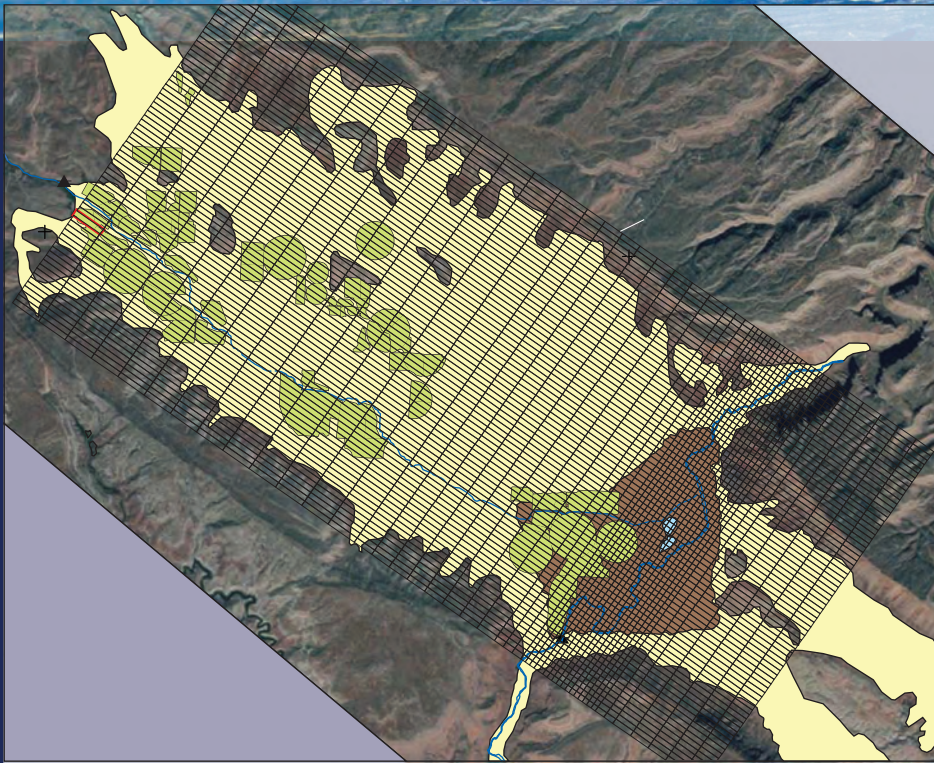


Prepared in cooperation with the Bureau of Reclamation

# Simulation of Groundwater Flow and Brine Discharge to the Dolores River in the Paradox Valley, Montrose County, Colorado



Scientific Investigations Report 2024–5038

**Cover.** Paradox Valley, Montrose County, Colo., view looking northwest toward the La Sal Mountains with model grid overlain from [figure 2](#) of this report (Used with permission from Wark Photography).

# **Simulation of Groundwater Flow and Brine Discharge to the Dolores River in the Paradox Valley, Montrose County, Colorado**

By Charles E. Heywood, Suzanne S. Paschke, M. Alisa Mast, and  
Kenneth R. Watts

Prepared in cooperation with the Bureau of Reclamation

Scientific Investigations Report 2024–5038

**U.S. Department of the Interior**  
**U.S. Geological Survey**

## U.S. Geological Survey, Reston, Virginia: 2024

For more information on the USGS—the Federal source for science about the Earth, its natural and living resources, natural hazards, and the environment—visit <https://www.usgs.gov> or call 1–888–392–8545.

For an overview of USGS information products, including maps, imagery, and publications, visit <https://store.usgs.gov/> or contact the store at 1–888–275–8747.

Any use of trade, firm, or product names is for descriptive purposes only and does not imply endorsement by the U.S. Government.

Although this information product, for the most part, is in the public domain, it also may contain copyrighted materials as noted in the text. Permission to reproduce copyrighted items must be secured from the copyright owner.

### Suggested citation:

Heywood, C.E., Paschke, S.S., Mast, M.A., and Watts, K.R., 2024, Simulation of groundwater flow and brine discharge to the Dolores River in the Paradox Valley, Montrose County, Colorado: U.S. Geological Survey Scientific Investigations Report 2024–5038, 47 p., <https://doi.org/10.3133/sir20245038>.

### Associated data for this publication:

Heywood, C.E., Mast, M.A., and Paschke, S.S., 2024, MODFLOW-6 model of variable-density groundwater flow and brine discharge to the Dolores River in the Paradox Valley, Colorado: U.S. Geological Survey data release, <https://doi.org/10.5066/P9ZW0FH5>.

U.S. Geological Survey, 2022, USGS water data for the Nation: U.S. Geological Survey National Water Information System database, <https://doi.org/10.5066/F7P55KJN>.

U.S. Geological Survey, 2024a, USGS 09169500 Dolores River at Bedrock, CO, in USGS water data for the Nation: U.S. Geological Survey National Water Information System database, <https://doi.org/10.5066/F7P55KJN>. [Site information directly accessible at <https://waterdata.usgs.gov/monitoring-location/09169500/all-graphs/#period=P7D>.]

U.S. Geological Survey, 2024b, USGS 09171100 Dolores River near Bedrock, CO, in USGS water data for the Nation: U.S. Geological Survey National Water Information System database, <https://doi.org/10.5066/F7P55KJN>. [Site information directly accessible at <https://waterdata.usgs.gov/monitoring-location/09171100/all-graphs/#period=P7D>.]

ISSN 2328-0328 (online)

## Contents

|  |    |
|--|----|
| Abstract.....  | 1  |
| Introduction.....  | 2  |
| Paradox Valley Unit .....  | 5  |
| Purpose and Scope .....  | 5  |
| Previous Investigations.....   | 6  |
| Hydrogeology of Study Area .....   | 6  |
| Hydrogeologic Units.....   | 7  |
| Climate and Precipitation .....  | 7  |
| Evapotranspiration.....  | 8  |
| Groundwater Recharge .....   | 8  |
| Dolores River .....  | 9  |
| West Paradox Creek.....  | 11 |
| Occurrence and Movement of Brine.....  | 11 |
| Aquifer Hydraulic Properties .....   | 12 |
| Model Development and Parameterization.....  | 12 |
| Modeling Strategy .....  | 14 |
| Spatial Discretization .....   | 15 |
| Distribution of Hydrogeologic Units.....   | 15 |
| Time Discretization .....  | 15 |
| Boundary Conditions .....  | 15 |
| Groundwater Withdrawals.....   | 16 |
| Specified-Flow Boundaries.....   | 17 |
| Recharge .....   | 17 |
| Groundwater Underflow .....  | 17 |
| Hydraulic Head-Dependent Flow Boundaries .....   | 18 |
| Evapotranspiration .....   | 18 |
| Stream Leakage .....   | 18 |
| Simulated Initial Conditions .....   | 19 |
| Calibration of the Groundwater Model .....   | 19 |
| Observed Groundwater Levels.....   | 19 |
| Observed Groundwater Concentrations .....  | 21 |
| Parameter Values and Sensitivities.....  | 21 |
| Simulation of Groundwater Flow and Brine Discharge in the Paradox Valley.....            | 22 |
| Simulated Water Budget .....   | 22 |
| Simulated Groundwater Levels .....   | 22 |
| Simulated Total Dissolved Solids Concentrations in Groundwater.....                      | 27 |
| Simulated Total Dissolved Solids Mass-Flux Budget.....                                   | 27 |
| Simulated Groundwater Withdrawals.....   | 30 |
| Simulated Streamflow and Total Dissolved Solids Concentrations of the Dolores River..... | 32 |
| Simulated Mass Flux to the Dolores River.....  | 33 |
| Model Uncertainty and Limitations.....   | 34 |
| Numerical Dispersion.....  | 34 |
| Breccia as a Source of Brine .....   | 34 |

|  |    |
|--|----|
| Other Sources of Model Uncertainty .....   | 35 |
| Brine Management Scenarios .....   | 38 |
| Scenario 1: Simulated Brine Discharge with No Brine Extraction .....                           | 39 |
| Scenario 2: Simulated Brine Discharge with Reduced Brine Extraction .....                      | 39 |
| Scenario 3: Simulated Brine Discharge with Brine Extraction for 9 Months Each Year .....       | 39 |
| Scenario 4: Simulated Brine Discharge with Reduced Irrigation-Return Flow.....                 | 40 |
| Scenario 5: Simulated Brine Discharge During a 5-Year Drought with No Brine<br>Extraction..... | 40 |
| Scenario Comparison.....   | 41 |
| Additional Research .....  | 42 |
| Summary.....   | 43 |
| Acknowledgments.....   | 45 |
| References Cited.....  | 45 |

## Figures

|  |    |
|--|----|
| 1. Map showing locations of the Paradox Valley Unit pumping and injection wells, irrigated land, and U.S. Geological Survey streamgages in the Paradox Valley, Montrose County, Colo.....  | 3  |
| 2. Map showing extent of the finite-difference model grid, alluvium of the Paradox Valley, collapse breccia, and irrigated land and locations of Paradox Valley Unit pumping and observation wells and U.S. Geological Survey streamgages in the Paradox Valley, Colo..... | 4  |
| 3. Schematic diagram showing the aquifer system below the Dolores River, the distribution of freshwater and brine in the alluvial aquifer, and the flow direction of groundwater toward the river in the Paradox Valley, Colo. ....  | 7  |
| 4. Graph showing monthly precipitation from January 1997 to May 2005 in the Paradox Valley, Colo.....  | 8  |
| 5. Graph showing average monthly freshwater pan evaporation in the Paradox Valley, Colo., 1975–1977. ....  | 9  |
| 6. Graph showing average monthly observed and simulated streamflow for the Dolores River at Bedrock in the Paradox Valley, Colo., 1987–2025 .....  | 10 |
| 7. Graph showing average monthly total dissolved solids concentrations estimated from specific conductance for the Dolores River at Bedrock and Dolores River near Bedrock in the Paradox Valley, Colo., 1987–2020.....  | 11 |
| 8. Map showing specific conductance in the Dolores River as it flows across the Paradox Valley, Colo., and locations of Paradox Valley Unit pumping wells.....   | 13 |
| 9. Graph showing estimated and simulated monthly total dissolved solids mass removed by Paradox Valley Unit pumping wells in the Paradox Valley, Colo., 1996–2020 .....  | 17 |
| 10. Graph showing monthly precipitation for 1987–2020 throughout the Paradox Valley floor and adjacent highlands .....   | 18 |
| 11. Graphs showing observed and simulated streamflow for the Dolores River near Bedrock in the Paradox Valley, Colo., 1987–2020 .....  | 20 |
| 12. Graph showing estimated and simulated total dissolved solids concentrations for the Dolores River near Bedrock in the Paradox Valley, Colo., 1987–2020.....  | 20 |

|  |    |
|--|----|
| 13. Bar graphs showing <i>A</i> , simulated monthly transient water budget for the 33-year simulation in the Paradox Valley, Colo., 1987–2020, and <i>B</i> , simulated monthly transient storage values and changes in storage for the 33-year simulation for the Paradox Valley, Colo., 1987–2020 .....  | 24 |
| 14. Map showing simulated water-table altitude for July 2007, locations of the Paradox Valley Unit pumping and observation wells, and extent of alluvium and collapse breccia in the Paradox Valley, Colo.....   | 25 |
| 15. Hydrographs of observed and simulated groundwater levels for observation wells near the Dolores River in the Paradox Valley, Colo.....   | 26 |
| 16. Map showing simulated water-table altitude and total dissolved solids concentrations in groundwater in the top model grid layer for November 2020, Paradox Valley, Colo.....   | 28 |
| 17. Graphs showing <i>A</i> , simulated monthly transient total dissolved solids mass-flux budget for the 33-year simulation in the Paradox Valley, Colo., 1987–2020, and <i>B</i> , monthly simulated transient total dissolved solids storage mass-flux values and changes in storage for the 33-year simulation in the Paradox Valley, Colo., 1987–2020 ..... | 29 |
| 18. Graph showing estimated and simulated monthly total dissolved solids mass flux to the Dolores River, Paradox Valley, Colo., 1987–2020.....   | 33 |
| 19. Graph showing estimated and simulated total dissolved solids mass flux removed by Paradox Valley Unit pumping wells for the 33-year simulation and alternative representations of the breccia as a constant-flux source in the Paradox Valley, Colo., 1987–2020 .....  | 37 |
| 20. Graph showing estimated and simulated total dissolved solids mass flux to the Dolores River for the 33-year simulation and alternative representations of the breccia as a constant-flux source in the Paradox Valley, Colo., 1987–2020.....   | 37 |
| 21. Graph showing simulated total dissolved solids mass flux withdrawn from Paradox Valley Unit pumping wells in scenarios 2 and 3 in the Paradox Valley, Colo., 2021–2025 .....   | 39 |
| 22. Graph showing total dissolved solids mass flux to the Dolores River simulated for five management scenarios at the Paradox Valley Unit in the Paradox Valley, Colo., 2021–2025 .....   | 41 |

## Tables

|  |    |
|--|----|
| 1. Irrigated area estimated recharge rate from irrigation-return flow and annualized recharge rate by crop type in the Paradox Valley, Colo. ....  | 9  |
| 2. Dimensions of Paradox Valley Unit pumping wells in the Paradox Valley, Colo., and percentage of time used during 1996–2020 .....  | 16 |
| 3. Calibrated parameter values for hydraulic properties or boundary conditions used in the groundwater model of the Paradox Valley, Colo., and sensitivities of hydraulic head and concentration to model parameters ..... | 21 |
| 4. Simulated water-budget components averaged during the 1,000-year, 33-year, pre-Paradox Valley Unit, and post-Paradox Valley Unit simulation periods for the Paradox Valley, Colo. ....                                  | 23 |
| 5. Simulated total dissolved solids mass-flux budget components averaged during the 33-year, pre-Paradox Valley Unit, and post-Paradox Valley Unit simulation periods for the Paradox Valley, Colo. ....                   | 30 |

|    |  |    |
|----|--|----|
| 6. | Estimated and simulated volume of groundwater, total dissolved solids concentrations, and total dissolved solids mass flux withdrawn from Paradox Valley Unit pumping wells for different simulation periods for the Paradox Valley, Colo.....                                   | 31 |
| 7. | Observed and simulated streamflow and estimated and simulated total dissolved solids concentrations and total dissolved solids mass flux to the Dolores River near Bedrock, in the Paradox Valley, Colo., 1987–2020.....   | 32 |
| 8. | Simulated total dissolved solids mass-flux budget components for average 33-year, constant-breccia flux, and increased constant-breccia flux simulations for the Paradox Valley, Colo., 1987–2020.....   | 36 |
| 9. | Simulated 5-year average values of total dissolved solids mass flux withdrawn from Paradox Valley Unit pumping wells, total dissolved solids mass flux to the Dolores River, and evapotranspiration for five management scenarios for the Paradox Valley, Colo., 2021–2025 ..... | 40 |

## Conversion Factors

U.S. customary units to International System of Units

| Multiply                                   | By       | To obtain                               |
|--|----------|---|
| Length                                     |          |   |
| inch (in)                                  | 2.54     | centimeter (cm)                         |
| foot (ft)                                  | 0.3048   | meter (m)                               |
| mile (mi)                                  | 1.609    | kilometer (km)                          |
| mile, nautical (nm)                        | 1.852    | kilometer (km)                          |
| yard (yd)                                  | 0.9141   | meter (m)                               |
| Area                                       |          |   |
| acre                                       | 4,047    | square meter (m <sup>2</sup> )          |
| acre                                       | 0.4047   | hectare (ha)                            |
| acre                                       | 0.004047 | square kilometer (km <sup>2</sup> )     |
| square foot (ft <sup>2</sup> )             | 0.0929   | square meter (m <sup>2</sup> )          |
| section (640 acres or 1 square mile)       | 259.0    | square hectometer (hm <sup>2</sup> )    |
| square mile (mi <sup>2</sup> )             | 259.0    | hectare (ha)                            |
| square mile (mi <sup>2</sup> )             | 2.59     | square kilometer (km <sup>2</sup> )     |
| Volume                                     |          |   |
| gallon (gal)                               | 0.003785 | cubic meter (m <sup>3</sup> )           |
| cubic foot (ft <sup>3</sup> )              | 0.0283   | cubic meter (m <sup>3</sup> )           |
| cubic yard (yd <sup>3</sup> )              | 0.7645   | cubic meter (m <sup>3</sup> )           |
| acre-foot (acre-ft)                        | 1,233.50 | cubic meter (m <sup>3</sup> )           |
| Flow rate                                  |          |   |
| foot per day (ft/d)                        | 0.3048   | meter per day (m/d)                     |
| cubic foot per day (ft <sup>3</sup> /d)    | 0.0283   | cubic meter per day (m <sup>3</sup> /d) |
| cubic foot per second (ft <sup>3</sup> /s) | 244.68   | cubic meter per day (m <sup>3</sup> /d) |
| gallon per day (gal/d)                     | 0.003785 | cubic meter per day (m <sup>3</sup> /d) |



| <b>Multiply</b>                            | <b>By</b> | <b>To obtain</b>                               |
|--|-----------|--|
| acre-foot per year (acre-ft/yr)            | 3.37939   | cubic meter per day (m <sup>3</sup> /d)        |
| Load                                       |           |  |
| pound per day (lb/d)                       | 0.4535    | kilogram per day (kg/d)                        |
| tons per year (tons/yr)                    | 2.484     | kilogram per day (kg/d)                        |
| Mass                                       |           |  |
| pound avoirdupois (lb)                     | 0.4535    | kilogram (kg)                                  |
| Density                                    |           |  |
| pound per cubic foot (lb/ft <sup>3</sup> ) | 16.0205   | kilogram per cubic meter (kg/m <sup>3</sup> )  |
| pound per cubic foot (lb/ft <sup>3</sup> ) | 0.01602   | gram per cubic centimeter (g/cm <sup>3</sup> ) |
| Hydraulic conductivity                     |           |  |
| foot per day (ft/d)                        | 0.3048    | meter per day (m/d)                            |
| Hydraulic gradient                         |           |  |
| foot per mile (ft/mi)                      | 0.1894    | meter per kilometer (m/km)                     |

International System of Units to U.S. customary units

| <b>Multiply</b>                         | <b>By</b> | <b>To obtain</b>                           |
|---|-----------|--|
| Length                                  |           |  |
| centimeter (cm)                         | 0.3937    | inch (in)                                  |
| meter (m)                               | 3.281     | foot (ft)                                  |
| kilometer (km)                          | 0.6214    | mile (mi)                                  |
| kilometer (km)                          | 0.5400    | mile, nautical (nm)                        |
| meter (m)                               | 1.094     | yard (yd)                                  |
| Area                                    |           |  |
| square meter (m <sup>2</sup> )          | 0.0002471 | acre                                       |
| hectare (ha)                            | 2.471     | acre                                       |
| square kilometer (km <sup>2</sup> )     | 247.1     | acre                                       |
| square meter (m <sup>2</sup> )          | 10.76     | square foot (ft <sup>2</sup> )             |
| square hectometer (hm <sup>2</sup> )    | 0.003861  | section (640 acres or 1 square mile)       |
| hectare (ha)                            | 0.003861  | square mile (mi <sup>2</sup> )             |
| square kilometer (km <sup>2</sup> )     | 0.3861    | square mile (mi <sup>2</sup> )             |
| Volume                                  |           |  |
| cubic meter (m <sup>3</sup> )           | 264.2     | gallon (gal)                               |
| cubic meter (m <sup>3</sup> )           | 35.31     | cubic foot (ft <sup>3</sup> )              |
| cubic meter (m <sup>3</sup> )           | 1.308     | cubic yard (yd <sup>3</sup> )              |
| cubic meter (m <sup>3</sup> )           | 0.0008107 | acre-foot (acre-ft)                        |
| Flow rate                               |           |  |
| meter per day (m/d)                     | 3.281     | foot per day (ft/d)                        |
| cubic meter per day (m <sup>3</sup> /d) | 35.31     | cubic foot per day (ft <sup>3</sup> /d)    |
| cubic meter per day (m <sup>3</sup> /d) | 0.0004087 | cubic foot per second (ft <sup>3</sup> /s) |
| cubic meter per day (m <sup>3</sup> /d) | 264.2     | gallon per day (gal/d)                     |
| cubic meter per day (m <sup>3</sup> /d) | 0.295911  | acre-foot per year (acre-ft/yr)            |
| Load                                    |           |  |
| kilogram per day (kg/d)                 | 2.205     | pound per day (lb/d)                       |

| <b>Multiply</b>                                | <b>By</b> | <b>To obtain</b>                           |
|--|-----------|--|
| kilogram per day (kg/d)                        | 0.40262   | tons per year (tons/yr)                    |
| <b>Mass</b>                                    |           |  |
| kilogram (kg)                                  | 2.205     | pound avoirdupois (lb)                     |
| <b>Density</b>                                 |           |  |
| kilogram per cubic meter (kg/m <sup>3</sup> )  | 0.06242   | pound per cubic foot (lb/ft <sup>3</sup> ) |
| gram per cubic centimeter (g/cm <sup>3</sup> ) | 62.4220   | pound per cubic foot (lb/ft <sup>3</sup> ) |
| <b>Hydraulic conductivity</b>                  |           |  |
| meter per day (m/d)                            | 3.281     | foot per day (ft/d)                        |
| <b>Hydraulic gradient</b>                      |           |  |
| meter per kilometer (m/km)                     | 5.27983   | foot per mile (ft/mi)                      |

Temperature in degrees Celsius (°C) may be converted to degrees Fahrenheit (°F) as follows:

$$^{\circ}\text{F} = (1.8 \times ^{\circ}\text{C}) + 32.$$

Temperature in degrees Fahrenheit (°F) may be converted to degrees Celsius (°C) as follows:

$$^{\circ}\text{C} = (^{\circ}\text{F} - 32) / 1.8.$$

## Datum

Vertical coordinate information is referenced to the North American Vertical Datum of 1988 (NAVD 88).

Horizontal coordinate information is referenced to the North American Datum of 1983 (NAD 83).

Altitude, as used in this report, refers to distance above the vertical datum.

## Supplemental Information

Concentrations of chemical constituents in water are given in either milligrams per liter (mg/L) or kilograms per cubic meter (kg/m<sup>3</sup>). In this report, mass flux is reported in both the International System of Units (kilograms per day) and the U.S. customary units (tons per year). U.S. customary units are included to be consistent with Bureau of Reclamation reporting standards.

## Abbreviations

|             |                             |
|-------------|-----------------------------|
| ET          | evapotranspiration          |
| MAW         | Multi-aquifer well          |
| PVU         | Paradox Valley Unit         |
| Reclamation | Bureau of Reclamation       |
| SFR         | Streamflow routing          |
| TDS         | total dissolved solids      |
| TVD         | total variation diminishing |
| USGS        | U.S. Geological Survey      |

# Simulation of Groundwater Flow and Brine Discharge to the Dolores River in the Paradox Valley, Montrose County, Colorado

By Charles E. Heywood, Suzanne S. Paschke, M. Alisa Mast, and Kenneth R. Watts

## Abstract

Salinity, or total dissolved solids (TDS), of the Colorado River affects agricultural, municipal, and industrial water users and is an important concern in the Western United States. In the Paradox Valley of southwestern Colorado, natural discharge of sodium-chloride brine to the Dolores River from the underlying core of a salt-valley anticline accounts for about 6 percent of the salinity load to the Colorado River. Formation of the Paradox Valley began during the Miocene, and subsequent erosion exposed the Pennsylvania Paradox Formation in the core of the anticline where a cap rock, collapse features, breccia, and sodium-chloride saturated brine developed at the top of the exposed salt diapir. The discharge of brine to the Dolores River is affected by these dissolution features, along with seasonal hydrologic conditions and density-dependent flow between older dense brine and the younger fresh groundwater in the overlying alluvial aquifer. To reduce TDS concentrations in the Dolores River through the Paradox Valley, the Bureau of Reclamation has pumped brine from a series of shallow wells adjacent to the river since July 1996. The pumped brine is collected and piped to a deep disposal well where it is injected into the Mississippian Leadville Limestone at a depth of about 4,570-meters below land surface. The pumping and injection operation is collectively known as the Paradox Valley Unit (PVU), and by 2015, the PVU had substantially reduced TDS concentrations in the Dolores River by about 70 percent. Since 2019, injection-pressure limits and related seismic activity have constrained deep-well injection and thus brine pumping at the PVU.

In cooperation with the Bureau of Reclamation, the U.S. Geological Survey developed a MODFLOW-6 three-dimensional, variable-density groundwater flow and TDS transport model of the Paradox Valley to evaluate the effects of PVU pumping operations on brine discharge to the Dolores River and to guide additional research. The finite-difference model grid consists of 76 rows and 48 columns oriented from northwest to southeast in alignment with valley topography and groundwater-flow directions in the near-surface freshwater alluvial aquifer. A 7-layer hydrogeologic framework was

developed from existing datasets to represent the alluvial aquifer, cap rock, collapse breccia, and groundwater flow and TDS transport from the underlying Paradox Formation salt to the Dolores River. The model represents a 33-year transient calibration period from 1987 through 2020 that includes pre-PVU conditions from 1987 through June 1996 and post-PVU conditions from July 1996 through 2020. A 1,000-year simulation of groundwater flow and coupled TDS transport computed the initial conditions for the subsequent 33-year transient simulation. Observations of precipitation, streamflow, evaporation, agricultural land use, and PVU brine pumping rates were used to specify appropriate boundary conditions to the model representing time-varying recharge, tributary streamflow, groundwater underflow, evapotranspiration (ET), and PVU pumping. Values for average monthly streamflow and TDS concentration at the upstream streamgage, the Dolores River at Bedrock (USGS streamgage 09169500), were specified as model input where the Dolores River enters Paradox Valley. Observed pumping from the PVU, water levels and TDS concentrations in groundwater, and streamflow and estimated TDS concentrations at the downstream streamgage, the Dolores River near Bedrock (USGS streamgage 09171100), were calibration targets that constrained the manual calibration of model parameters representing aquifer hydraulic conductivity, storage, streambed conductance, recharge, and (ET).

Two primary model-calibration targets were the match between observed and simulated TDS mass flux from PVU pumping wells and the match between estimated and simulated TDS mass flux to the Dolores River. The simulated TDS mass withdrawn by pumping wells is calculated by the model as the product of the assigned pumping rate and simulated groundwater TDS concentrations. Because actual pumping rates were assigned as simulated values, the total simulated PVU pumping for the 33-year calibration is within 0.5 percent of the observed values. However, simulated concentrations and thus mass flux of TDS withdrawn by the PVU pumping wells were consistently about 26 percent less than observed values for all the simulated time periods (33-year simulation, pre-PVU, and post-PVU). The representation of brine inflow was explored through additional modeling to evaluate the effect of the simulated brine source on groundwater TDS concentrations. Results indicated that a saturated-salt

## 2 Simulation of GW Flow and Brine Discharge to the Dolores River in the Paradox Valley, Montrose County, Colorado

constant-flux brine source best replicated the magnitude and transient pattern observed for TDS mass flux from PVU pumping wells.

The simulated TDS mass flux to the Dolores River is compared to estimates based on observed streamflow and specific conductance (SC) data for the downstream streamgage. The calibrated model provided a close fit of simulated to measured streamflow at the downstream streamgage, and the calibrated model fit to estimated TDS concentrations at the downstream streamgage was reasonable. The greatest differences between simulated and estimated values occurred during drought periods from June 2000 to March 2003, May 2012 to June 2013, and October 2013 to October 2014, when simulated TDS concentrations in the river were greater than estimated concentrations. In general, simulated TDS mass flux to the river for the pre-PVU period is in good agreement with estimated values (2-percent difference), but the model overestimated TDS mass flux to the river by about 41 percent during the post-PVU period. The model uncertainty with respect to TDS mass flux to the river indicates other processes or model parameters not well represented by the model are affecting the system, especially during drought. During model calibration, the most sensitive parameters were identified as vertical hydraulic conductivity of the alluvial aquifer, conductance of the Dolores River streambed, ET extinction depth and rate, and recharge rate.

Five 5-year scenarios of conditions for 2021–25 were simulated to assist evaluation of alternative strategies to manage the discharge of brine into the Dolores River. The first scenario simulates no PVU pumping and serves as a base case for comparison to the other scenarios. Two scenarios simulate the effects of varying withdrawal timing at an annual rate about one-third less than during 2010 through 2018. During high-flow spring snowmelt runoff periods when brine discharge is naturally minimized, PVU pumping does not substantially affect salinity in the Dolores River, and comparison of these two scenarios indicates that scheduling brine withdrawals during times of low river stage is nearly as effective at reducing TDS mass flux to the river as pumping brine year-round. Cessation of pumping during periods of high river stage may be advantageous for system maintenance, brine injection, and seismic-risk reduction. The fourth scenario tested the effect of reducing irrigation-return flow on brine discharge and predicted a slight reduction of TDS mass flux to the Dolores River, but not as great a reduction as that of using the PVU to remove brine. The fifth scenario simulated 5 years of drought conditions without PVU pumping and indicates brine discharge during drought about 15 percent greater than during average hydrologic conditions. Results from scenario 5 are consistent with the calibrated model results and indicate that aquifer properties and ET processes and parameters may be affecting simulation results during drought.

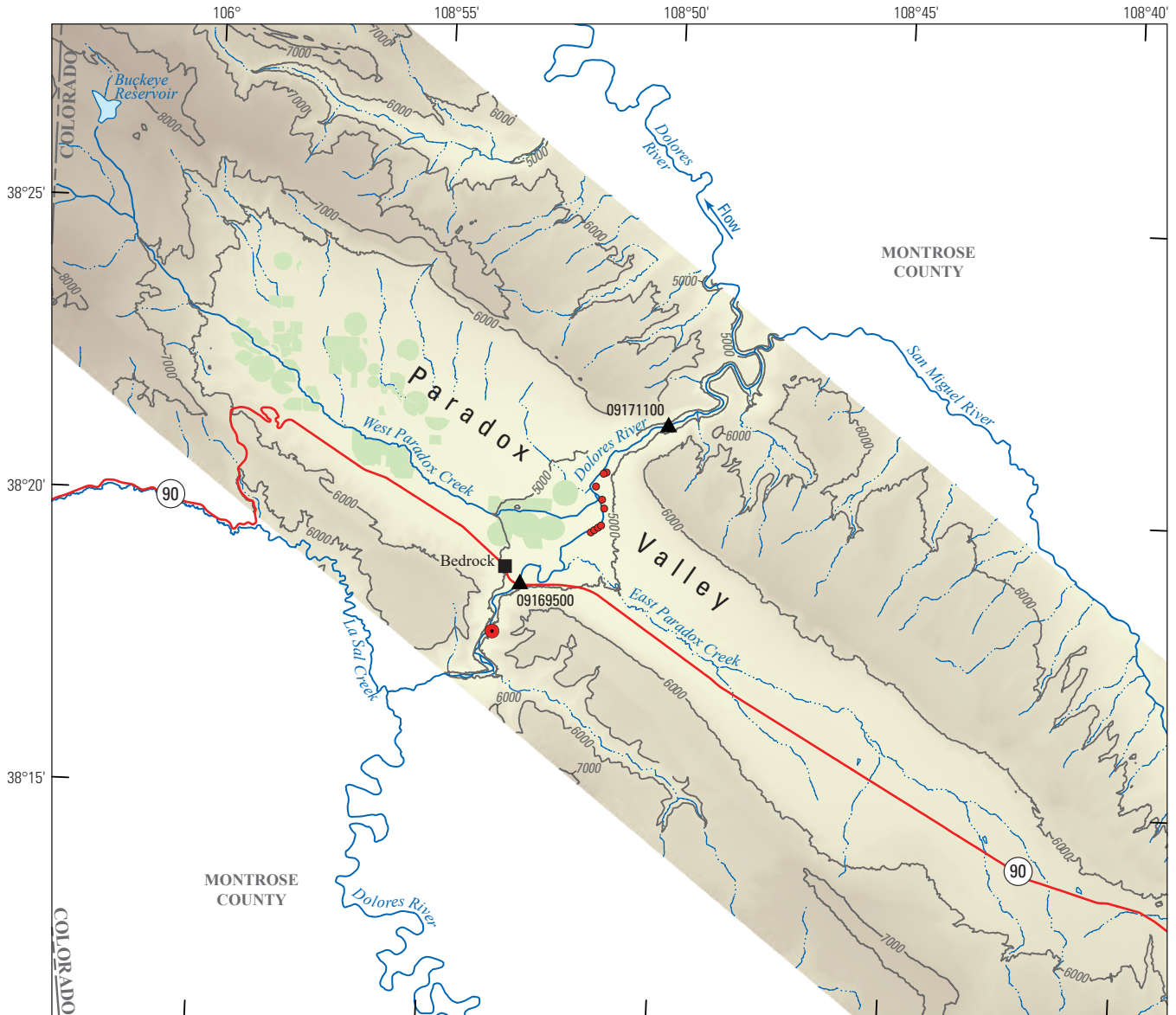
The Paradox Valley groundwater model provides a reasonable overall match to observed conditions in the Dolores River. The model is useful for evaluating relative differences between brine management scenarios to inform PVU

operational decisions and to identify gaps in data and process understanding. Representation of the brine source, hydraulic-conductivity parameters, and recharge and ET processes were identified as potential areas for additional field and modeling research. Additional research in the Paradox Valley might include field-data collection that provides additional information on the hydrogeologic framework, groundwater levels, groundwater TDS concentrations, stream characteristics, and aquifer properties. Additional modeling efforts could benefit from applying advanced tools for model development, calibration, and visualization including parameter-estimation and sensitivity analysis. Statistical evaluation of known model uncertainties such as hydraulic conductivity, streambed conductance, representations of the brine source, recharge, and ET could improve the match between simulated and estimated TDS mass flux from PVU pumping wells and to the Dolores River further informing model predictions and system understanding for the Paradox Valley.

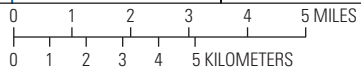
## Introduction

The Colorado River and its tributaries supply water for about 40 million people and irrigation of about 22,300 square kilometers (km<sup>2</sup>) in the Western United States, making it an important water resource in the region. Salinity, or total dissolved solids (TDS), is a primary water-quality constituent of concern in the Colorado River Basin, affecting agricultural, municipal, and industrial water users. Salinity in the Upper Colorado River Basin (fig. 1) is derived primarily in arid parts of the basin from interactions of groundwater and surface water and with soluble minerals in underlying sedimentary rocks (Tuttle and Grauch, 2009). Water-use processes, including irrigation, reservoir evaporation, and municipal and industrial wastewater discharges, can also increase salinity concentrations and accelerate the release of naturally occurring dissolved solids to streams (Tuttle and Grauch, 2009). During water year 1991, about 57 percent of the salinity load in the Colorado River upstream from its confluence with the Green River was from natural geologic sources (Kenney and others, 2009).

The Dolores River is a major tributary of the Colorado River historically accounting for about 6 percent of the salinity load to the Colorado River, and the primary source of salinity to the Dolores River is the Paradox Valley (Kenney and others, 2009; fig. 2). The Paradox Valley is a topographic basin bounded by faults that outline the geologic structure and expose the collapsed core of a salt-valley anticline (Hite and Lohman, 1973). The salt-anticline core is an elongated northwest-to-southeast trending salt diapir composed of the Pennsylvanian Paradox Formation of the Hermosa Group (herein Paradox Formation; Elston and Shoemaker, 1961; Cater and Craig, 1970). A cap rock, collapse features, breccia, and salt-saturated brine developed at the top of the exposed salt diapir during valley formation and erosion that began



Base from U.S. Geological Survey digital data, 2021  
 Universal Transverse Mercator projection, zone 13 north  
 North American Datum of 1983



**EXPLANATION**

- Elevation**—Elevation in feet
  - 8,500
  - 4,800
- Irrigated land**
- Perennial stream**
- Intermittent stream**
- Topographic contour**—Contour interval 1,000 feet. Datum is North American Vertical Datum of 1988
- U.S. Geological Survey streamgage and identifier**
- Paradox Valley Unit injection well**
- Paradox Valley Unit pumping well**

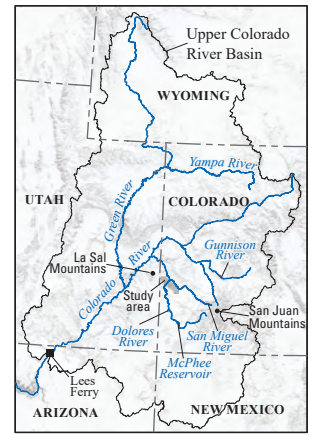


**Figure 1.** Locations of the Paradox Valley Unit pumping and injection wells, irrigated land, and U.S. Geological Survey streamgages in the Paradox Valley, Montrose County, Colo. (Bureau of Reclamation [Reclamation], 2022; U.S. Geological Survey, 2022; Paschke and Mast, 2024).

4 Simulation of GW Flow and Brine Discharge to the Dolores River in the Paradox Valley, Montrose County, Colorado

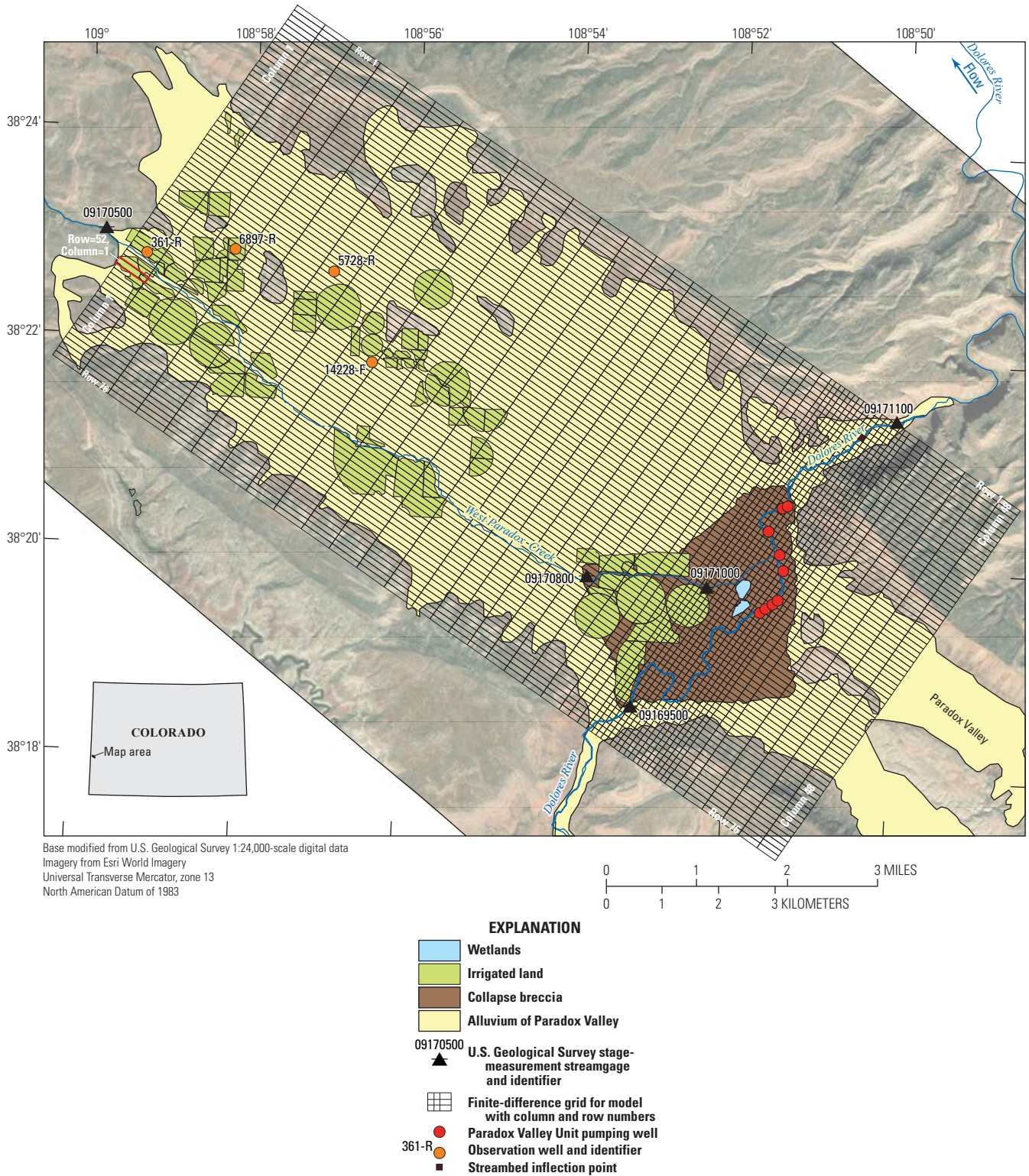


**Figure 2.** Extent of the finite-difference model grid, alluvium of the Paradox Valley, collapse breccia, and irrigated land and locations of Paradox Valley Unit pumping and observation wells and U.S. Geological Survey streamgages in the Paradox Valley, Colo. (U.S. Geological Survey, 2022; Heywood and others, 2024; Paschke and Mast, 2024).

during the Miocene and continued through the Quaternary (Gutiérrez, 2004; Paschke and others, 2024). The brine in the cap rock and breccia is much older than the overlying freshwater and dense because of its salt content, and the density difference between the brine and the overlying freshwater aquifer drives density-dependent gradients and flow of brine into the base of the alluvial aquifer and the Dolores River (Paschke and others, 2024). It is this discharge of brine from the Paradox Formation that causes the observed increases in salinity as the river crosses the valley (Mast and Terry, 2019). A large collapse breccia feature near the center of the valley as well as seasonal hydrologic conditions also affect hydraulic gradients and thus discharge of brine to the river (Mast and Terry, 2019; Paschke and others, 2024).

## Paradox Valley Unit

To reduce salinity concentrations in the Dolores River, the Bureau of Reclamation (Reclamation) operates the Paradox Valley Unit (PVU) in the Paradox Valley. The PVU project consists of nine shallow pumping wells near the Dolores River that extract brine from the base of the alluvial aquifer and one injection well about 4.8 kilometers (km) southwest of the pumping wells where the brine is deep-well injected for disposal (fig. 1). The PVU is a Reclamation project authorized by the Colorado River Basin Salinity Control Act of 1974 (Public Law 93–320) to construct salinity-control projects in the Colorado River Basin (Reclamation, 2021). The PVU pumping wells are located adjacent to the river along its southeast bank (fig. 1) and are completed below the freshwater-brine interface and above the base of the alluvial aquifer at depths that range from 14.8 to 32.3 meters (m) below land surface (Reclamation, 1978b). Brine is pumped from the nine pumping wells at a total rate in the range of about 940 to 1,223 cubic meters per day ( $\text{m}^3/\text{d}$ ) (Reclamation, 2022). The PVU pumping lowers the freshwater-brine interface beneath the river thereby reducing discharge of brine to the river (Paschke and others, 2024). The pumped brine is collected and piped to the deep disposal well (the injection well) where it is injected into the Mississippian Leadville Limestone at depths of 4,288 to 4,833 m below land surface (Watts, 2000; Block and others, 2015; fig. 1).

The PVU system was developed in the 1970s and 1980s with a test phase of intermittent pumping and injection occurring from 1991 to 1993 (Reclamation, 1978b, 2022; Block and others, 2015). Regular operation of the PVU began July 1, 1996 (Block and others, 2015). The period of PVU operation prior to July 1, 1996, is herein described as the pre-PVU period, and the period of PVU operation after July 1, 1996, is herein described as the post-PVU period. By 2015, the PVU had reduced TDS concentrations in the Dolores River by as much as 70 percent compared to pre-PVU conditions (Mast, 2017) indicating that continued operation of the PVU supports reduction of the salinity load of the Dolores and Colorado Rivers.

After more than 20 years of injection, increased fluid pressure has induced earthquake seismicity in the area (King and others, 2014). Seismicity induced by PVU injection has increased since 2016 (Denlinger and O’Connell, 2020), and, on March 4, 2019, injection operations, and thus PVU pumping, were immediately suspended after the occurrence of a 4.5 magnitude earthquake in the region (the largest to date attributed to PVU operations) (Reclamation, 2022). Except for a short pumping period in the spring 2020, PVU operations remained ceased from March 2019 to June 2022 (Reclamation, 2022). On June 1, 2022, the PVU temporarily resumed operations for a six-month trial period with a reduced injection rate of about  $625 \text{ m}^3/\text{d}$ , or about two-thirds of past operations, to gather additional information and guide potential future operational decisions (Reclamation, 2022). Further brine disposal into the Leadville Limestone may be limited, and Reclamation is considering alternative strategies to manage brine disposal through an Environmental Impact Statement process (Reclamation, 2022). Operation of the existing PVU pumping and injection wells may continue at a reduced rate until an alternative strategy is implemented.

To evaluate the efficacy of alternative PVU pumping operations and to guide additional research in the Paradox Valley, the U.S. Geological Survey (USGS), in cooperation with Reclamation, developed a numerical groundwater model of the Paradox Valley and PVU pumping that simulates groundwater flow and TDS concentrations beneath the valley, streamflow and TDS concentrations in the Dolores River, PVU pumping, and other groundwater-surface-water interaction processes. The model quantifies the temporal variations of brine discharge into the Dolores River for a 33-year model-calibration period from 1987 to 2020 and provides a useful tool for evaluating the effects of hydrologic processes on brine discharge to the Dolores River.

## Purpose and Scope

The purpose of this report is to present results of groundwater flow and TDS transport simulations for the Paradox Valley, Colorado, developed by the USGS in cooperation with Reclamation. The report describes a numerical model of variable-density groundwater flow and TDS transport implemented with the MODFLOW-6 computer program (Langevin and others, 2017, 2020, 2021) for the purposes of evaluating the effects of PVU pumping operations on TDS discharge to the river and guiding additional research.

The MODFLOW-6 simulations were designed to simulate TDS concentrations in the Paradox Valley groundwater system and in the Dolores River. The model grid encompasses the Paradox Valley floor and is oriented from northwest to southeast in alignment with groundwater-flow directions. As described in the “Model Development and Parameterization” section of this report, the model simulates groundwater flow in the near-surface alluvial aquifer and TDS transport from the underlying Paradox Formation to the alluvial aquifer and

the Dolores River using a 7-layer hydrogeologic framework based on geospatial datasets from Paschke and Mast (2024) and the Colorado Water Conservation Board and Colorado Division of Water Resources (2021). Model input files for hydrologic boundary conditions representing PVU pumping, recharge, groundwater underflow, evapotranspiration, and stream leakage were developed from previous studies (Paschke and others, 2024 and the “Hydrogeology of the Study Area” of this report) as described in the “Boundary Conditions” section of this report.

The groundwater model represents a 33-year calibration period from October 1987 through November 2020 that includes pre-PVU conditions from 1987 through June 1996 and post-PVU conditions from July 1996 through 2020. The MODFLOW-6 simulations were manually calibrated to observations and estimates of groundwater levels, streamflow, and TDS concentrations in groundwater and surface water as described in the “Calibration of the Groundwater Model” section of this report. The simulated brine discharge to the Dolores River is compared to estimates (Mast, 2017; Heywood and others, 2024) based on streamflow and specific conductance (SC) data for the Dolores River, and simulation results for the calibration period are described in the “Simulation of Groundwater Flow and Brine Discharge in the Paradox Valley” section of this report. The simulations also were used to evaluate four management scenarios and the effect of drought on brine discharge to the river for a simulated prediction period from 2021 through 2025 as described in the “Brine Management Scenarios” section of this report. Three of the management scenarios compare the effects of reducing PVU groundwater withdrawals by different amounts, and the fourth scenario tests the effect of reducing irrigation-return flow on brine discharge to the Dolores River. The simulated drought is a continuation of conditions existing since June 2020. Simulation results are used to identify data and modeling gaps for the Paradox Valley in the “Model Uncertainty and Limitations” section of this report and areas for additional evaluation in the “Additional Research” section of this report. The model input files, source and executable codes, and model output files from the calibration and scenario simulations are published in a USGS data release (Heywood and others, 2024).

## Previous Investigations

Konikow and Bedinger (1978) described the groundwater-flow system in the Paradox Valley, the problem of TDS discharge into the Dolores River, and the effect of contrasting densities between freshwater and brine fluids on the hydraulics of the groundwater-flow system. Reclamation (1978a, b) documented the design and implementation of the PVU for brine pumping from the shallow aquifer and for deep reservoir reinjection. Mast (2017) estimated the magnitudes of TDS mass flux into the Dolores River before and during operation of the PVU. Mast and Terry (2019) documented the

effects of Dolores River stage on the discharge of TDS into the river. A summary of USGS hydrologic, geologic, and geophysical investigations in the Paradox Valley area is presented in Paschke and others (2024), where they describe a conceptual model of groundwater flow and brine discharge that provided the framework for building the numerical model described in this report.

## Hydrogeology of the Study Area

The Paradox Valley is a structural and topographic basin about 25 miles long and 3–5 miles wide (Fenneman, 1931) located in Montrose County, Colorado, near the Colorado-Utah border (fig. 1). Topography of the area is characterized by plateaus dissected by canyons with large topographic relief resulting from rapid downcutting by the Colorado River and its tributaries since the Miocene (Hite and Lohman, 1973; Gutiérrez, 2004). The Paradox Valley, on the southeast flank of the La Sal Mountains, is oriented along the northwest to southeast axis of the underlying salt anticline (Hite and Lohman, 1973). The floor of the Paradox Valley has an altitude of about 1,500 m (about 4,900 feet [ft]) near the Dolores River and is relatively flat compared to the surrounding uplands (fig. 1). The paradox of the Paradox Valley is that the Dolores River crosses the salt-anticline valley perpendicular to its northwest to southeast trend and about midway along the valley axis. The Dolores River enters and leaves the Paradox Valley through deep canyons incised through the surrounding Paleozoic and Mesozoic rocks (Mast, 2017; Paschke and others, 2024). Uplands at the northwestern end of the Paradox Valley and mesas on the northeastern and southwestern sides of the valley rise about 305 m above the valley floor. Major land uses in the valley include rangeland and about 2,700 acres of irrigated cropland and pastureland located northwest of the river (Mast, 2017; fig. 2).

The hydrogeology of the Paradox Valley can be generally characterized as an unconfined freshwater aquifer in alluvial deposits (an alluvial aquifer) underlain by brine that occurs in the brecciated cap rock and underlying salt deposits of the exposed Paradox Formation (Paschke and others, 2024; fig. 3). The brine is dense because of its salt content and is estimated as at least 10,000 years old, much older than fresh groundwater in the overlying alluvial aquifer (Gardner and Newman, 2023; Paschke and others, 2024). Density-dependent gradients support upward flow of brine into the alluvial aquifer and toward the Dolores River, and both freshwater from the alluvial aquifer and brine discharge to the river. As the Dolores River crosses the Paradox Valley, it gains salinity, or TDS, from discharge of the brine (Reclamation, 1978b; Mast and Terry, 2019). A large collapse breccia feature near the center of the valley as well as seasonal hydrologic conditions also affect hydraulic gradients and thus discharge of brine to the river (Mast and Terry, 2019; Paschke and others, 2024). During spring snowmelt runoff, when river stage is highest,



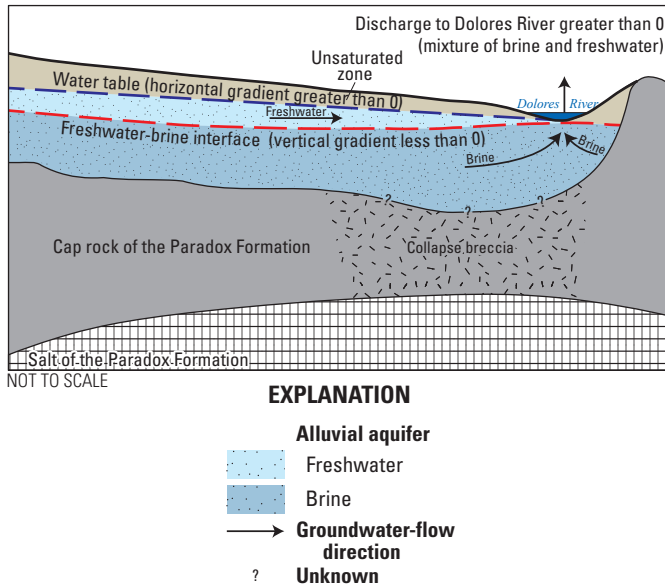


**Figure 3.** Aquifer system below the Dolores River, the distribution of freshwater and brine in the alluvial aquifer, and the flow direction of groundwater toward the river in the Paradox Valley, Colo. (modified from Hubbert, 1953).

the freshwater-brine interface is depressed beneath the riverbed, and brine discharge to the river is minimized (Mast and Terry, 2019). As much as 70 percent of the annual salinity gain across the valley occurs from December through March during the winter low-flow months (Mast, 2017) when river stage is lowest, and the freshwater-brine interface rises to near the land surface. (Mast and Terry, 2019).

## Hydrogeologic Units

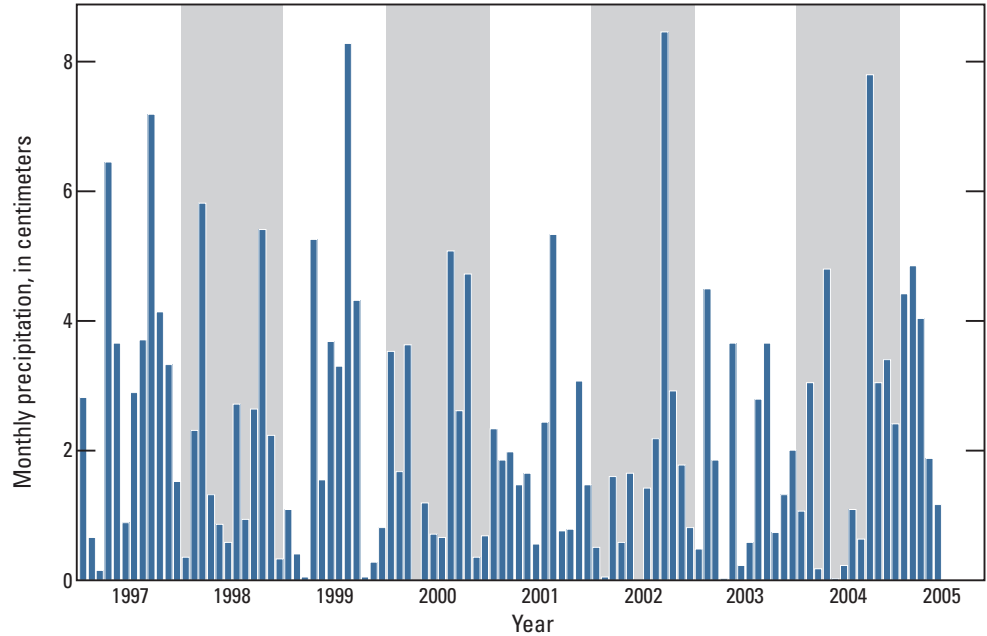
Quaternary alluvial and aeolian deposits overlie bedrock along the floor of the Paradox Valley forming an unconfined alluvial aquifer with a water table near the land surface (Paschke and others, 2024). The uppermost deposits are eolian and consist of as much as 3 meters (m) of indistinctly bedded light-red silt and sand that has been partly reworked by water and mixed with sheet wash (Cater and Craig, 1970). The alluvial deposits generally consist of 1.5–4.6 m of silty sand that overlies layers of sand, sand and gravel, gravel, and clay (Reclamation, 1978b) sourced from the Dolores River and its tributaries within the valley and East and West Paradox Creeks. Total thickness of the alluvial deposits ranges from 15.2 to 51.8 m, and the saturated thickness is greatest near the center of the valley along the Dolores River, where a collapse feature has been mapped in the underlying bedrock (Reclamation, 1978a; Paschke and others, 2024; fig. 2).

Evaporative salt deposits of the Paradox Formation form the core of the Paradox Valley anticline, underlie the alluvial aquifer, and are exposed along the floor of the Paradox Valley southeast of the Dolores River (Paschke and others, 2024). Salt in the Paradox Formation is predominantly halite (70–80 percent), with interbedded shale; anhydrite and other evaporite minerals; and dolomite (Geldon, 2003). The salt diapir at the center of the Paradox Valley anticline is as much as 3,700 m thick (King and others, 2014). A cap rock is present at the top of the exposed salt diapir that formed as circulating groundwater dissolved the more soluble minerals, potash (potassium chloride), and halite (sodium chloride), leaving behind a karstic residuum of less soluble minerals and rocks (Gutiérrez, 2004). The cap rock is largely devoid of sodium chloride and contains a high proportion of anhydrite, gypsum, dolomite, and clay (Reclamation, 1978b; Gutiérrez, 2004). The cap rock which is exposed on the floor of the Paradox Valley, has an estimated thickness ranging from about 120 to 150 m near the Dolores River to about 400 m at the southeastern end of the valley (Paschke and others, 2024). In the center of the Paradox Valley is an apparent collapse feature (fig. 2) where the cap rock has been brecciated (broken up) and is referred to as “collapse breccia” (Reclamation, 1978b). The collapse breccia, although similar to the cap rock in composition, is mixed with rock fragments and alluvial deposits indicating that subsidence of this feature was contemporaneous with deposition of Quaternary alluvial deposits (Gutiérrez, 2004). The collapse breccia is described in drilling logs from wells and test holes at the PVU as “brecciated gypsiferous crumbly shale” as much as 150 m thick and overlain by more than 30 m of alluvial deposits (Reclamation, 1978b). The collapse breccia is softer and more permeable compared to the unbrecciated cap rock and surrounding undeformed consolidated rocks (Reclamation, 1978b).

## Climate and Precipitation

Climate of the Paradox Valley is semiarid (Cater and Craig, 1970). Annual precipitation throughout the valley floor averaged 34.3 cm for the period from 1980 to 2017 and ranged from a minimum of 17.8 cm in 1989 to a maximum of 47.0 cm in 1983 (PRISM Climate Group, 2021; Paschke and others, 2024). The valley receives variable amounts of precipitation throughout the year, with maximum precipitation to the valley floor falling as rain during the summer months (Western Regional Climate Center, 2020; fig. 4). Precipitation increases with topography and is greatest in upland areas along the flanks of the La Sal Mountains, Utah, northwest of the valley (fig. 1). A mean annual precipitation of 76.8 cm was recorded at the La Sal Mountain Snow Telemetry (SNOTEL) network station at an altitude of 2,929 m from 1981 to 2020 (Natural Resources Conservation Service, 2020).

**Figure 4.** Monthly precipitation from January 1997 to May 2005 in the Paradox Valley, Colo. (Western Regional Climate Center, 2020).



## Evapotranspiration

Weir and others (1983) estimated annual potential evapotranspiration (ET) in the valley to vary with altitude from about 60 cm above 4,000 m to about 137 cm below 1,500 m, with an average of about 90 cm. The altitude of the Paradox Valley floor ranges from about 1,500 m near the Dolores River to about 1,700 m at the north-west end, indicating annual ET throughout most of the valley floor is between 90 and 137 cm. The freshwater pan-evaporation rate is a measurement of potential ET, which varies seasonally with temperature, humidity, solar incidence, and wind. The average monthly freshwater pan-evaporation rate measured on the valley floor from 1975 to 1977 (fig. 5) was zero during December through February, increasing to 30 cm during June (Reclamation, 1978b).

Based on the predominant soil type (sandy loam) and vegetative cover (pasture) in the Paradox Valley, the ET from the water table, known as groundwater ET, likely ceases at about 2–3 m below land surface (Shah and others, 2007). This depth of the water table below land surface at which groundwater ET approaches zero is termed the “ET extinction depth,” and is a model parameter in MODFLOW-6 (Banta, 2000; Langevin and others, 2017). Near the river, root transpiration may be limited to shallower soil depths because of salty groundwater near the land surface that may limit vegetation root depths.

## Groundwater Recharge

Precipitation recharge is the fraction of precipitation that reaches the water table to recharge the saturated groundwater system. Precipitation recharge is spatially and temporally variable and dependent upon the duration and intensity of precipitation; land cover and vegetation; soil type; surface slope; depth to the water table; temperature; humidity; ET; and other factors. Estimates of recharge by model-independent methods applied to a similar arid desert area in the Western United States range from 6 to 10 percent of the recorded precipitation (Hood and Waddell, 1968); although other studies indicate lower rates of precipitation recharge in semiarid climates where ET exceeds precipitation. For example, Paschke (2011)

estimated recharge as 1–2 percent of precipitation for the Denver Basin aquifer system in semiarid eastern Colorado. Given an average annual precipitation of 27.2 cm for the period 1997–2005 in the Paradox Valley (Western Regional Climate Center, 2020), a 6–10-percent recharge rate would yield 1.6–2.7 cm of annual precipitation recharge.

Irrigation is another potential source of recharge to the groundwater system. Application rates of irrigation water and consumptive use by crops in the Paradox Valley are not well documented, so the magnitude of recharge from irrigation-return flow was estimated based on crop types and corresponding areas of irrigation. A 2005 map of areas and types of irrigated crops northwest of the Dolores River (Colorado Water Conservation Board and Colorado Division of Water Resources, 2005) was used to estimate the magnitude of irrigation return flows (recharge) to the water table beneath about 1,100 hectares of irrigated cropland in the Paradox Valley. Areas of irrigated alfalfa were assumed to have an average recharge rate from return flows of about 12.5 centimeters per year (cm/yr), corn of about 6.5 cm/yr, and grass pasture and small grains of about 4.0 cm/yr each (table 1). Based on the crop-type fractions and crop-type specific recharge rates in table 1, the annualized recharge rate is about 1,808 cubic meters per day ( $m^3/d$ ). Because the irrigation season generally is 6 months or less, the recharge rate from irrigation-return flows is estimated at about 4,600  $m^3/d$  during the irrigation season. Actual recharge rates may differ because of annual variations in planted crop types, irrigated areas, and efficiencies and may range from 50 to 200 percent of this estimate.

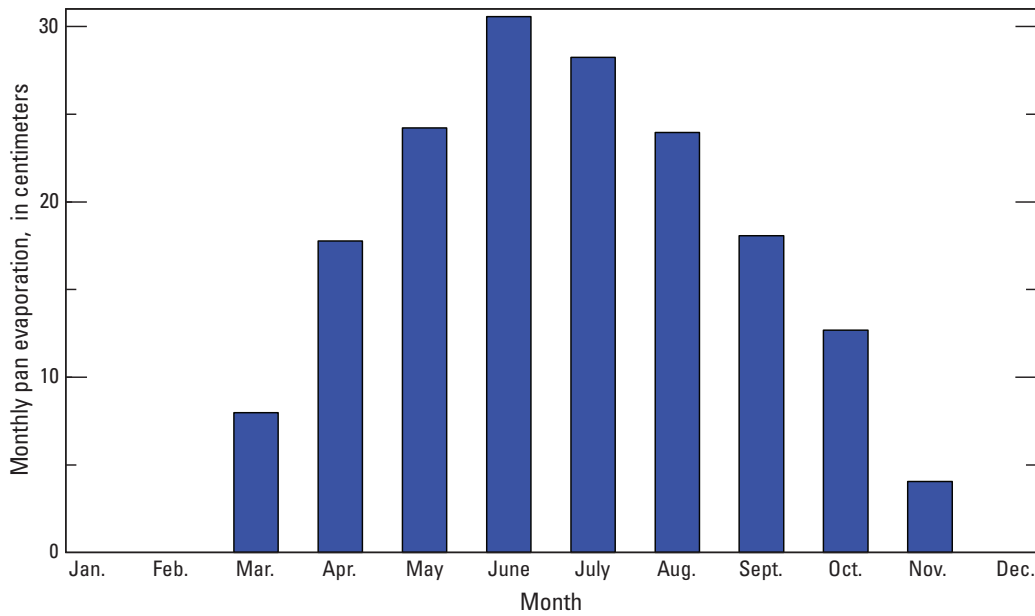


**Figure 5.** Average monthly freshwater pan evaporation in the Paradox Valley, Colo. (Reclamation, 1978b), 1975–1977.

### Dolores River

The Dolores River and West Paradox Creek are the only perennial streams in the Paradox Valley (fig. 1). East Paradox Creek, which drains the southeastern part of the valley, is ephemeral. The Dolores River originates as snowmelt runoff from the San Juan Mountains southeast of the valley and joins the Colorado River near the Colorado-Utah state line draining an area upstream from the Paradox Valley of about 5,242 square kilometers (km<sup>2</sup>). Streamflow in the Dolores River upstream from the Paradox Valley has been regulated by releases from McPhee Reservoir (about 177 km upstream) since July 1984, when the McPhee Dam was completed (Voggeser, 2001).

The average monthly streamflow in the Dolores River was calculated from daily values of streamflow where the Dolores River enters the Paradox Valley (Dolores River at Bedrock USGS streamgauge 09169500), referred to herein as the “upstream streamgauge” (U.S. Geological Survey, 2024a) and where the river exits the valley (Dolores River near Bedrock USGS streamgauge 09171100), referred to herein as the “downstream streamgauge” (U.S. Geological Survey, 2024b; figs. 1, 2). The average monthly streamflow observed at the

upstream streamgauge for the period October 1, 1987, through November 30, 2020, was 545,792 m<sup>3</sup>/d and ranged from 4,404 to 7,934,231 m<sup>3</sup>/d (U.S. Geological Survey, 2024a; fig. 6). The average monthly streamflow at the downstream streamgauge for this period was 561,667 m<sup>3</sup>/d and ranged from 4,233 to 7,875,514 m<sup>3</sup>/d (U.S. Geological Survey, 2024b). Streamflow at the downstream streamgauge was generally greater than at the upstream streamgauge from 1980 to 2020, with an increase from 7,340 to 9,786 m<sup>3</sup>/d between the two streamgages. This difference is mostly attributable to inflow from groundwater seepage, with minor contributions from West Paradox Creek and overland precipitation runoff.

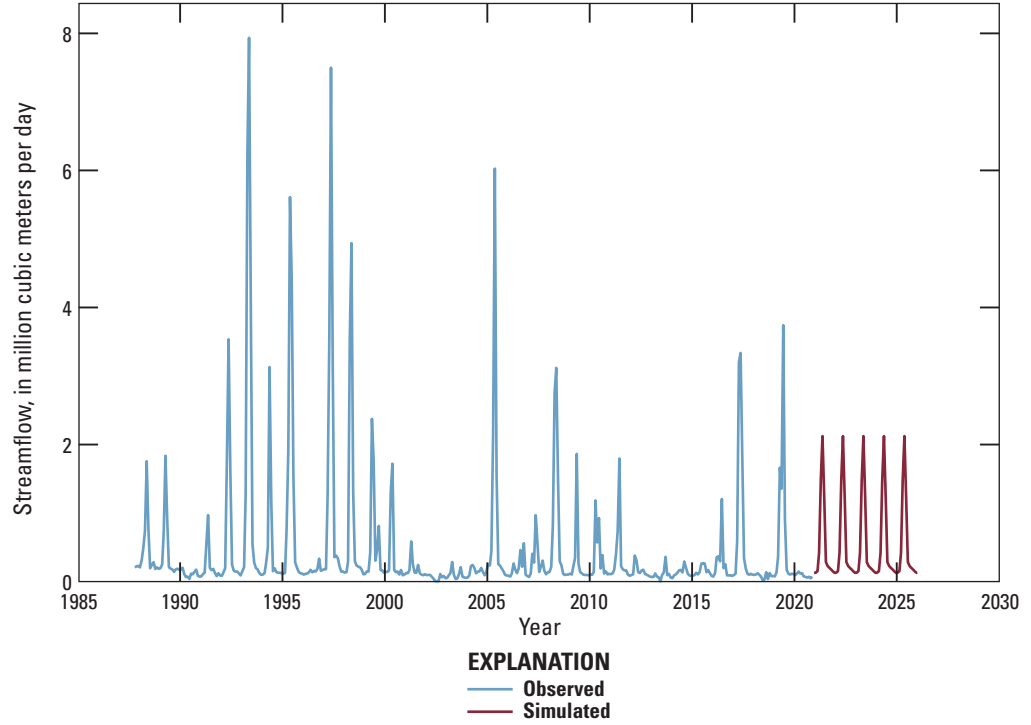
In general, streamflow in the Dolores River has declined during the period of record reflecting upstream reservoir operations and more frequent periods of drought during the past two decades. For example, the average streamflow of 330,288 m<sup>3</sup>/d for the period 2000 to 2017 is about one third of the average annual streamflow of 890,554 m<sup>3</sup>/d for the wetter period from 1985 to 1999 (Paschke and others, 2024). On a seasonal scale, Dolores River streamflow generally exhibits an annual cycle of peak runoff during the spring snowmelt season from late March through June followed by a low-flow

**Table 1.** Irrigated area estimated rate of irrigation-return flow and annualized recharge rate by crop type in the Paradox Valley, Colo.

[Percentage of irrigated area and irrigation return flow from Colorado Water Conservation Board and Colorado Division of Water Resources (2005)]

| Category  | Grass pasture | Small grains | Corn grain | Alfalfa |
|---|---------------|--------------|------------|---------|
| Percentage of irrigated area                      | 33            | 35           | 12         | 20      |
| Irrigated area, in hectares                       | 363           | 385          | 132        | 220     |
| Irrigation return flow, in centimeters per year   | 4             | 4            | 6.5        | 12.5    |
| Annualized recharge rate, in cubic meters per day | 398           | 422          | 235        | 753     |

**Figure 6.** Average monthly observed and simulated streamflow for the upstream streamgauge Dolores River at Bedrock, (U.S. Geological Survey streamgauge 09169500) in the Paradox Valley, Colo., 1987–2025. Observed data from U.S. Geological Survey (2024a) and simulated values from Heywood and others (2024).



(base flow) period during the winter months from November through February (Mast, 2017). Localized rain storms can generate peak flows during the summer months.

The effect of the PVU on the TDS mass flux to the Dolores River is based on analysis of continuous measurements of SC and streamflow from the upstream streamgauge (USGS streamgauge 09169500) and the downstream station (USGS streamgauge 09171100) to estimate daily TDS concentrations at each streamgauge using a regression model (Mast, 2017; U.S. Geological Survey, 2024a; 2024b). Estimated daily TDS concentrations are reported through 2015 in Mast (2017), and for this report, they were extended through 2020 using the same methods; the results are provided in Heywood and others (2024). Calculation of the estimated monthly TDS concentration was weighted by the daily streamflow shown in equation 1:

$$C_{\text{mon}} = \frac{\sum_{i=1}^n C_i Q_i}{\sum_{i=1}^n Q_i} \quad (1)$$

where

- $C_{\text{mon}}$  is the monthly concentration of TDS,
- $i$  is the day of the month,
- $n$  is the number of days in the month,
- $Q_i$  is the average streamflow on day  $i$ , and
- $C_i$  is the TDS concentration on day  $i$ .

The flow-weighted monthly TDS concentration from December 1987 to November 2020 at the upstream streamgauge (USGS streamgauge 09169500) was 457 milligrams per liters (mg/L) and ranged from 164 to 922 mg/L (fig. 7). The average monthly TDS concentration during this period at the downstream streamgauge (USGS streamgauge 09171100) was 1,541 mg/L and ranged from 160 to 9,061 mg/L (fig. 7). The TDS concentration in the Dolores River is greater at the downstream streamgauge than at the upstream streamgauge because of brine discharge from the aquifer system into the river between the two streamgages. The increase in TDS mass flux to the river between the two streamgages is termed the “net load” and is served to the National Water Information System (NWIS) database for the downstream streamgauge Dolores River near Bedrock (USGS streamgauge 09171100) (U.S. Geological Survey, 2024b). Prior to PVU test operations that began in 1991, the average annual TDS mass flux to the river across the Paradox Valley was estimated at about 137,900 tons per year (Mast, 2017). During the post-PVU period, from 1996 to 2015, the TDS mass flux to the river was about 43,300 tons per year, which represents a TDS mass flux reduction of about 70 percent compared to pre-PVU conditions (Mast, 2017). The TDS mass flux to the Dolores River varies with time, in part, because of the effect river stage has on the hydraulic-head gradient of the groundwater beneath the river (Mast, 2017) and in part because of the effects from PVU pumping wells. All streamflow and SC data for USGS streamgages 09169500 and 09171100 used in these calculations are available in the USGS NWIS database (U.S. Geological Survey, 2024a; 2024b).

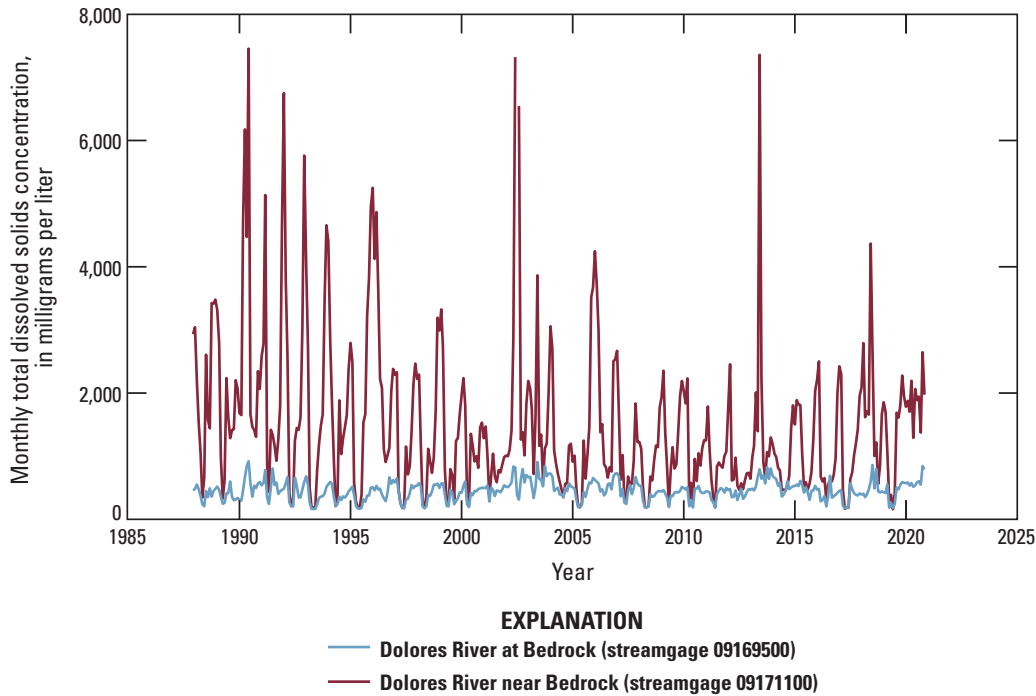


**Figure 7.** Average monthly total dissolved solids concentrations estimated from specific conductance for the upstream streamgage Dolores River at Bedrock (U.S. Geological Survey streamgage 09169500) and downstream streamgage Dolores River near Bedrock (U.S. Geological Survey streamgage 09171100) in the Paradox Valley, Colo., 1987–2020. Estimated concentrations from Mast (2017) and Heywood and others (2024).

## West Paradox Creek

West Paradox Creek originates in the upland areas flanking the La Sal Mountains northwest of the Paradox Valley (fig. 1). The creek flows through the Paradox Valley from the northwest toward the Dolores River, where it infiltrates the shallow alluvium recharging wetlands and the alluvial aquifer along its course (Paschke and others, 2024; fig. 2). Streamflow in West Paradox Creek has been regulated since 1988 by releases from Buckeye Reservoir to supply irrigation diversions in the Paradox Valley. From 1988 to July 2020, monthly reservoir releases ranged from 0 to 77,800 m<sup>3</sup>/d and typically occurred during the irrigation season from April to October (Colorado Water Conservation Board and Colorado Division of Water Resources, 2021).

Streamflow in West Paradox Creek was previously measured at three USGS streamgages (fig. 2). Average monthly streamflow in West Paradox Creek ranged from 475 to 145,000 m<sup>3</sup>/d and averaged 21,000 m<sup>3</sup>/d, as was measured at USGS streamgage 09170500 at the northwest end of the valley (fig. 2) from October 1944 through August 1952. Average monthly streamflow measured at USGS streamgage 09171000 during this period, which is about 13-km downstream from 09170500 (fig. 2), ranged from 7 to 80,000 m<sup>3</sup>/d and averaged 10,900 m<sup>3</sup>/d. Streamflow magnitudes at these two streamgages were not in phase during this period, possibly because of irrigation diversions between the two streamgages. The average monthly streamflow at a third streamgage on West Paradox Creek (USGS streamgage 09170800; fig. 2) ranged from 7,200 to 93,000 m<sup>3</sup>/d and averaged 22,000 m<sup>3</sup>/d from August 1971 through September 1973 (U.S. Geological Survey, 2022).

## Occurrence and Movement of Brine

Cap rock, collapse features, breccia, and salt-saturated groundwater or “brine” developed at the top of the exposed Paradox Formation salt diapir during valley formation since the Miocene (Hite and Lohman, 1973; Gutiérrez, 2004). The brine is a sodium-chloride type water (Paschke and others, 2024) with groundwater TDS concentrations approaching the saturated concentration of sodium chloride in water of about 354,000 mg/L. In observation wells near the Dolores River, sampled by Reclamation from June through October 1977, TDS concentrations ranged from 255,000 to 285,000 mg/L (Reclamation, 1978b). Groundwater pumped from the PVU pumping wells had an average TDS concentration around 257,000 mg/L during the period of operation, which is more than 7 times greater than typical seawater (Hem, 1985). The brine is dense because of its salt content and is estimated as at least 10,000 years old, much older than fresh groundwater in the overlying alluvial aquifer (Gardner and Newman, 2023; Paschke and others, 2024). The density difference between the brine and the overlying freshwater aquifer drives density-dependent gradients and flow of brine from the cap rock into the base of the alluvial aquifer and to the Dolores River (Paschke and others, 2024).

Brine from the collapse breccia and underlying salt is considered the primary source of TDS to the alluvial aquifer, PVU pumping wells, and Dolores River. Paschke and others (2024) summarize previous studies that describe the depth and distribution of brine beneath the Paradox Valley to the extent of limited available data. The Paradox Formation and associated brine is likely widespread at depth beneath the valley

(Reclamation, 1978b). Previous geophysical studies (Ball and others, 2015; 2020; Mast and Terry, 2019) provide spatial data on the three-dimensional extent of the brine, although there are limited groundwater-level and TDS monitoring data away from the PVU to define the full spatial extent and depth of the brine. Brine discharge from the collapse breccia and alluvial aquifer to the Dolores River occurs in two primary reaches and is not uniform throughout the valley reach (Reclamation, 1978b), which contributes to spatial variations in the SC (and TDS) of the river (fig. 8). The spatial variation in brine discharge could be caused by structural features, variations in the depth to the top of bedrock, and the freshwater-brine interface as well as variations in aquifer properties and PVU pumping. Aquifer properties for hydraulic conductivity are represented in the model by parameters for aquifer horizontal and vertical hydraulic conductivity and streambed conductance. Because the PVU pumping wells affect the capture of brine in the vicinity of the PVU, they likely also affect the locations of brine discharge to the river.

A large collapse breccia feature near the center of the valley as well as seasonal hydrologic conditions also affect hydraulic gradients and thus discharge of brine to the river (Mast and Terry, 2019; Paschke and others, 2024). For example, horizontal water-table gradients from the northwest part of the valley flatten near the center of the valley where saturated thickness and transmissivity of the collapse breccia feature are greatest (Paschke and others, 2024). Horizontal and vertical gradients for the water table and freshwater-brine interface control brine discharge to the river and are affected by river stage (Mast, 2017; Mast and Terry, 2019). During spring snowmelt runoff, when river stage is highest, the freshwater-brine interface is depressed beneath the riverbed, and brine discharge to the river is minimized (Mast and Terry, 2019). Brine discharge to the river is greatest during the winter low-flow months when river stage is lowest, and the freshwater-brine interface rises to near the land surface (Mast and Terry, 2019), with as much as 70 percent of the annual salinity gain across the valley occurring from December through March (Mast, 2017).

## Aquifer Hydraulic Properties

Aquifer properties of hydraulic conductivity and storage are reported from constant-rate pumping tests and specific-capacity tests conducted by Reclamation (Reclamation, 1978b; Paschke and Mast, 2024) and a large-scale aquifer test at the PVU conducted by the USGS (Newman, 2021; Paschke and others, 2024).

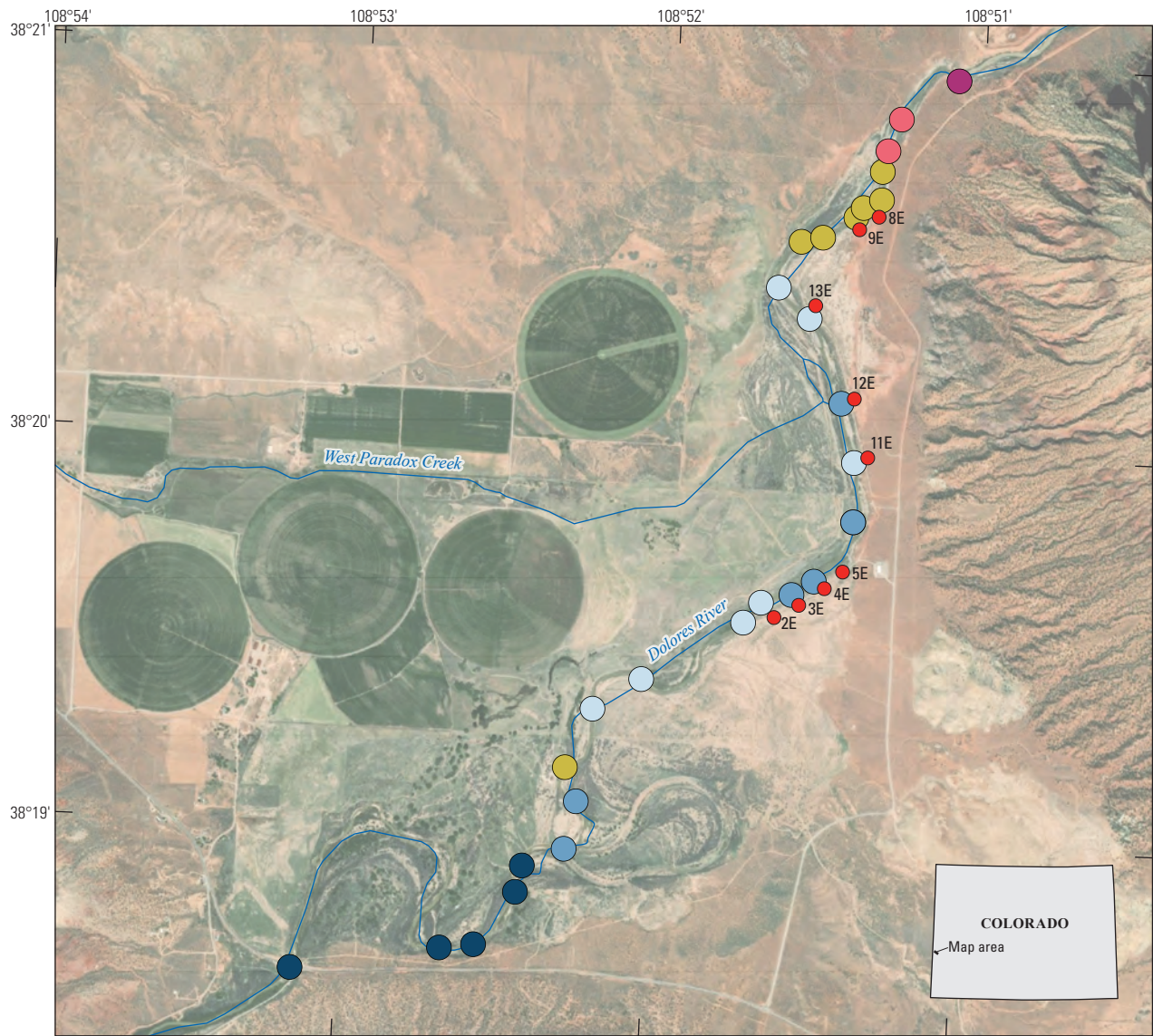
Aquifer transmissivity (T) of the alluvial aquifer near the PVU ranged from 0.26 to 0.96 square meter (m<sup>2</sup>) per minute based on analyses of a 48-hour constant-rate pumping test with four observation wells, indicating aquifer heterogeneity (Reclamation, 1978b). The saturated thickness of 28.1 m for the alluvial aquifer at the pumping well (Reclamation, 1978b)

was used as saturated thickness (b) to convert the transmissivity (T) values to horizontal hydraulic conductivity (K<sub>x</sub>) values according to the relation  $K_x = T/b$  (Fetter, 1994) that range from 13 to 49 meters per day (m/d), with a geometric mean of 20 m/d. Results from analysis of specific-capacity tests conducted from 1973 to 1984 (Paschke and Mast, 2024) indicate slightly lesser K<sub>x</sub> values for the alluvial aquifer than the pumping test ranging from 0.2 to 19 m/d, with a geometric mean of 4 ft/d. Storativity (S) values reported for the alluvial aquifer (Reclamation, 1978b) were converted to specific storage (S<sub>s</sub>) estimates by dividing by the saturated thickness (b; Fetter, 1994) and range from  $1.1 \times 10^{-5}$  per meter (m<sup>-1</sup>) to  $1.9 \times 10^{-4}$  m<sup>-1</sup>, with a median of  $9.1 \times 10^{-5}$  m<sup>-1</sup>. Based on an analysis of pumping tests completed in 2013 in the Paradox Valley, Newman (2021) reported K<sub>x</sub> values for the alluvial aquifer range from 0.08 to 53 m/d. Analyses of 2013 slug testing on a single alluvial aquifer well yielded K<sub>x</sub> values ranging from 1.4 to 40 m/d, with a median of 5.8 m/d (Newman, 2021; Paschke and others, 2024).

For the collapse breccia, aquifer T and S were estimated from two constant-flow pumping tests with as many as six observation wells (Reclamation, 1978b). Transmissivity of the collapse breccia ranged from 0.103 to 0.896 m<sup>2</sup> per minute (Reclamation, 1978b). Although the collapse breccia was reportedly 55.5 m thick at the pumping well (Reclamation, 1978b), pumping through the 15.5-m well screen may not have uniformly stressed the depth intervals of this aquifer. Nevertheless, the 55.5-m value for the thickness of the collapse breccia was used to convert the transmissivity values to estimates of K<sub>x</sub> that ranged from 2.7 to 23 m/d, with a geometric mean of 7.3 m/d and a median of 7.6 m/d. The collapse breccia K<sub>x</sub> values are similar in magnitude to those for the alluvial aquifer and are several orders of magnitude greater than K<sub>x</sub> values reported for the unbrecciated cap rock, which ranged from  $9.3 \times 10^{-5}$  to 0.21 m/d, with a geometric mean of  $1.1 \times 10^{-2}$  ft/d (Wollitz and others, 1982). Specific storage (S<sub>s</sub>) estimates for the collapse breccia ranged from  $8.25 \times 10^{-6}$  m<sup>-1</sup> to  $1.5 \times 10^{-4}$  m<sup>-1</sup>, with a median of  $1.73 \times 10^{-5}$  m<sup>-1</sup> (Reclamation, 1978b).

## Model Development and Parameterization

There are multiple approaches to simulating variable-density groundwater-flow systems that feature a freshwater-brine interface like that observed in the alluvial aquifer of the Paradox Valley. These approaches are exemplified in several models, including sharp-interface models, such as SHARP (Essaid, 1990) and SWI (Bakker and others, 2013) and models that integrate groundwater flow and solute transport such as SEAWAT (Langevin and others, 2017), SUTRA (Provost and Voss, 2019), and MODFLOW-6 (Langevin and others, 2017, 2020, 2021). Although a sharp-interface model can simulate



Base modified from U.S. Geological Survey 1:24,000-scale digital data  
 Imagery from Esri World Imagery  
 Universal Transverse Mercator, zone 13  
 North American Datum of 1983

0 0.25 0.5 0.75 1 MILE  
 0 0.25 0.5 0.75 1 KILOMETER

**EXPLANATION**

- 2E Paradox Valley Unit pumping well and identifier
- Specific conductance of the Dolores River, in microsiemens per centimeter, June 2013**
- Less than 10,000
- 10,000 to 19,999
- 20,000 to 29,999
- 30,000 to 39,999
- 40,000 to 49,999
- 50,000 to 60,000

**Figure 8.** Specific conductance in the Dolores River as it flows across the Paradox Valley, Colo., and locations of Paradox Valley Unit pumping wells. The specific conductance data are from a survey completed by the Bureau of Reclamation on June 24–25, 2013 (Mast, 2017).

transient changes in the position of the freshwater–brine interface, the integrated groundwater-flow and solute-transport model was preferred for this study to quantify the mass transport of brine among components of the coupled groundwater and surface-water system. Numerical dispersion presents a limitation inherent with numerical transport models, which can degrade the accuracy of simulated concentrations, particularly near steep gradients across a simulated interface (Langevin and others, 2020). This dispersion effectively “smooths” simulated concentrations across a freshwater-brine interface, thereby increasing the width of the simulated transition zone between freshwater and brine and may, therefore, preclude accurate numerical representation of a sharp freshwater-brine interface, unless very refined and computationally expensive discretization is used.

Having considered these benefits and limitations, the computer program MODFLOW-6 (Langevin and others, 2017, 2020, 2021) was selected because it can simulate groundwater flow and solute transport, as well as the effects of variable solute concentrations on groundwater density and flow. Other important capabilities of MODFLOW-6 for the Paradox Valley modeling include its capacity to integrate streamflow routing with mass solute transport and simulate the volumetric flow and solute mass transport between the groundwater system and the river. The inability of the program to simulate a sharp freshwater-brine interface was a limitation of using MODFLOW-6 (Langevin and others, 2020).

The sodium-chloride brine in the Paradox Valley was simulated as a chemically conservative solute for which concentrations are not affected by chemical reactions or decay. Although heterogeneous aquifer properties likely cause dispersive mixing, the vertical transition zone between freshwater and brine beneath the Dolores River in the Paradox Valley is thought to be relatively thin (Ball and others, 2020; Paschke and others, 2024). Although the second order total variation diminishing (TVD) scheme used by this effort for solving the advective-dispersion equation produced less numerical dispersion than alternative schemes available in the Groundwater Transport (GWT) Model of MODFLOW-6, numerical dispersion nevertheless smoothed concentrations above and below the simulated freshwater-brine interface. Because this numerical dispersion over-represented the hydrodynamic dispersion across the freshwater-brine interface, additional aquifer dispersivity was not specified in the model. The effect of brine concentration on groundwater density and flow was simulated by using the Buoyancy Package of MODFLOW-6 (Langevin and others, 2020), which uses a variable-density form of Darcy’s Law. The buoyancy correction for the variable-density flow was calculated as a linear function of the solute concentration (eq. 2):

$$\rho = \rho_f + \frac{\partial \rho}{\partial C} C \quad (2)$$

where

$C$  is solute concentration (mass per cubic length),

$\rho$  is fluid density (mass per cubic length),

$\rho_f$  is the density of freshwater =1,000 kilograms per cubic meter ( $\text{kg}/\text{m}^3$ ), and

$\partial \rho / \partial C = 0.597257$  is the slope of the linear equation of state that relates fluid density to solute concentration.

Variable-density effects on wellbore flow and aquifer-stream interaction also were simulated with the Multi-Aquifer Well Transport (MAW) and Streamflow Transport (SFT) Packages of MODFLOW-6, respectively (Langevin and others, 2021).

## Modeling Strategy

Because of the numerical coupling among simulated groundwater flow, TDS concentrations, and density in a variable-density model, a quasi-steady-state simulation is needed to set up initial conditions for transient simulations. The spatial distribution of TDS, and hence density, affects path lines of groundwater flow and is, in turn, affected by the distribution and variability of hydraulic stresses (such as, recharge, groundwater ET, river stage, and well pumping) on the groundwater system. If hydraulic stresses remain relatively constant through time, this coupling of TDS concentration distribution and groundwater flow eventually equilibrates, resulting in a stable or “steady-state” concentration distribution. Subsequent transient changes to simulated hydraulic stresses cause changing simulated conditions for groundwater flow and solute transport such that simulated TDS concentrations and brine discharge to the Dolores River in the transient model are sensitive to the specified initial TDS concentration distribution. Specification of an initial TDS concentration distribution reasonably consistent with the groundwater-flow field is thus necessary to accurately simulate groundwater flow and avoid temporal concentration trends unrelated to the transient hydraulic stresses of interest.

To account for this coupling between computed groundwater flow and TDS concentrations, modifications of boundary conditions and other model parameter values during model



calibration required iteratively running 1,000-year (quasi-steady state) and 33-year transient simulations for the model calibration period 1987–2020. For each parameter-value iteration, TDS concentration and head distributions at the end of the 1,000-year “equilibration simulation” were specified as initial conditions for the subsequent 33-year simulation, in which stream flow, recharge, and pumping stresses varied. Although the TVD solver algorithm has less numerical dispersion and was used for the 33-year simulations, the substantially longer model runtime required by TVD was not tractable for the 1,000-year simulation, which instead used the upstream weighting scheme as a numerical solution (Langevin and others, 2021).

## Spatial Discretization

To discretize data corresponding to the geographic area being modeled (model domain), a mathematical grid was created that encompassed the Paradox Valley floor northwest of the Dolores River, uplands bordering the valley, and part of the valley southeast of the Dolores River (fig. 2). To align the grid with topography and principal directions of groundwater flow in the Paradox Valley, the grid is oriented 35 degrees (clockwise) about the northwest corner with respect to true north. The finite-difference model grid consists of 7 vertical layers of cells, with each containing 76 rows that are 100 m long and 48 columns that range from 100 to 600 m wide. The top layer of the model domain corresponds to the land-surface altitude at the center of each cell (node), as derived from a digital elevation model of the Paradox Valley (U.S. Geological Survey, 2023). This top layer generally represents the alluvial aquifer; to maintain a relatively consistent layer thickness along the Dolores River, the bottom altitude of the top layer slopes down to the northeast at a gradient of 1 meter per kilometer ( $-0.0001$ ). The bottom altitude of the top layer between columns 1 and 13 also slopes down to the southeast at an average gradient of  $-0.0167$  so that the top layer thickness approximates the alluvial aquifer thickness where that aquifer exists. The underlying layers 2–7 represent either bedrock units or the alluvial aquifer and progressively increase to a thickness of 20 m for layer 7, which has a flat bottom at an altitude of 1,463 m.

## Distribution of Hydrogeologic Units

Data in the model layers are zoned to represent the known and estimated spatial distribution of alluvium in the Paradox Valley, the underlying collapse breccia at the top of the exposed Paradox Formation, and surrounding Mesozoic consolidated rocks. The alluvium in the Paradox Valley generally is on the order of 10 m thick and as much as about 52 m thick in the central part of the valley beneath the Dolores River (Paschke and others, 2024). The surficial extent of alluvium in the Paradox Valley (fig. 2) is represented in the top (surface) layer of the model. Because the thickness of

the top layer exceeds the thickness of the valley alluvium in the northwest part of the model domain, underlying consolidated rocks are also represented in the top layer in decreasing proportion between column 1 (the northwest side of the model domain) and column 19. Model layers 2 through 7 represent consolidated rocks except where the alluvium is thickest near the river. In this area, the alluvium extends into deeper layers in a stepwise fashion down through layer 6. The Paradox Formation is simulated in model layer 7. The hydraulic properties assigned to these hydrogeologic units are summarized in the “Parameter Values and Sensitivities” section of this report.

## Time Discretization

The 1,000-year quasi-steady-state simulation was discretized with one steady-state stress period followed by one transient stress period containing 1,000 annual time-steps. The subsequent 33-year transient simulation encompassed the time from October 1, 1987, through November 30, 2020 (1987–2020), and represents time before and during PVU operations. In this report, October 1, 1987, through June 1996 is designated as the “pre-PVU” period, and July 1996 through November 2020 is designated as the “post-PVU” period. The year 1987 was discretized with one stress period, during which average annual groundwater recharge and average streamflow during 1987 were specified. The years 1988 through 2020 generally were discretized with monthly stress periods (28, 29, 30, or 31 days); however, to simulate times when hydraulic stresses were changing (mainly PVU pumping), some months after April 1999 were discretized with multiple shorter stress periods (between 2 and 23 days). The length of each stress period used in the model is documented in the data release associated with this publication (Heywood and others, 2024).

## Boundary Conditions

Establishing similarity of boundary conditions and water budgets between the 1,000- and 33-year simulations was necessary to avoid erroneous simulation of storage changes and water-level trends during the 33-year simulation. The average magnitudes of the specified-flow boundary conditions (representing recharge and groundwater underflow) that varied in time during the 33-year simulation were specified as constant values for the 1,000-year simulation to maintain similarity of flow budgets between the simulations. Similarity of the average magnitude of head-dependent fluxes (representing ET and stream leakage) during the 33-year and 1,000-year simulations was maintained by specification of a constant average of maximum ET rates and average stage of the Dolores River during the 1,000-year simulation. Although irrigation did not occur during most of the 1,000-year simulation, a similar flow for West Paradox Creek was specified because the streamflow now diverted for irrigation likely infiltrated into the alluvial aquifer before irrigated agriculture.

The northeast and southwest sides of the model domain are where Mesozoic rocks border the Paradox Valley near probable groundwater divides and are represented as no-flow boundaries. The southeast side of the model domain crosses the Paradox Valley where alluvium is thin and mostly unsaturated. Because there is relatively little recharge to the deeper low-permeability rocks in the southeast part of the model domain, groundwater flow in this area is considered negligible, and the southeast side of the model is represented as a no-flow boundary. Estimated inflows from the highlands flanking the La Sal Mountains to the northwest are specified into the top layer on the northwest side of the model.

The inflow of brine from the Paradox Formation is the conceptual source of TDS to the alluvial aquifer and the Dolores River, although groundwater flow through the Paradox Formation is considered negligible compared to flow within the more permeable alluvium (Konikow and Bedinger, 1978). Accordingly, no flow is simulated through the bottom of the model, except for the area where the collapse breccia is mapped. In this area, an influx of brine from beneath the model domain is specified into the bottom model layer (layer 7). This brine inflow is the primary simulated source of TDS to the model and was represented as a constant concentration, time-varying flux. Timing of this inflow was simulated as correlated to precipitation in the highland recharge area, where higher hydraulic potentials could induce groundwater flow through deeper regional flow paths.

## Groundwater Withdrawals

Groundwater withdrawals from nine PVU pumping wells adjacent to the Dolores River were simulated with the MAW package of MODFLOW-6 (Langevin and others, 2021). Although values for total withdrawals coinciding with MAW data boundaries were specified, these withdrawals are considered head-dependent boundaries because the flow among individual model cells and the MAW boundary depends upon the

head difference between the MAW boundary and model cell. Well-screen interval lengths of the PVU pumping wells range from 3.8 to 10.4 m and are represented with data in model layers 2 or 3 to allow simulation of intra-borehole flow. When pumping wells are idle, this intra-borehole flow can redistribute variable-density groundwater between model layers where hydraulic head differences exist between layers.

Reclamation provided records of the monthly withdrawal for nine PVU pumping wells, which totaled 7.95 million cubic meters ( $\text{m}^3$ ; 2.1 billion gallons) during the operational period from July 1996 through May 2020. To improve the efficiency of capturing brine that may have discharged to the river, pumping was greatest from PVU pumping wells near river reaches where SC measurements increase (fig. 8; table 2). The monthly withdrawals (starting July 1996) are available in Heywood and others (2024) for each well, in units of  $\text{m}^3/\text{d}$ . Withdrawals were suspended for 3 months after a magnitude 4.4 earthquake on January 24, 2013, and during occasional shorter maintenance periods (Reclamation, 2022). The average withdrawal rate from July 1996, to when operations were shut down after the magnitude 4.5 earthquake on March 4, 2019, was about  $962 \text{ m}^3/\text{d}$  (including a 3-month shutdown during 2013). Assuming the average concentration of the pumped brine from July 1996 to March 2019 was  $257,000 \text{ mg/L}$ , the estimated average rate of TDS mass extraction during that period was  $247,178 \text{ kg/d}$  or about  $99,518 \text{ tons per year}$  (tons/yr; fig. 9).

Records of monthly withdrawals for PVU pumping wells were not available during PVU operational testing from July 1991 through April 1995. During this period, Reclamation had records of the injection rate into the PVU injection well, and this was used to assign withdrawal rates to PVU pumping wells in the model during the testing phase. Injected water during this testing period was withdrawn primarily from four PVU pumping wells (2E, 3E, 4E, and 5E) and mixed with 30-percent fresh water. In the model, one-fourth of the total groundwater withdrawn (70 percent of the total injected water) was specified from each of the four PVU pumping wells for

**Table 2.** Dimensions of Paradox Valley Unit pumping wells in the Paradox Valley, Colo., and percent of time used during 1996–2020.

[Well dimensions from Reclamation (1978b). Use based on pumping schedule in Heywood and others (2024). m, meters]

| Well name | Screen top (m) | Screen bottom (m) | Screen length (m) | Well radius (m) | Use (percent) |
|-----------|----------------|-------------------|-------------------|-----------------|---------------|
| 2E        | 1,495.43       | 1,483.08          | 12.35             | 0.153           | 19            |
| 3E        | 1,494.12       | 1,486.50          | 7.62              | 0.107           | 12            |
| 4E        | 1,496.61       | 1,490.51          | 6.10              | 0.10            | 20            |
| 5E        | 1,494.51       | 1,485.06          | 9.45              | 0.107           | 11            |
| 8E        | 1,495.37       | 1,490.80          | 4.57              | 0.153           | 14            |
| 9E        | 1,494.63       | 1,490.82          | 3.81              | 0.153           | 14            |
| 11E       | 1,496.15       | 1,487.92          | 8.23              | 0.107           | 2.6           |
| 12E       | 1,495.70       | 1,486.55          | 9.15              | 0.10            | 0.5           |
| 13E       | 1,494.97       | 1,484.61          | 10.36             | 0.10            | 7.2           |

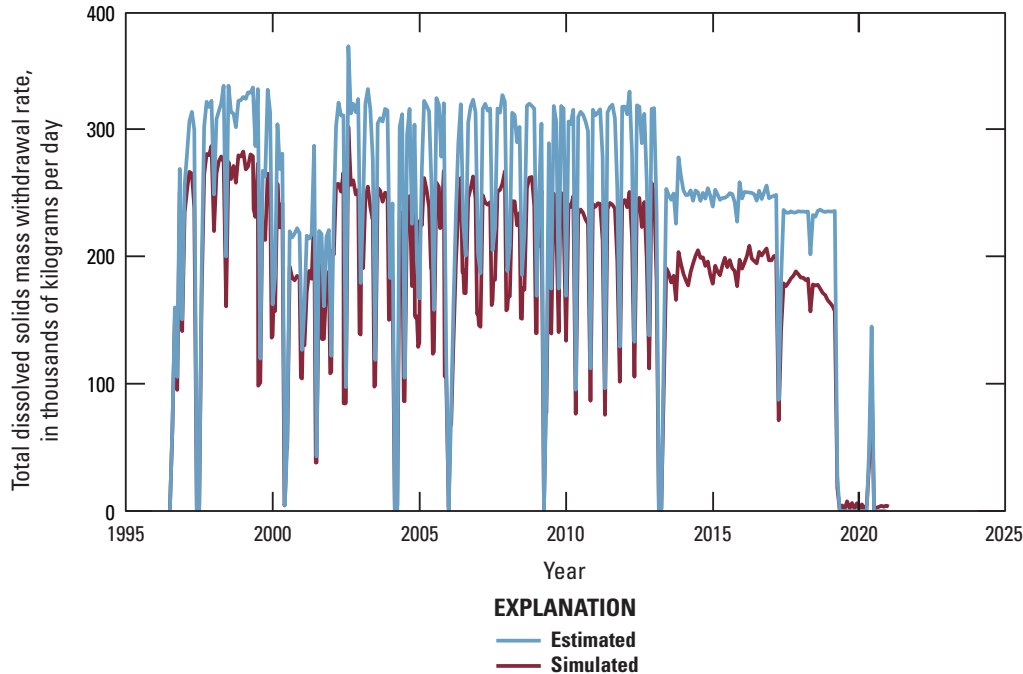


**Figure 9.** Estimated and simulated monthly total dissolved solids mass removed by Paradox Valley Unit pumping wells in the Paradox Valley, Colo., 1996–2020. Estimated and simulated data from Heywood and others (2024).

this testing period. Groundwater withdrawn during the test period totaled 431,537 m<sup>3</sup>, but pumping was episodic, with most occurring during 1993–94.

## Specified-Flow Boundaries

Specified-flow boundaries were used to simulate recharge from precipitation, irrigation-return flow, and water coming from the highlands northwest of the model domain that contributes to groundwater underflow. Irrigation-return flows are part of the specified water diverted from West Paradox Creek, which is simulated as a head-dependent boundary and described in the “Stream Leakage” section of this report.

## Recharge

Model-input for recharge to the water table was specified to simulate infiltration of areal precipitation and irrigation water diverted from West Paradox Creek. Infiltration of precipitation recharge was specified to all cells in the top model layer. Average monthly precipitation data (1980–2020) for the Paradox Valley floor and adjacent highland recharge area were obtained from the PRISM climate data website (PRISM Climate Group, 2021). For the 1,000-year simulation, 1.86 cm/yr was specified as the long-term average recharge rate from infiltrated precipitation. During the subsequent 33-year simulation, this component of recharge was specified as 6 percent of the monthly precipitation (fig. 10) spatially distributed throughout the Paradox Valley floor, based on gridded climate data obtained from the PRISM Climate Group (2021).

During the simulated 6-month irrigation season from April to September, an inflow of 4,616 m<sup>3</sup>/d was specified to represent irrigation-return flows from water diverted from West Paradox Creek, which were distributed to mapped irrigation areas in the model (fig. 2) at rates (table 1) corresponding to crop types planted in 2005 (Colorado Water Conservation Board and Colorado Division of Water Resources, 2005). Simulation of the remaining flow and recharge from West Paradox Creek is described in the “Stream Leakage” section of this report.

## Groundwater Underflow

Shallow and deep groundwater underflows were simulated to represent additional groundwater inputs to the Paradox Valley. Drainage from the La Sal Mountains provides surface runoff to West Paradox Creek and potentially groundwater underflow from the northwest to the groundwater system in the Paradox Valley. Shallow groundwater underflow from the La Sal Mountains into the northwest side of the model domain was simulated as 1,700 m<sup>3</sup>/d distributed amongst 5 top-layer cells near West Paradox Creek in column 1. Deep groundwater underflow was simulated into the base of the model domain to represent brine inflow from the Paradox Formation. Although the detailed hydrogeologic structure beneath the valley alluvium and surrounding the Paradox Valley is uncertain, such underflow may be driven by the difference in hydraulic potential between highland recharge areas and brine discharge near the Dolores River, and TDS flux to the Dolores River described by Mast (2017) can be interpreted to relate to prior-year precipitation. For deep underflow in the 1,000-year

simulation, a constant value of 1,320 m<sup>3</sup>/d was specified into model layer 7 (the model base) near the Dolores River to simulate groundwater and brine inflow into the model domain. To evaluate the potential pressure-diffusion time lag between the recharge area and the deepest model layer, input for this underflow was varied through time by scaling the flow to the precipitation amount in the highlands recharge area for the preceding 8-month period (PRISM Climate Group, 2021; fig. 10) for the 33-year simulation. Representation of the brine inflow is explored as a source of model uncertainty in the “Breccia as a Source of Brine” section of this report.

## Hydraulic Head-Dependent Flow Boundaries

This section presents head-dependent boundary conditions for ET and stream leakage used in the groundwater model. Evapotranspiration and stream leakage were simulated using different packages available in MODFLOW-6. The inputs for ET were based on pan-evaporation measurements, and stream leakage was based on streamflow measurements and channel geometry of the Dolores River and West Paradox Creek.

### Evapotranspiration

The MODFLOW-6 Evapotranspiration (EVT) package, which was used in the model, simulates ET rate as a linear function that decreases with the distance of the water table below land surface (Banta, 2000; Langevin and others, 2021). Evapotranspiration rate varies from the specified maximum rate where the water table is at land surface to zero at the “ET extinction depth” of 1 m below land surface. For the

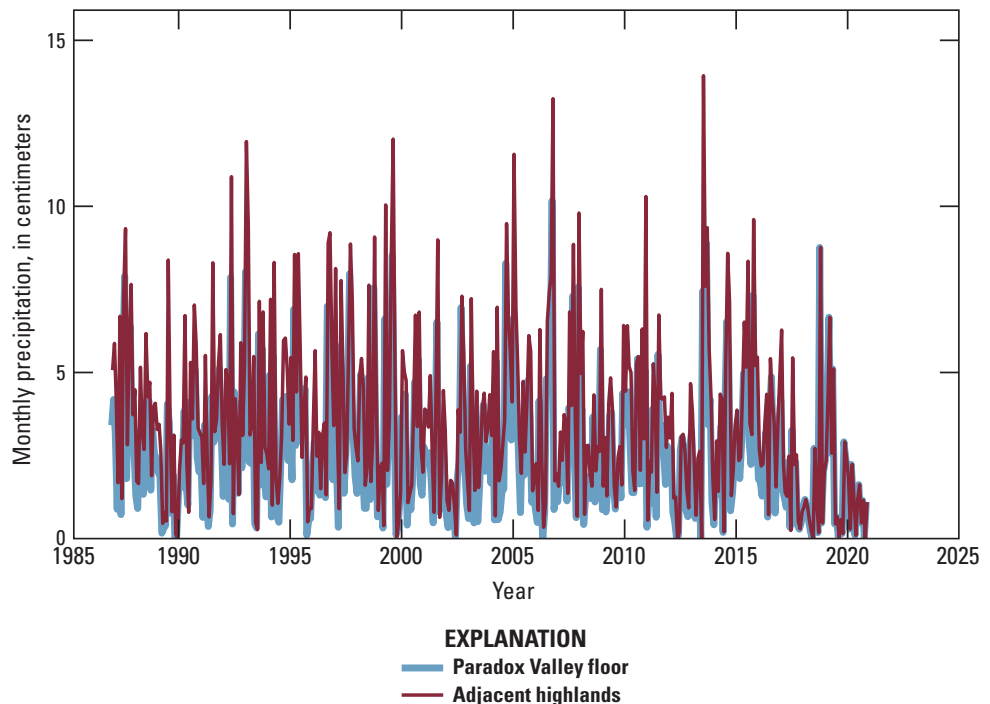
1,000-year simulation, the input for the maximum annual ET rate was set to 1.37 m based on the estimate of Weir and others (1983). To input the maximum rate for each month to the 33-year simulation, the monthly pan-evaporation rates observed in the Paradox Valley (fig. 5) were used to scale the average-annual rate. No ET was simulated for three winter months, and the maximum rate was simulated during June.

### Stream Leakage

Groundwater flow between the Dolores River and the shallow alluvial aquifer was simulated as a hydraulic head-dependent flux with the Streamflow routing (SFR) package of MODFLOW-6 (Langevin and others, 2021). Because the position of the hydraulic head of the river affects flows between the surface-water and groundwater system, and the river stage is calculated with respect to the streambed altitude, an accurate measurement of the streambed altitude was needed. To obtain accurate altitudes for the two streamgages on the Dolores River, a real-time-kinematic (RTK) Global Positioning System (GPS) survey (accuracy within about 5 cm) of reference markers at each streamgage was done on September 12, 2017. The results yielded streamgage altitudes of 1,506.57 m (above the North American Vertical Datum of 1988) for the upstream streamgage (USGS streamgage 09169500; U.S. Geological Survey, 2024a) and 1,497.05 m for the downstream streamgage (USGS streamgage 09171100; U.S. Geological Survey, 2024b).

The SFR package was applied along the section of the Dolores River intersecting the grid (fig. 2), and a stream reach was defined for each connected groundwater model cell. The streambed conductance between each reach of the

**Figure 10.** Monthly precipitation for 1987–2020 throughout the Paradox Valley floor and adjacent highlands. Data from PRISM Climate Group (2021).



Dolores River and connected groundwater model cells was proportional to the length of the Dolores River transecting each cell. The Manning Equation is used in the SFR package to calculate the river stage from the specified channel width, streambed slope and roughness, and simulated flow within each reach. Based on air photos and field observations, a river width of 10 m was specified for the length of the Dolores River in the model domain. A roughness coefficient for the streambed of 0.03 was estimated by comparison to analogous rivers documented by Barnes (1967). The measured streambed altitudes were specified at the upstream and downstream streamgage locations and at an inflection point about 700-m upstream from the downstream streamgage, where the streambed slope steepens downstream (fig. 2). From this inflection point, the upstream slope of the streambed is  $7.56 \times 10^{-4}$ , and the downstream slope is  $3.27 \times 10^{-3}$ . A time series of average monthly streamflow at the upstream streamgage (fig. 6) from October 1, 1987, through November 30, 2020, was specified as inflow to the simulated stream reach. For each stream reach simulated downstream from the starting point, streamflow was computed as the sum of inflow from the upstream reach and seepage to or from the connected aquifer model cell.

Stream recharge from West Paradox Creek to the alluvial aquifer also was simulated using the SFR package of MODFLOW-6. West Paradox Creek was not gaged during the timeframe of the simulations; instead, outflow from Buckeye Reservoir was used to specify inflow variations to West Paradox Creek for the SFR package. For periods when Buckeye Reservoir was not releasing water, the minimum streamflow observed from October 1944 through August 1952 at USGS streamgage 09170500 was used to estimate an input value of  $1,223 \text{ m}^3/\text{d}$  to represent the base-flow component for West Paradox Creek inflow. Streambed altitudes at four points were extracted from a digital elevation model (U.S. Geological Survey, 2023) to specify the streambed slope of West Paradox Creek, which decreases from about 0.022 in the western part of the model grid to about 0.005 upstream from the Dolores River. A constant stream width of 2 m and roughness coefficient of 0.03 was specified for all reaches of West Paradox Creek.

## Simulated Initial Conditions

A steady-state head solution was calculated for the first stress period of the 1,000-year simulation with initial heads specified as a constant altitude of 1,634 m, which was above the base of the top model layer. Subsequent transient head solutions were insensitive to the initial head distribution. Initial TDS concentrations for the 1,000-year simulation were distributed uniformly within each model layer to represent freshwater in the top 3 model layers, and an observed brine concentration of  $270 \text{ kg/m}^3$  (Reclamation, 1978b) was assigned in the lower 4 model layers. Constant TDS concentrations of  $270 \text{ kg/m}^3$  were specified in a subset (161 cells) of the lower model layers that represent the collapse breccia

for the 1,000-year simulation. Heads and TDS concentrations simulated at the end of the 1,000-year simulation were saved and used to define the initial head and TDS concentration conditions for the 33-year simulation.

## Calibration of the Groundwater Model

The groundwater model was calibrated by adjusting model boundary conditions and parameter values within reasonable limits to match simulated water levels, flows, and concentrations to observed or estimated values. The term “observed values” is used for variables with direct observations including streamflow and groundwater levels, and the term “estimated values” is used for variables estimated by regression or composite measurements, including TDS concentrations, TDS mass flux to the river, and groundwater concentrations. Observed and simulated streamflow are depicted on figure 11, and estimated and simulated TDS concentrations for the downstream streamgage are depicted on figure 12. Manual adjustment of model parameters was iterated with multiple realizations of boundary specifications to achieve the calibrated model simulations.

## Observed Groundwater Levels

By 1978, Reclamation had installed a total of 65 groundwater observation wells near both sides of the Dolores River in the Paradox Valley (Reclamation, 1978b). Altitudes of 29 of the Reclamation observation wells within 0.5 km of the Dolores River were remeasured during a RTK GPS survey (in 2017) to an accuracy within about 5 cm. Water-level measurements taken by Reclamation from June 24, 2005, to January 19, 2016, in 25 of these wells were used to calibrate the model (data in Heywood and others, 2024). Although records of the total depth and screen-interval depths for these observation wells are not available in Reclamation (1978b), the wells are assumed to be completed within the alluvial aquifer. The random error associated with individual tape or transducer water-level measurements is likely on the order of 1 cm. Additional uncertainty in water-level measurements also is introduced by (1) vertical groundwater head gradients as much as 0.18 that exist in the collapse breccia under the Dolores River (Paschke and others, 2024), which generally are upward but may reverse direction during times of high river stage and (2) increases in groundwater salinity and density with depth, which cause lower apparent groundwater-level observations. If uncertainty in the depth of the observation-well screen interval is on the order of 10 m, a vertical hydraulic gradient of 0.1 may contribute 1 m to the error associated with the water-level measurements, which is an order of magnitude greater than the other sources of error in water-level observations. For these reasons, differences between simulated and observed water levels less than 1 m were considered acceptable during model calibration.

**Figure 11.** Observed and simulated streamflow for the downstream streamgage Dolores River near Bedrock, in the Paradox Valley, Colo. (U.S. Geological Survey streamgage 09171100), 1987–2020. Observed data from U.S. Geological Survey (2024a) and simulated values from Heywood and others (2024).

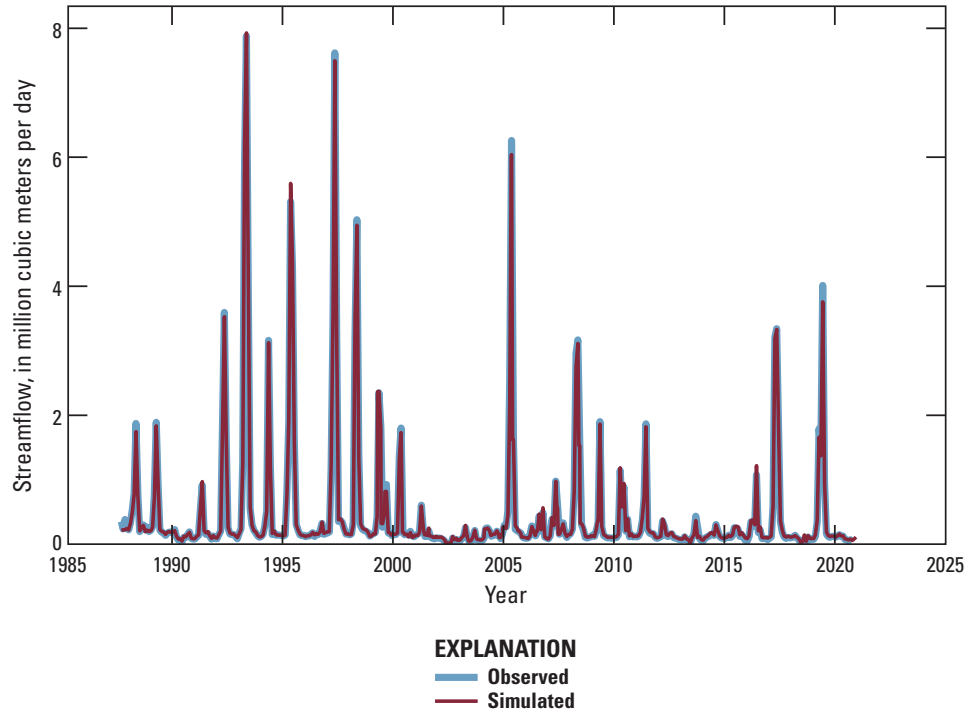
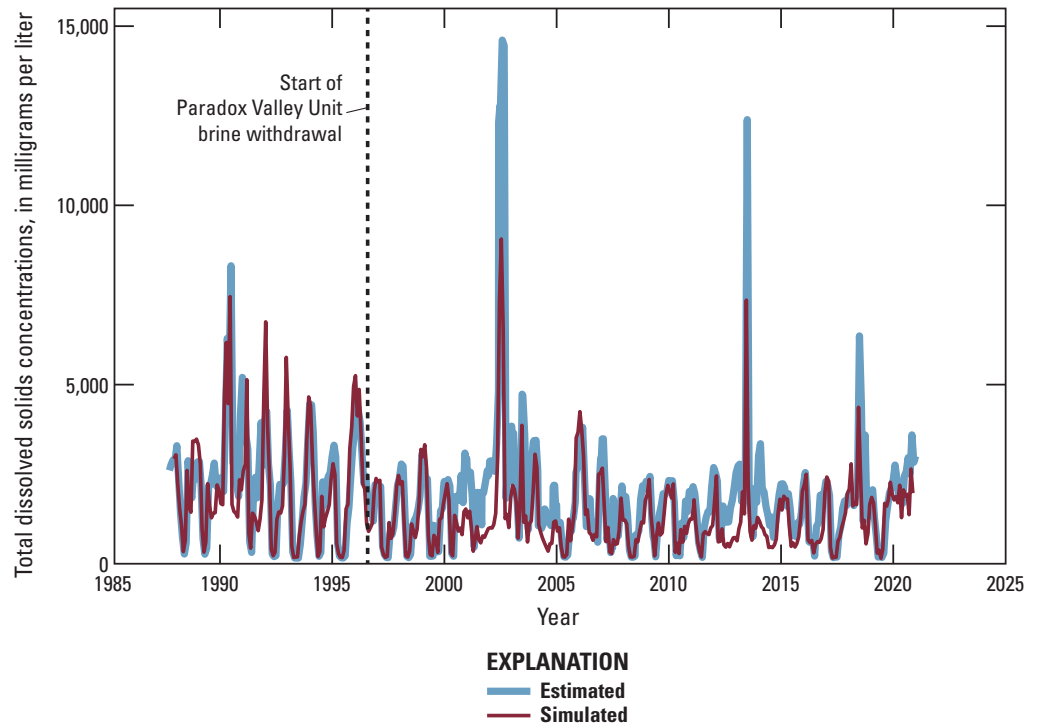


**Figure 12.** Estimated and simulated total dissolved solids concentrations for the downstream streamgage Dolores River near Bedrock, in the Paradox Valley, Colo. (U.S. Geological Survey streamgage 09171100), 1987–2020. Estimated concentrations from Mast (2017) and Heywood and others (2024). Simulated concentrations from Heywood and others (2024).



Accurate water-level observations in wells farther from the Dolores River in the Paradox Valley are scarce. To constrain aquifer transmissivity in the simulation, four water-level measurements were obtained from the Colorado Water Conservation Board and Colorado Division of Water Resources (2021) for wells 361-R, 6897-R, 5728-F, and 14228-F, which are located 7–11 km northwest of the Dolores River (fig. 2). These water-level measurements were assigned as observations for corresponding columns of the model grid. Well 361-R is located in column 1, so its measurement was assigned to all rows in column 1. The measurement for 6897-R was assigned to all rows in column 3, the measurement for 5728-F was assigned to all rows in column 6, and the measurement for 14228-F was assigned to all rows in column 8 (fig. 2).

### Observed Groundwater Concentrations

Concentrations of TDS observed in Reclamation observation wells near the Dolores River from June through October 1977 ranged from 255,000 to 285,000 mg/L (Reclamation, 1978b). Similar concentration values are indicated by observations of the specific gravity of the combined

mixture of PVU-pumped brine, which has had a concentration of about 257,000 mg/L consistently throughout the operation of the PVU (Reclamation, 2022).

### Parameter Values and Sensitivities

Paschke and others (2024) summarize published estimates of hydraulic properties of hydrogeologic units in and around the Paradox Valley. A trial-and-error process was necessary to determine appropriate input values for model parameters representing these properties in the simulations. The selected parameter values (table 3) are all within the range of published estimates for the corresponding hydraulic properties. A qualitative sensitivity analysis of the simulated water levels and TDS concentrations in the river was completed during the trial-and-error calibration. Parameter values that had an appreciable sensitivity on simulated groundwater hydraulic heads and TDS concentrations are denoted as “yes” in table 3. Values of parameters with negligible sensitivity were not well constrained by the calibration dataset and were fixed at a reasonable or published value. Although the hydraulic properties represented by parameters denoted “yes\*” do not appear in the transport equation, their effect on heads simulated near the

**Table 3.** Calibrated parameter values for hydraulic properties or boundary conditions used in the groundwater model of the Paradox Valley, Colo., and sensitivities of hydraulic head and concentration to model parameters (Heywood and others, 2024).

[Hydraulic head sensitivity: yes, appreciable sensitivity; neg, negligible sensitivity; \*, substantially affected brine discharge. m/d, meters per day; m<sup>-1</sup>, 1/meters; m, meter; TDS, total dissolved solids; —, not applicable]

| Hydraulic property or boundary condition | Hydrogeologic unit  | Calibrated parameter value         | Hydraulic head sensitivity | Concentration sensitivity |
|--|---------------------|------------------------------------|----------------------------|---------------------------|
| Horizontal hydraulic conductivity        | Alluvial aquifer    | 22 m/d                             | yes                        | neg                       |
|  | Collapse breccia    | 10 m/d                             | neg                        | neg                       |
|  | Consolidated rocks  | 0.1 m/d                            | neg                        | neg                       |
| Vertical hydraulic conductivity          | Alluvial aquifer    | 2.0 m/d                            | yes                        | yes*                      |
|  | Collapse breccia    | 1.0 m/d                            | neg                        | neg                       |
|  | Consolidated rocks  | 0.1 m/d                            | neg                        | neg                       |
|  | Streambed sediments | 0.17 m/d                           | neg                        | yes*                      |
| Specific yield                           | Alluvial aquifer    | 0.25                               | yes                        | neg                       |
|  | Consolidated rocks  | 0.01                               | neg                        | neg                       |
| Specific storage                         | Alluvial aquifer    | 1x10 <sup>-5</sup> m <sup>-1</sup> | yes                        | neg                       |
|  | Collapse breccia    | 1x10 <sup>-5</sup> m <sup>-1</sup> | neg                        | neg                       |
|  | Consolidated rocks  | 3x10 <sup>-6</sup> m <sup>-1</sup> | neg                        | neg                       |
| Effective porosity                       | Alluvial aquifer    | 0.25                               | n/a                        | yes                       |
|  | Collapse breccia    | 0.05                               | n/a                        | yes                       |
|  | Consolidated rocks  | 0.01                               | n/a                        | neg                       |
| Evapotranspiration extinction depth      | All                 | 1 m                                | yes                        | yes*                      |
| Evapotranspiration rate                  | All                 | Variable                           | yes                        | yes*                      |
| Recharge rate                            | All                 | Variable                           | yes                        | yes*                      |
| TDS concentration initial condition      | All                 | Variable                           | —                          | yes                       |

Dolores River substantially affected brine discharge and consequently simulated TDS concentrations in the river. Because of the limited spatial extent or accuracy of groundwater-level observations used in the model, a detailed simulation of aquifer heterogeneity and variability of hydraulic properties within hydrogeologic units was not feasible.

## Simulation of Groundwater Flow and Brine Discharge in the Paradox Valley

In this section, model results for the 1,000-year, 33-year (1987–2020), pre-PVU (October 1987–June 1996), and post-PVU (July 1996–November 2020) simulation periods are described. Modeled water budgets, groundwater levels, groundwater TDS concentrations, groundwater TDS pumping rates, streamflow, stream TDS concentrations, and changes to TDS flux to the Dolores River are presented and compared for the different simulation periods.

### Simulated Water Budget

The simulated water budgets for the calibrated model averaged during the 1,000-year, 33-year, pre-PVU, and post-PVU simulation periods are shown in [table 4](#) for each water-budget component. For MODFLOW simulations in general, positive values for water-budget components indicate flow into the groundwater system from that component, and negative values represent flow out of the groundwater system to the specified component. For storage, positive values represent water into the groundwater system from storage or decreases in groundwater storage, and negative values indicate water out of the groundwater systems and into storage or increases in groundwater storage.

The average magnitudes of the specified-flux boundary conditions (representing recharge and groundwater underflow) were specified for the 1,000-year quasi-steady-state simulation and varied in time during the 33-year simulation, as described in the “Boundary Conditions” section of this report. Similarly, for head-dependent flux boundaries, the average maximum ET rate and average river stage during the 33-year simulation were specified for the 1,000-year simulation. Maintenance of water-budget similarity between the 1,000-year and 33-year simulations ([table 4](#)) was necessary to avoid erroneous water-level trends and storage changes during the 33-year simulation.

For the 33-year simulation, sources of recharge to the groundwater system include precipitation recharge, recharge from irrigation-return flows, inflow from the northwest highlands, and inflow from the underlying breccia. Stream leakage, primarily from West Paradox Creek, also is a large inflow to the groundwater system, and there are small inflows from PVU pumping wells and aquifer storage. Outflows are to ET, stream leakage primarily to the Dolores River, PVU pumping

wells, and aquifer storage. Net flow from recharge includes inflow from the sources of recharge minus the outflow to ET. Evapotranspiration generally exceeds inflow from recharge for the 1,000-year and the 33-year simulations. The net flows for stream leakage include inflows and outflows for West Paradox Creek and the Dolores River. Although the Dolores River has losing and gaining reaches that vary with seasonal changes in river stage, groundwater flow, including brine discharge, is predominantly out of the aquifer system into the river. In contrast, seepage from West Paradox Creek predominantly recharges the aquifer system, as indicated by the positive net inflow value.

The transient water budget for the 33-year simulation ([figs. 13A, 13B](#)) indicates the seasonality of groundwater inflows and outflows. Stream inflows, primarily from West Paradox Creek, precipitation recharge, irrigation recharge, and ET flow rates peak during spring snowmelt runoff and the subsequent summer months, whereas inflow from the northwest highlands and underlying breccia are held constant in the simulations. Outflow to streams, primarily the Dolores River, is greatest during the fall and winter months when river stage is lowest and when brine discharges to the river. Storage changes during the 33-year simulation are in response to transient changes in streamflow, recharge, and groundwater withdrawals. Increases in storage (negative net change in storage) are simulated during periods of high streamflow and decreases in storage (positive net change in storage) are simulated during periods of low streamflow ([fig. 13B](#)). The storage results are consistent with the conceptual understanding of the groundwater system that aquifer storage increases in response to recharge from the Dolores River during high streamflow, and aquifer storage decreases as groundwater discharges to the river during periods of low streamflow. Groundwater flow and storage changes within the unsaturated zone were not simulated such that flow to and from unconfined storage represents changes in pore-space saturation below the water table. Flow to and from confined storage simulates the elastic response of water and the aquifer matrix to changing pressures. Withdrawals from PVU pumping wells are small in comparison to other water-budget components ([fig. 13A](#)).

### Simulated Groundwater Levels

Contours of the water-table altitudes ([fig. 14](#)) simulated for model layer 1 for November 30, 2020, indicate groundwater potentials approximately perpendicular to the water-table contours and flow away from West Paradox Creek, which is consistent with the conceptual understanding that West Paradox Creek is a source of recharge to the alluvial aquifer. Simulated and observed hydrographs at observation wells near West Paradox Creek at the west end of the valley ([fig. 15A](#)) and near the Dolores River ([fig. 15B](#)) illustrate the magnitude of inter-annual water-level variations simulated in the top layer of the model and do not indicate substantial trends in water levels during the 33-year simulation period. Groundwater flow



**Table 4.** Simulated water-budget components averaged during the 1,000-year, 33-year, pre-Paradox Valley Unit, and post-Paradox Valley Unit simulation periods for the Paradox Valley, Colo. (Heywood and others, 2024).

[By MODFLOW-6 convention, inflows to the groundwater model are positive, and outflows are negative. The pre-PVU period is October 1987–June 1996. The post-PVU period is July 1996–November 2020. PVU, Paradox Valley Unit; m<sup>3</sup>/d, cubic meters per day; —, not determined]

| Budget component   | 1,000-year simulation | 33-year simulation | Range for 33-year simulation | Pre-PVU period | Post-PVU period |
|--|-----------------------|--------------------|------------------------------|----------------|-----------------|
| Inflows, in m <sup>3</sup> /d                            |                       |                    |                              |                |                 |
| Infiltrated precipitation                                | 6,097                 | 6,152              | 0 to 23,170                  | 6,363          | 5,965           |
| Irrigation-return flow                                   | 2,315                 | 2,315              | 0 to 4,629                   | 2,249          | 2,335           |
| Northwest underflow                                      | 1,700                 | 1,700              | —                            | 1,700          | 1,700           |
| Deep breccia underflow                                   | 1,240                 | 1,295              | 20 to 4,368                  | 1,416          | 1,232           |
| Stream leakage inflow                                    | 13,832                | 13,836             | 2,836 to 67,463              | 11,414         | 14,311          |
| PVU pumping wells  | —                     | 3                  | 0 to 63                      | 4              | 4               |
| Unconfined storage                                       | 81                    | 7,683              | 1,103 to 23,876              | 8,268          | 7,639           |
| Confined storage   | 5                     | 37                 | 1 to 1,816                   | 49             | 34              |
| Total in   | 25,240                | 33,021             | —                            | 31,463         | 33,219          |
| Outflows, in m <sup>3</sup> /d                           |                       |                    |                              |                |                 |
| Evapotranspiration                                       | −14,265               | −14,002            | 0 to −42,744                 | −13,262        | −14,129         |
| Stream leakage outflow                                   | −10,893               | −10,862            | −1,688 to −18,294            | −10,826        | −10,890         |
| PVU pumping wells  | —                     | −714               | 0 to −1,451                  | −139           | −868            |
| Unconfined storage                                       | −77                   | −7,411             | −400 to −49,161              | −7,206         | −7,299          |
| Confined storage   | −5                    | −32                | 0 to −147                    | −29            | −33             |
| Total out  | −25,240               | −33,021            | —                            | −31,463        | −33,219         |
| Net flows, in m <sup>3</sup> /d                          |                       |                    |                              |                |                 |
| Net recharge (recharge inflows minus evapotranspiration) | −4,153                | −3,835             | −41,024 to 33,868            | −2,950         | −4,129          |
| Net stream leakage West Paradox Creek                    | 10,759                | 10,382             | −425 to 45,528               | 8,010          | 11,111          |
| Net stream leakage Dolores River                         | −7,817                | −7,630             | −15,403 to 21,770            | −7,423         | −7,693          |
| Net PVU pumping wells                                    | 0                     | −710               | 0 to −1,451                  | −135           | −864            |
| Net unconfined storage                                   | —                     | 272                | −44,325 to 23,062            | 1,062          | 340             |
| Net confined storage                                     | —                     | 5                  | −145 to 1,750                | 19             | 1               |
| Net total storage (confined plus unconfined)             | —                     | 277                | −44,421 to 23,167            | 1,062          | 341             |

from the northwest toward the Dolores River in a direction about perpendicular to the water-table contours, and water-table contours curve around the river indicating groundwater discharge in the valley (fig. 14). There is a downward-moving component of flow where groundwater is recharged in the northwest part of the model domain, and there is an upward-moving component near the Dolores River where groundwater discharge occurs. A relatively minor amount of groundwater is simulated for an area southeast of but flowing toward the Dolores River.

The well hydrographs illustrate the effect of the Dolores River stage on observed and simulated water levels, particularly in observation wells 8E25, MR4E, and 5E25 near the Dolores River (figs. 15D–F). These wells indicate notable water-level rises during June 2007 and 2008 that correspond to relatively high stages of the Dolores River during the same periods.

The hydrograph of well 3E2 (fig. 15H) contains five measurements that are outliers, being about 1 m higher than the measurement trend; they are also anomalous when compared to simulated and observed water-level trends in

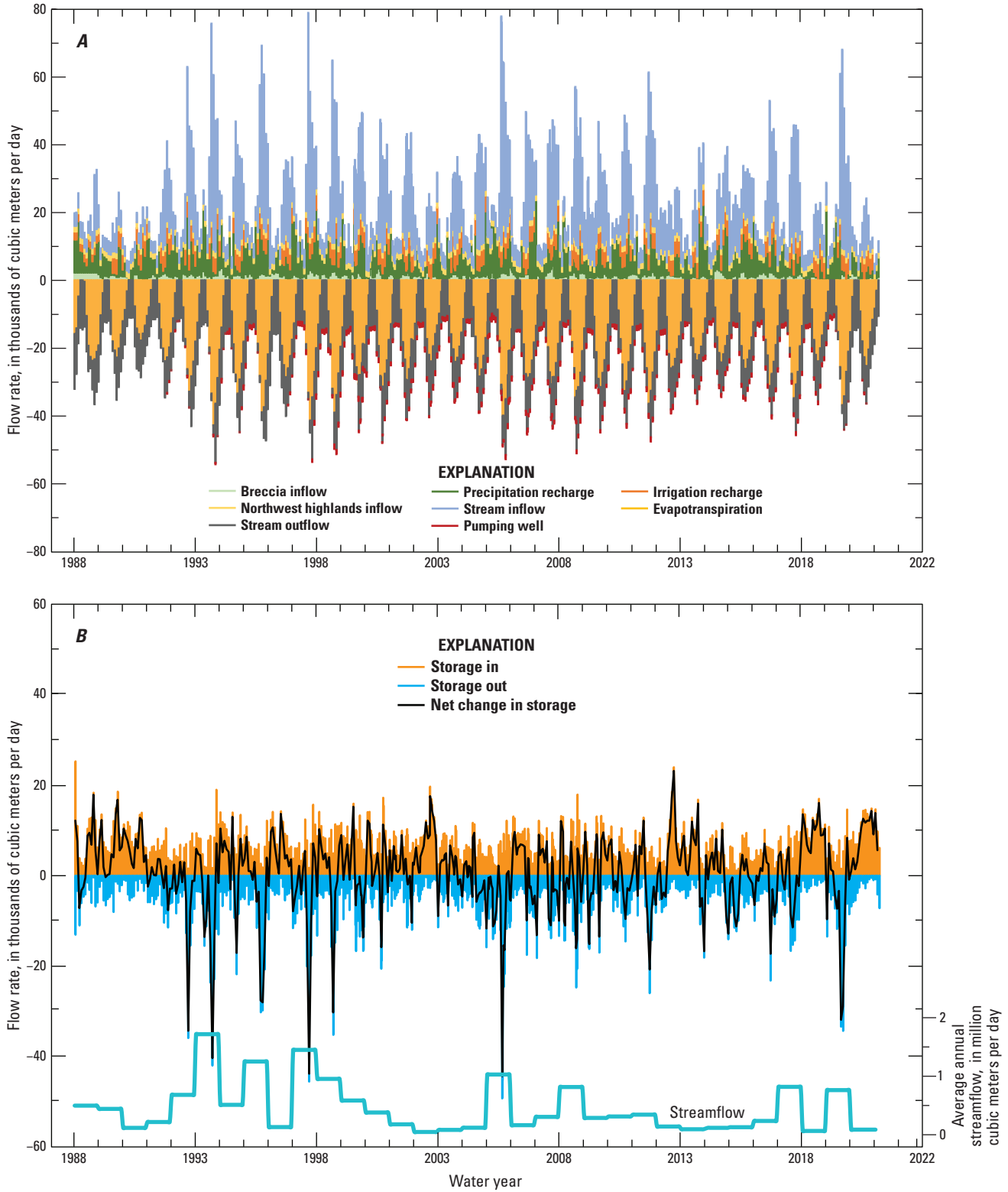


**Figure 13.** A, Simulated monthly transient water budget for the 33-year simulation for the Paradox Valley, Colo., 1987–2020. (Heywood and others, 2024); and B, simulated monthly transient storage values and net changes in storage for the 33-year simulation for the Paradox Valley, Colo., 1987–2020. (Heywood and others, 2024).

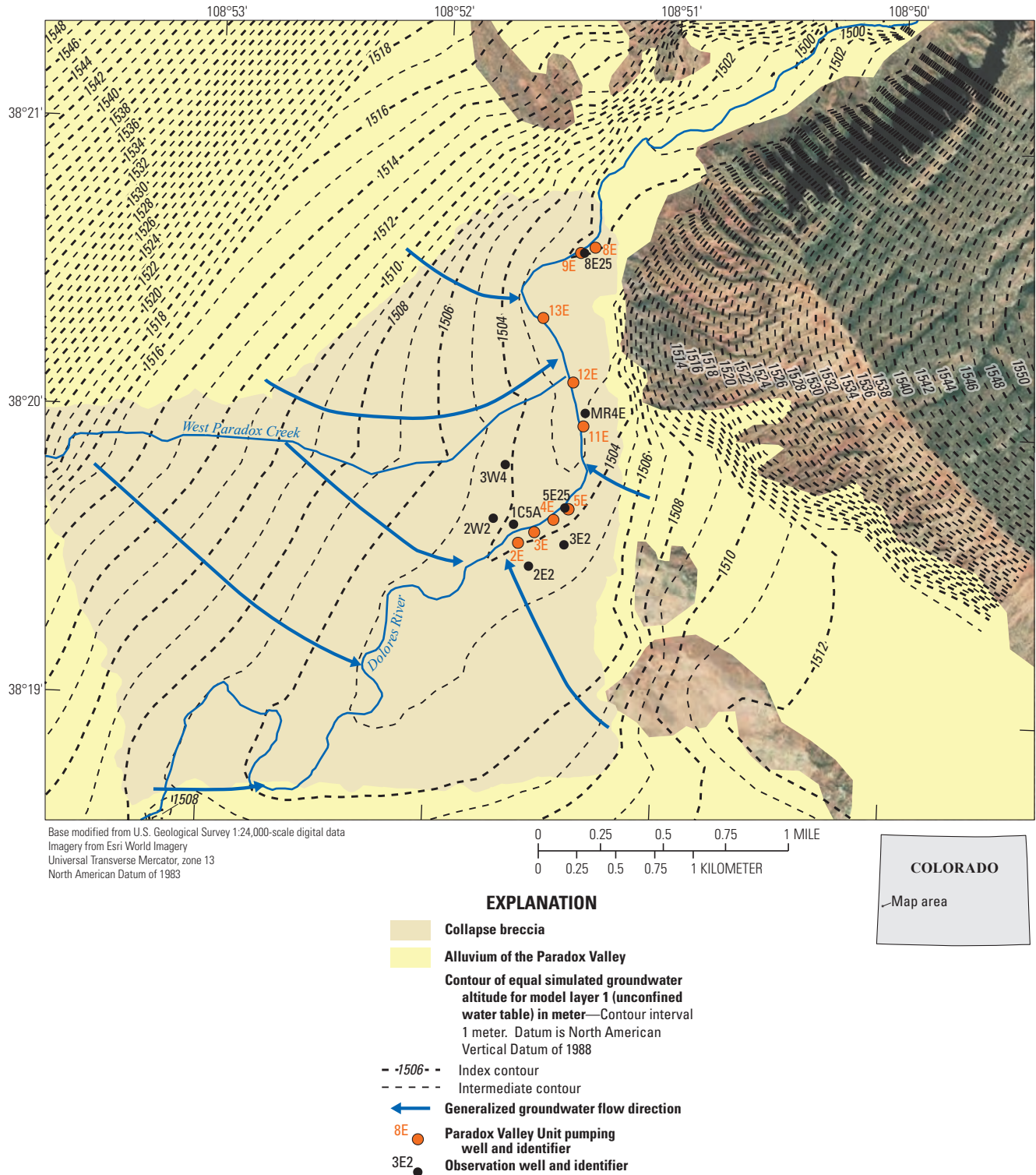


**Figure 14.** Simulated water-table altitude for July 2007 (data from Heywood and others, 2024), locations of Paradox Valley Unit pumping and observation wells, and extent of alluvium and collapse breccia in the Paradox Valley, Colo. (Reclamation, 1978b; Paschke and Mast, 2024).

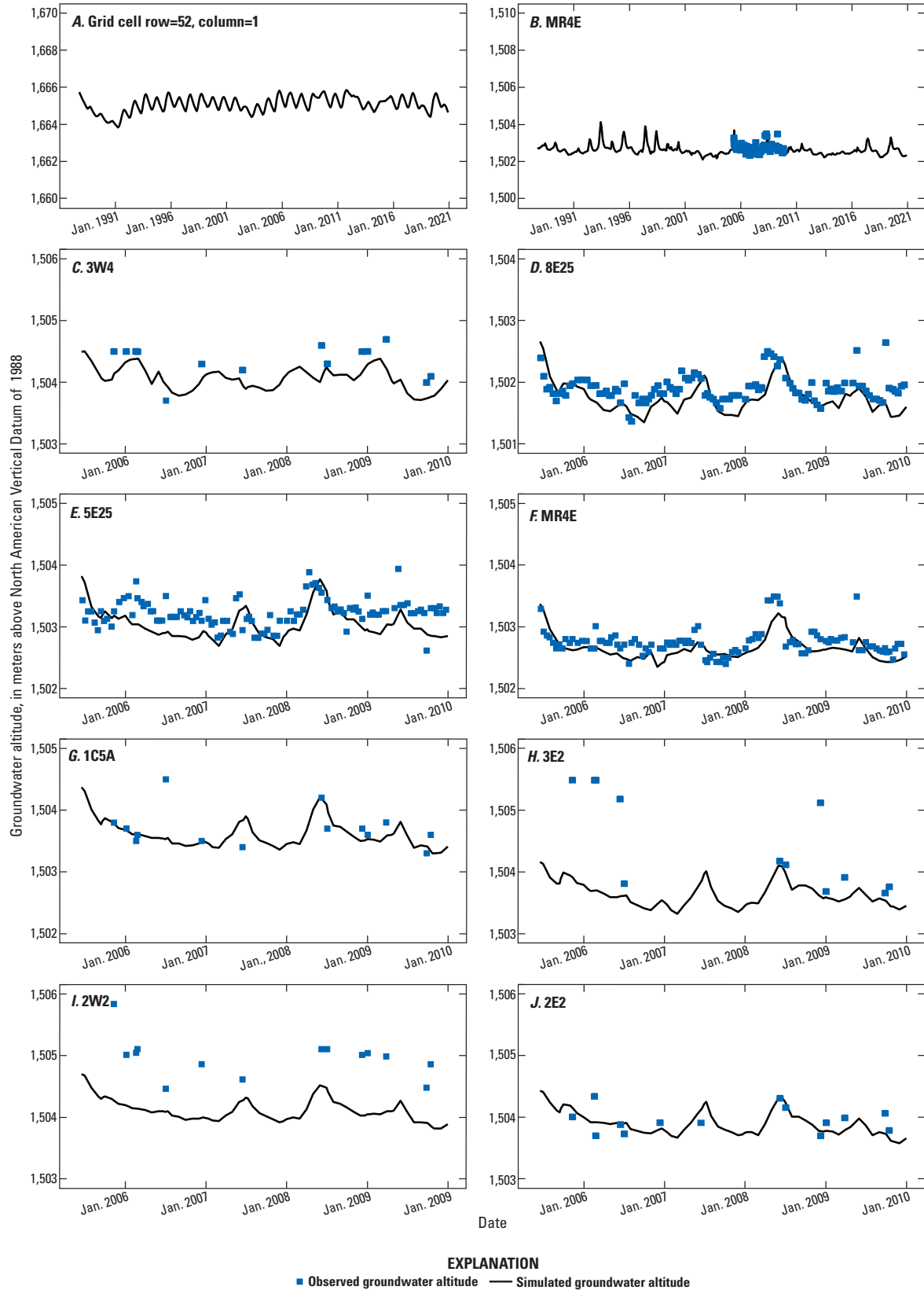


**Figure 15.** Observed and simulated groundwater levels for observation wells near the Dolores River in the Paradox Valley, Colo. For each hydrograph (A–J), names of the observation wells correspond to locations on [figure 14](#) (Heywood and others, 2024).

other observation wells. Site 3E2 contains two piezometers with screens at unknown, but differing, depth intervals. These anomalies are possibly explained by water-level measurements being made in different piezometers at different times. It should be noted that measurement anomalies also appear in water-level hydrographs from some other wells that contain two or three piezometers.

## Simulated Total Dissolved Solids Concentrations in Groundwater

Simulated TDS values in shallow groundwater represented in the top layer of the model for November 2020 (fig. 16) were greater than 100 mg/L. These values are typical of TDS distributions simulated during seasons when the Dolores River stage is relatively low. The areas with simulated groundwater concentrations greater than 40,000 mg/L are along the river near PVU pumping wells. Of the PVU pumping wells, 11E, 12E, and 13E (fig. 16) were the least used (table 2), and SC of the river was not observed to increase within the reach adjacent to these wells during the June 24–25, 2013, river survey (fig. 8). The lack of change in TDS of the river around 11E, 12E, and 13E may indicate that actual groundwater concentrations in this area are less than the simulated concentrations or that this area is not a zone of groundwater discharge. The simulated TDS concentrations of groundwater during times of higher river stage that typically occur during the spring were generally less than during times of low river stage but have a similar spatial distribution, which is consistent with observed conditions.

## Simulated Total Dissolved Solids Mass-Flux Budget

The simulated TDS mass-flux budget for the calibrated model averaged during the 33-year simulation period is shown in table 5 for each budget component. Similar to the water budget, positive values for the mass-flux budget components indicate TDS inflows to the groundwater system from that component, and negative values represent TDS outflows from the groundwater system. For storage, positive values indicate decreases in TDS storage (TDS into the groundwater system from storage), and negative values indicate increases in TDS storage (TDS out of the groundwater system and into storage).

The primary sources of simulated TDS to the groundwater system are groundwater inflow from the underlying breccia and aquifer storage, whereas inflow from streams and the PVU pumping wells are minor sources of simulated TDS. Mass flux from the underlying breccia represents the brine source in the valley and was simulated by assigning constant TDS concentrations to variable inflows to model cells in layer 7 that represent the base of the collapse breccia beneath the Dolores River. At the beginning of the 33-year simulation, initial TDS concentrations were assigned to the bottom 4 model

layers representing the breccia using ending values from the 1,000-year simulation, as described in the “Simulated Initial Conditions” section of this report and these initial conditions are a source of TDS from aquifer storage in the 33-year simulation. Recharge from precipitation, irrigation-return flows, and groundwater inflow from the northwest highlands were not assigned TDS concentrations and thus are not simulated sources of TDS. Simulated output of TDS from the groundwater system is to ET, PVU pumping wells, the Dolores River, and aquifer storage.

The transient TDS mass-flux budget for the 33-year simulation (figs. 17A, B) indicates the simulated seasonality of TDS fluxes in the groundwater system. Mass flux of TDS from the underlying collapse breccia is simulated as an assigned constant concentration multiplied by a time-varying water inflow scaled to precipitation rates in the La Sal Mountains with an 8-month time lag, as described in the “Hydraulic Head-Dependent Flow Boundaries” section of this report. This time-varying representation of TDS mass flux from the brine is a source of model uncertainty that may contribute to the low-bias in simulated TDS concentrations from PVU pumping wells described in the “Simulated Groundwater Withdrawals” and “Breccia as a Source of Brine” sections of this report. Simulated aquifer storage of TDS in the groundwater system is both a source and sink of TDS and changes in response to time-varying changes in TDS inflows, streamflow, and PVU withdrawals (fig. 17B). Increases in TDS storage (negative net change in storage) are simulated during periods of high streamflow and decreases in TDS storage (positive net change in storage) are simulated during periods of low streamflow (fig. 17B) consistent with the conceptual understanding of the groundwater system. Outflow of TDS is to ET, PVU pumping wells, and streams (primarily to the Dolores River; fig. 17A). Evapotranspiration is simulated for all months except November, December, and January, and simulated TDS flux to ET peaks during June, in response to warm air temperatures and active irrigation. The TDS mass flux to PVU pumping wells and the Dolores River and post-PVU changes to the system are described further in subsequent sections of this report.

Comparison of average annual streamflow for the downstream streamgage to simulated mass-flux budget rates (figs. 17A, B) indicates that during periods of low streamflow, TDS mass flux to ET is somewhat less than during periods of higher streamflow. Because ET is computed as a function of depth to water, lesser simulated ET mass-flux rates during periods of low streamflow would indicate that simulated depths to water are greater than the assigned simulation ET extinction depth of 1 m. The ET extinction-depth parameter is identified as a highly sensitive model parameter (table 3), and previous work indicates that ET extinction depth could be as much as 2–3 m, as described in the “Evapotranspiration” section of this report. Increasing the ET extinction depth would increase the TDS mass flux to ET and reduce the TDS mass flux to the Dolores River. In addition, comparison of ET mass-flux rates between pre- and post-PVU periods (table 5; fig. 17A) indicated that simulated TDS mass flux to ET

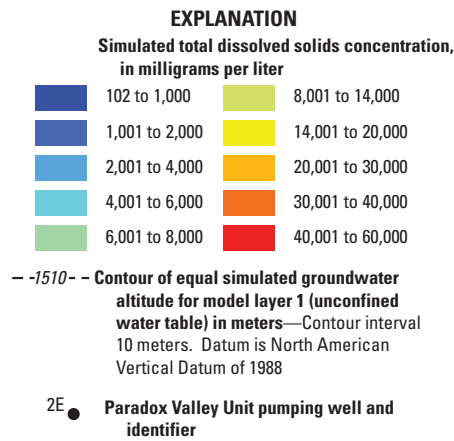
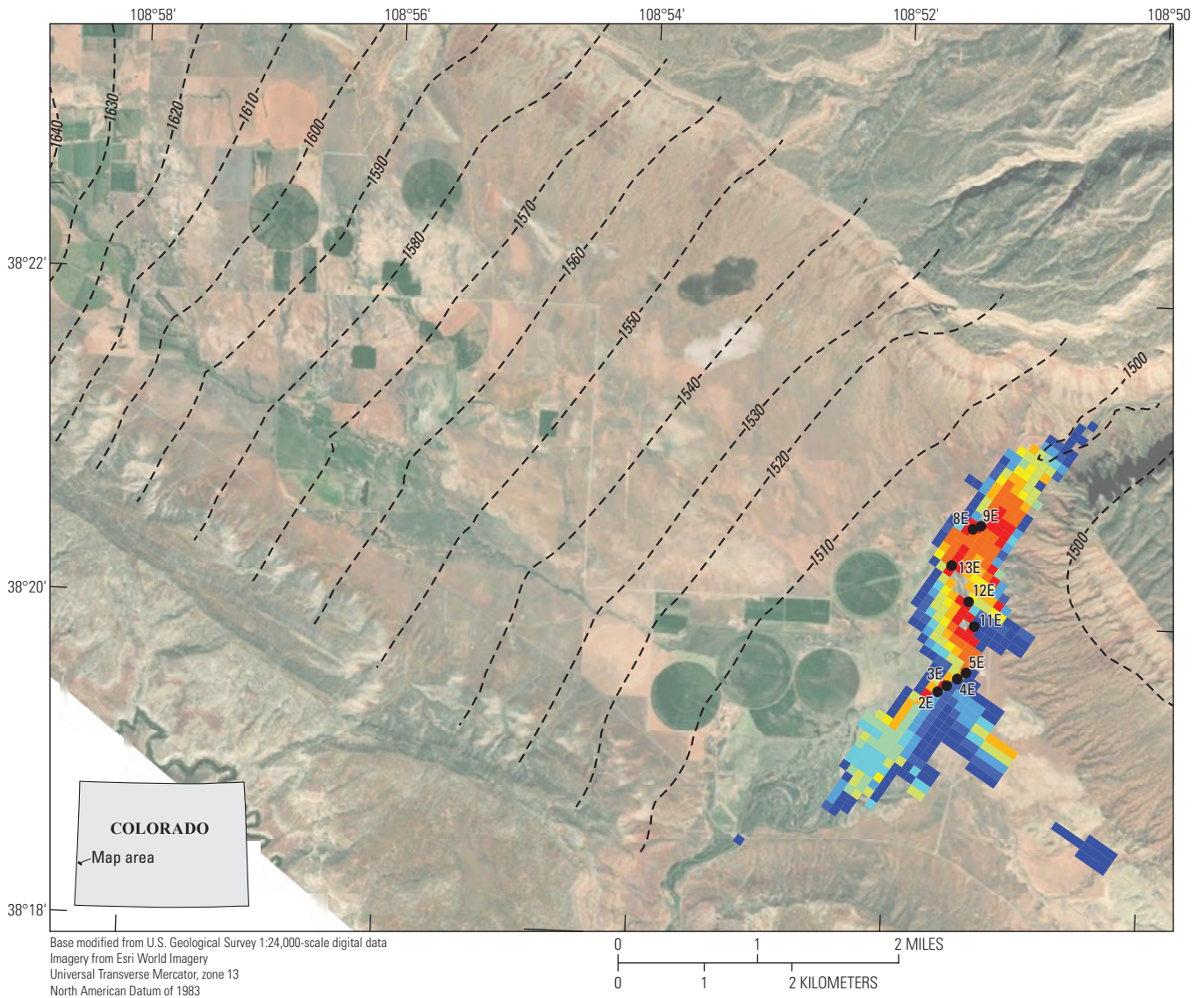


**Figure 16.** Simulated water-table altitude and total dissolved solids concentrations in groundwater in the top model grid layer for November 2020, Paradox Valley, Colo. (Heywood and others, 2024).

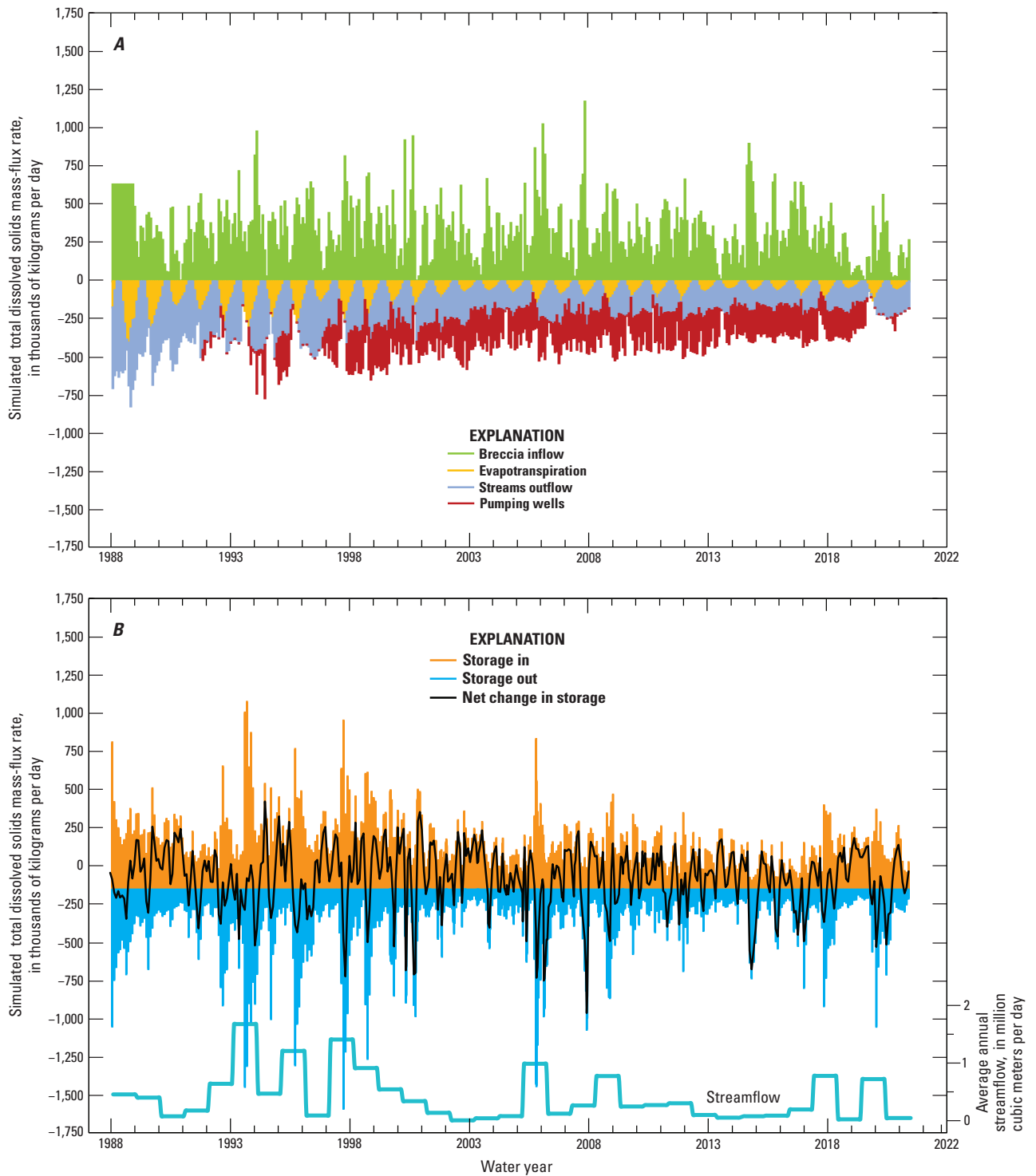


**Figure 17.** A, Simulated monthly transient total dissolved solids mass-flux budget for the 33-year simulation in the Paradox Valley, Colo., 1987–2020; and B, simulated monthly transient total dissolved solids storage mass-flux values and changes in storage for the 33-year simulation for the Paradox Valley, Colo., 1987–2020 (Heywood and others, 2024).

decreased by about 56 percent in the post-PVU period when PVU pumping wells captured TDS that was previously lost to ET. In the physical system, TDS removed from the groundwater system by ET would accumulate as evaporative salt deposits in the unsaturated zone above the water table, which is supported by observation of evaporative salt at the land surface in the Paradox Valley. These evaporative salt deposits at the land surface and in the unsaturated zone could be an additional source of TDS to the Dolores River and the groundwater system; however, because the unsaturated zone is not simulated by the model, the dissolution of evaporative deposits is not a simulated source of TDS. The shallow ET extinction depth simulated by the model as well as the inability of the model to simulate TDS input from the unsaturated zone are sources of model uncertainty.

### Simulated Groundwater Withdrawals

The simulated mass withdrawn from the groundwater system by PVU pumping wells is calculated by the model as the product of the assigned pumping rate and simulated TDS concentrations in the aquifer. The simulated pumping for the pre-PVU period totaled 433,400 m<sup>3</sup>, and the simulated pumping for the post-PVU period totaled 7,987,699 m<sup>3</sup>, which is within 0.5 percent of the estimated values of about 431,537 and 7,949,366 m<sup>3</sup> for the pre- and post-PVU periods, respectively (table 6). Concentrations of TDS withdrawn by the PVU pumping wells cannot be assigned in the model and are calculated based on the simulated concentration of groundwater withdrawn by each well. The depths and completion intervals of pumping wells (table 2) determine the location of groundwater capture. For the 33-year simulation, the simulated withdrawal TDS concentration for individual wells averaged 181,869 mg/L (table 6). For the pre-PVU period, from October 1987 to June 1996, the simulated

**Table 5.** Simulated total dissolved solids mass-flux budget components averaged during the 33-year, pre-Paradox Valley Unit, and post-Paradox Valley Unit simulation periods for the Paradox Valley, Colo. (Heywood and others, 2024).

[By MODFLOW-6 convention, inflows to the groundwater model are positive and outflows are negative. Pre-PVU period is October 1987–June 1996. Post-PVU period is July 1996–November 2020. Net mass flux also provided in tons per year for consistency with Bureau of Reclamation reporting. PVU, Paradox Valley Unit; kg/d, kilograms per day; —, not determined; tons/yr, tons per year]

| Budget component                         | 33-year simulation | Range of 33-year simulation | Pre-PVU period | Post-PVU period |
|--|--------------------|-----------------------------|----------------|-----------------|
| Mass-flux inflows, in kg/d               |                    |                             |                |                 |
| Infiltrated precipitation                | 0                  | —                           | 0              | 0               |
| Irrigation-return flow                   | 0                  | —                           | 0              | 0               |
| Northwest underflow                      | 0                  | —                           | 0              | 0               |
| Deep breccia underflow                   | 343,784            | 5,346 to 1,179,417          | 379,861        | 332,772         |
| Stream leakage inflow                    | 161                | 0 to 3,983                  | 225            | 142             |
| PVU pumping wells                        | 767                | 0 to 15,689                 | 941            | 714             |
| Total storage (confined plus unconfined) | 317,061            | 57,807 to 1,204,059         | 401,741        | 291,214         |
| Total in                                 | 661,773            | —                           | 782,768        | 624,842         |
| Mass-flux outflows, in kg/d              |                    |                             |                |                 |
| Evapotranspiration                       | −64,293            | 0 to −402,415               | −113,043       | −49,413         |
| Stream leakage outflow                   | −198,795           | 0 to −625,398               | −309,958       | −164,865        |
| PVU pumping wells                        | −144,731           | 0 to −351,650               | −33,365        | −178,724        |
| Total storage (confined plus unconfined) | −253,953           | −31,726 to −1,406,347       | −326,401       | −231,839        |
| Total out                                | −661,772           | —                           | −782,767       | −624,841        |
| Net mass flux, in kg/d                   |                    |                             |                |                 |
| Net flux to Dolores River                | −198,634           | 3,913 to −625,398           | −309,733       | −164,723        |
| Net PVU pumping wells                    | −143,965           | 38 to −351,490              | −32,425        | −178,010        |
| Net total storage                        | 63,108             | 564,463 to −792,211         | 75,340         | 59,375          |
| Net mass flux, in tons/yr                |                    |                             |                |                 |
| Net flux to Dolores River                | −79,974            | 1,575 to −251,798           | −124,705       | −66,321         |
| Net PVU pumping wells                    | −57,963            | 15 to −141,517              | −13,055        | −71,670         |
| Net total storage                        | 25,409             | 227,264 to −318,960         | 30,333         | 23,906          |



withdrawal TDS concentrations for individual wells averaged 128,664 mg/L, and for the post-PVU period, from July 1996 to November 2020, the simulated withdrawal TDS concentrations for individual wells averaged 198,217 mg/L (table 6). Specific-gravity measurements of the combined mixture from PVU pumping wells are relatively consistent through time and indicate an average withdrawal concentration of about 257,000 mg/L (Reclamation, 2022). For all of the simulated time periods (33-year simulation, pre-PVU, and post-PVU) simulated TDS concentrations of groundwater withdrawals are consistently and substantially less than the TDS concentrations estimated by specific-gravity measurements made at the PVU (table 6). The average simulated concentration withdrawn by PVU pumping wells during the post-PVU period (198,217 mg/L) is about 26 percent less than the estimated concentration of 257,000 mg/L (table 6).

The temporal variation of the simulated and estimated TDS mass flux from PVU pumping wells for the 33-year simulation indicates that although the temporal pattern of mass withdrawal is nearly replicated, the simulated mass-flux rates are consistently less than the estimated values (fig. 9). The average simulated TDS mass flux from PVU pumping wells

for the post-PVU period is 178,009 kilograms per day (kg/d; 71,670 tons/yr), which is about 26 percent less than the estimated mass withdrawal rate of 231,027 kg/d (93,016 tons/yr) and consistent with the low bias in simulated groundwater TDS concentrations for the same period (table 6). Similarly, the simulated mass-flux rate of 190,224 kg/d (76,588 tons/yr) for the period 1996–2015 was about 30 percent less than the estimated mass-flux rate of 258,309 kg/d (104,000 tons/yr) from Mast (2017; table 6). Because simulated PVU pumping rates for the 33-year simulation are specified in the model and were derived from PVU estimated pumping rates, simulated groundwater withdrawal from PVU pumping wells closely matched estimated values (table 6). The differences between simulated and estimated TDS mass flux from PVU pumping wells is caused by differences between the simulated and observed pumped groundwater TDS concentrations. These differences could be caused by several model limitations and uncertainties, including numerical dispersion, seasonal representation of brine inflow, model-parameter values, and other processes, including ET. These sources of model uncertainty are explored further in the “Model Uncertainty and Limitations” section of this report.

**Table 6.** Simulated and estimated volume of groundwater, total dissolved solids concentrations, and total dissolved solids mass flux withdrawn from Paradox Valley Unit pumping wells for different simulation periods for the Paradox Valley, Colo.

[Pre-PVU period is October 1987–June 1996. Post-PVU period is July 1996–November 2020. Mass flux also reported in tons per year for consistency with Bureau of Reclamation reporting. Simulated and estimated groundwater withdrawals from Heywood and others (2024). Estimated TDS mass flux for July 1996–November 2015 from Mast (2017). PVU, Paradox Valley Unit; m<sup>3</sup>, cubic meters; —, not applicable; TDS, total dissolved solids; mg/L, milligrams per liter; kg/d, kilograms per day; tons/yr; tons per year]

| Category  | 33-year simulation | Pre-PVU | Post-PVU  | Post-PVU (Mast, 2017) |
|---|--------------------|---------|-----------|-----------------------|
| Volume of groundwater withdrawals for PVU pumping wells |                    |         |           |                       |
| Simulated withdrawals (m <sup>3</sup> )                 | —                  | 433,400 | 7,987,699 | —                     |
| Estimated withdrawals (m <sup>3</sup> )                 | —                  | 431,537 | 7,949,366 | —                     |
| Ratio of simulated to estimated (percent)               | —                  | 100.4   | 100.5     | —                     |
| Difference simulated to estimated (percent)             | —                  | 0.43    | 0.48      | —                     |
| TDS concentrations for PVU pumping wells                |                    |         |           |                       |
| Simulated concentration (mg/L)                          | 181,869            | 128,664 | 198,217   | —                     |
| Estimated concentration (mg/L)                          | 257,000            | 257,000 | 257,000   | —                     |
| Ratio of simulated to estimated (percent)               | 71                 | 50      | 77        | —                     |
| Difference simulated to estimated (percent)             | –34                | –67     | –26       | —                     |
| TDS mass flux for PVU pumping wells                     |                    |         |           |                       |
| Simulated mass flux (kg/d)                              | 143,965            | 32,425  | 178,009   | 190,224               |
| Estimated mass flux (kg/d)                              | 184,308            | 39,176  | 231,027   | 258,309               |
| Simulated mass flux (tons/yr)                           | 57,963             | 13,055  | 71,670    | 76,588                |
| Estimated mass flux (tons/yr)                           | 74,206             | 15,773  | 93,016    | 104,000               |
| Ratio of simulated to estimated (percent)               | 78                 | 83      | 77        | 74                    |
| Difference simulated to estimated (percent)             | –25                | –19     | –26       | –30                   |

### Simulated Streamflow and Total Dissolved Solids Concentrations of the Dolores River

There is close correspondence between simulated and observed average monthly streamflow at the downstream streamgauge (USGS streamgauge 09171100; fig. 11; table 7). With regard to streamflow, a close fit of the simulation to observed values is expected because streamflow into the model is specified at the location of the upstream streamgauge (USGS streamgauge 09169500), and the magnitude of seepage to and from the groundwater system along the valley reach is relatively small compared to the magnitude of streamflow (table 7). The difference in streamflow from pre- to post-PVU periods also was accurately simulated within about 1 percent (table 7), with simulated and observed streamflow being substantially reduced between the pre-PVU and post-PVU periods, consistent with observed streamflow patterns. This observed reduction in streamflow (fig. 6) was likely caused by the 1984 impoundment of the upstream McPhee Reservoir (Voguesser, 2001) and subsequent controlled releases to the Dolores River as well as drought conditions in the later part of the record.

The largest differences between simulated and observed streamflow coincide with periods of high streamflow and may be caused by less accurate rating curves for high flows at either streamgauge, or the addition of streamflow from West Paradox Creek, which is not accurately specified in the model. Precipitation runoff and ephemeral streamflow from East Paradox Creek may also contribute to higher observed streamflow at the downstream streamgauge compared to the simulation because these flows are not included in the model.

The simulated TDS concentration for the Dolores River at the downstream streamgauge (USGS streamgauge 09171100) is shown on figure 12, in comparison to the estimated average monthly TDS concentration. Overall, simulated TDS concentrations for the downstream streamgauge are greater than estimated values for the simulation period (table 7); however, the fit of simulated to estimated values during the pre-PVU period (8-percent difference between simulated and estimated values) is closer than during the post-PVU period (35-percent difference between simulated and estimated values). Before the start of PVU operations in 1996, simulated peak concentrations, which generally occur during low river stages when groundwater discharge is greatest, are usually less than estimated TDS concentrations at the low stage. After 1996, simulated peak concentrations often match, but sometimes exceed

**Table 7.** Simulated and estimated (or observed) streamflow and total dissolved solids concentrations for and total dissolved solids mass flux to the Dolores River near Bedrock (U.S. Geological Survey streamgauge 09171100) in the Paradox Valley, Colo.

[Simulated values from Heywood and others (2024), Observed streamflow from USGS (2024b). Estimated total dissolved solids (TDS) from Mast (2017) and Heywood and others (2024). Units of tons per year also included for consistency with Bureau of Reclamation reporting preferences. pre-PVU, 1987–June 1996; post-PVU, July 1996–November 2020; PVU, Paradox Valley Unit; m<sup>3</sup>/d, cubic meters per day; —, not applicable; mg/L, milligrams per liter; tons/yr, tons per year; kg/day, kilograms per day]

| Category   | 33-year simulation | Pre-PVU | Post-PVU | Pre-PVU minus post-PVU | Percent difference post-PVU minus pre-PVU |
|--|--------------------|---------|----------|------------------------|---|
| Streamflow for Dolores River near Bedrock        |                    |         |          |                        |   |
| Simulated streamflow (m <sup>3</sup> /d)         | 471,782            | 650,401 | 417,261  | -233,140               | -44                                       |
| Observed streamflow (m <sup>3</sup> /d)          | 474,518            | 647,301 | 411,580  | -235,721               | -45                                       |
| Ratio of simulated to observed (percent)         | 99                 | 100     | 101      | 99                     | —   |
| Difference simulated to observed (percent)       | -0.6               | 0.5     | 1.4      | -1.1                   | —   |
| TDS concentration for Dolores River near Bedrock |                    |         |          |                        |   |
| Simulated concentration (mg/L)                   | 2,007              | 2,343   | 1,905    | 438                    | -21                                       |
| Estimated concentration (mg/L)                   | 1,555              | 2,166   | 1,342    | 824                    | -47                                       |
| Ratio of simulated to estimated (percent)        | 129                | 108     | 142      | 53                     | —   |
| Difference simulated to estimated (percent)      | 25                 | 8       | 35       | -61                    | —   |
| TDS mass flux for Dolores River near Bedrock     |                    |         |          |                        |   |
| Simulated mass flux (tons/yr)                    | 79,974             | 124,704 | 66,321   | -58,383                | -47                                       |
| Estimated mass flux (tons/yr)                    | 66,434             | 126,657 | 43,770   | -82,887                | -65                                       |
| Simulated mass flux (kg/d)                       | 198,634            | 309,731 | 164,724  | -145,008               | -47                                       |
| Estimated mass flux (kg/d)                       | 165,004            | 314,582 | 108,713  | -205,869               | -65                                       |
| Ratio of simulated to estimated (percent)        | 120                | 98      | 152      | 70                     | —   |
| Difference simulated to estimated (percent)      | 18                 | -2      | 41       | -35                    | —   |

estimated concentrations at the low stage. Concentration minima that occur during spring runoff when river stages are highest generally are accurately simulated. However, simulated TDS concentrations are notably greater than estimated concentrations from June 2000 to March 2003, May 2012 to June 2013, and October 2013 to October 2014. These differences between simulated and estimated TDS concentrations occur primarily during periods of drought and could be caused by the low bias in simulated groundwater concentrations withdrawn from PVU pumping wells or by actual conditions that differ from simulated conditions during drought. The effects of these differences on simulated TDS flux calculations in the river are described in the “Simulated Mass Flux to the Dolores River” section of this report.

### Simulated Mass Flux to the Dolores River

The simulated transient TDS mass flux to the Dolores River (fig. 18) represents the simulated sum of TDS mass flux to stream reaches, which, in the simulations, is equal to the TDS mass flux calculated as the product of streamflow and stream concentration at the downstream streamgage (USGS streamgage 09171100). Because simulated streamflow closely matches observed streamflow at the downstream streamgage (fig. 11; table 7), the simulated temporal variation

in TDS mass flux reflects the temporal variation in simulated stream concentrations (fig. 12). Monthly averages of the daily TDS mass flux estimated using the Mast (2017) regression model are depicted as “estimated” on figure 18 and listed in table 7 through 2020 for comparison. Mast (2017) estimated a 64-percent decrease in TDS mass flux to the river attributed to PVU pumping for the period 1996–2015 as the ratio of the reduction in TDS mass from pre-PVU to post-PVU conditions (195,222 kg/d or 78,600 tons/yr) to the pre-PVU TDS flux (302,767 kg/d or 121,900 tons/yr). This ratio was consistent when the post-PVU calculations by Mast (2017) were extended through the 33-year simulation period to November 2020 (Heywood and others, 2024), indicating about a 65-percent decrease in mass flux of total dissolved solids to the river (table 7).

In general, simulated mass flux to the river for the pre-PVU period is in good agreement with estimated values (2-percent difference; table 7), but model results vary from estimated values during the post-PVU period. Post-PVU, simulated TDS mass flux to the Dolores River decreased after the commencement of PVU operations in July 1996, presumably because of withdrawals from the PVU pumping wells (fig. 12). However, the simulated average post-PVU TDS mass flux to the river of 164,724 kg/d (66,321 tons/yr) is 41 percent greater than the average estimated post-PVU TDS mass flux to the river of 108,713 kg/d (43,770 tons/yr; table 7). The

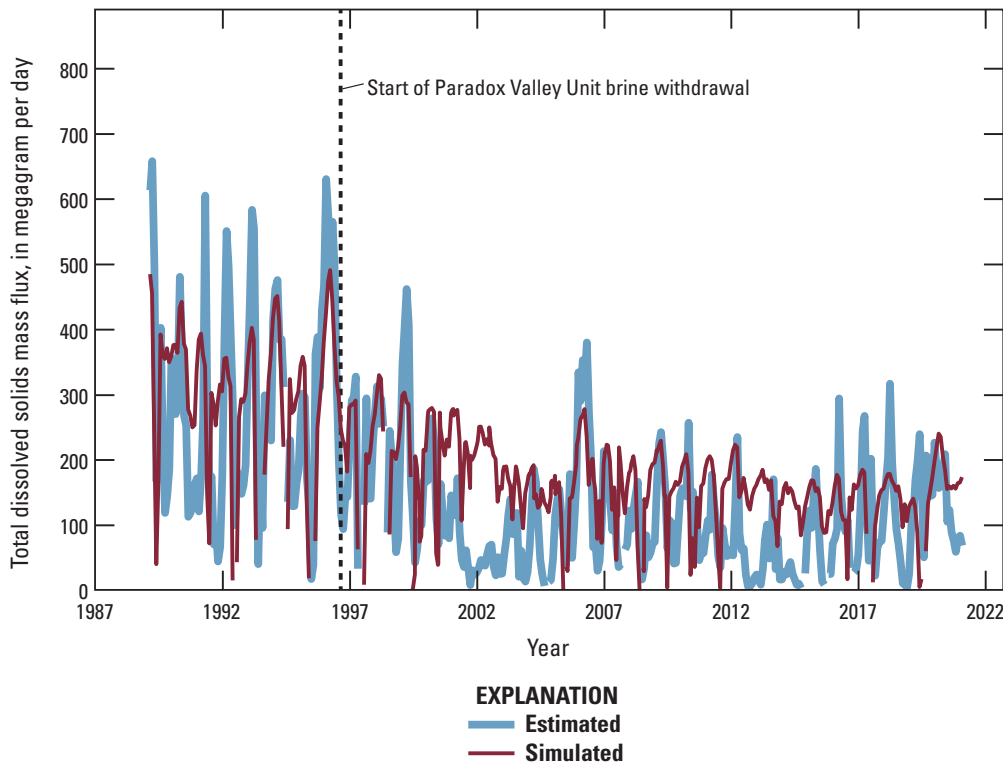


**Figure 18.** Estimated and simulated monthly total dissolved solids mass flux to the Dolores River in the Paradox Valley, Colo., 1987–2020. Estimated data from Mast (2017) and Heywood and others (2024). Simulated data from Heywood and others (2024).

model simulates a 47-percent reduction in TDS mass flux to the Dolores River from the pre- to post-PVU period, whereas estimated values indicate a 65-percent reduction during the same period, consistent with previous results (Mast, 2017). These results indicate that the groundwater model is overestimating stream TDS concentrations and thus TDS mass flux to the river. Simulated TDS mass flux appears greater than estimated TDS mass flux during drought periods from June 2000 to March 2003, May 2012 to June 2013, and October 2013 to October 2014 (figs. 11–13), which leads to the conclusion that simulated flux to the Dolores River does not provide a good match to estimated conditions during extended low-flow or drought conditions. These differences could be caused by the low bias for groundwater concentrations withdrawn from PVU pumping wells (26 percent less than estimated values for the post-PVU period) in addition to other model uncertainties, including numerical dispersion, seasonal representation of brine inflow, model-parameter values, and other processes, including ET. These sources of model uncertainty are explored further in the “Model uncertainty and Limitations” section of this report.

## Model Uncertainty and Limitations

Discrepancies between and relations among model results and observations indicate that, although the model provides a reasonable overall match to observed conditions in the Dolores River, there are sources of model uncertainty preventing a close match between simulated and estimated TDS mass flux from PVU pumping wells and the transient patterns of TDS mass flux to the Dolores River. The Paradox Valley groundwater flow and transport model underestimates brine removal from the PVU pumping wells and overestimates TDS mass flux to the river compared to observed conditions, which are the two primary known model-calibration targets. Potential sources of uncertainty that limit the model include numerical dispersion, representation of brine inflow from the breccia, model parameters, and other physical processes, including recharge and ET. Results from simulations exploring these model limitations and sources of uncertainty are described in the Numerical Dispersion”, “Breccia as a Source of Brine,” and “Other Sources of Model Uncertainty” sections of this report.

## Numerical Dispersion

Numerical dispersion is an artifact of the numerical solutions inherent to MODFLOW-6 that smooth the simulated vertical concentration gradient across the freshwater-brine interface and is a possible source of model uncertainty (Langevin and others, 2020). The PVU pumping wells are constructed with open-screen intervals below and near the freshwater–brine interface, and because the model effectively smooths the TDS concentration across the freshwater-brine

interface, simulated groundwater TDS concentrations captured by PVU pumping wells can be less than estimated values. This effect hindered the simultaneous simulation of accurate concentrations in the PVU wells near the river and was exacerbated by simulated infiltration of fresh water from the Dolores River that also diluted concentrations in the upper model layers. Although numerical dispersion may be reduced with sufficiently fine spatial and temporal discretization, testing of increased vertical discretization did not substantially reduce this dispersion and caused excessively long model execution times. The model does simulate the magnitude and variability of TDS mass flux from groundwater to the Dolores River and concentrations at the downstream streamgage reasonably well, except during drought conditions. A limitation is a simulated freshwater-saltwater interface that may be more vertically diffuse than the actual interface, which results in simulated TDS mass withdrawn by the PVU pumping wells of 190,224 kg/d (76,588 tons/yr) that is about three-quarters (74 percent) of the reported withdrawals of 258,309 kg/d (104,000 tons/yr; table 6; Mast, 2017). This underestimate of simulated mass flux from PVU pumping wells could be contributing to the overestimate of simulated mass flux to the river of 164,724 kg/d (66,321 tons/yr) compared to the Mast (2017) estimate of 108,713 kg/d (43,770 tons/yr; 41 percent greater; table 7). Conceptually, extracting less brine from the alluvial aquifer would allow more brine to discharge to the Dolores River, although this relation also can be affected by model parameters, such as vertical and horizontal hydraulic conductivity and streambed conductance, and other hydrologic processes such as recharge and ET.

## Breccia as a Source of Brine

Mass flux of TDS from the underlying collapse breccia is represented in the 33-year simulation using a constant-concentration time-varying water flux tied to precipitation rates in the La Sal Mountains 8-months prior, as described in the “Hydraulic Head-Dependent Flow Boundaries” section of this report. This flux is assigned to 31 cells in model layer 7 that underlie the mapped extent of collapse breccia beneath the Dolores River (fig. 2). Because there are no data with which to evaluate concentrations, rates, and timing of brine inflow from the underlying breccia, the representation of breccia as a source of brine inflow was explored to evaluate if increasing the simulated brine source would result in increased groundwater TDS concentrations and thus simulated TDS mass-flux rates from PVU pumping wells that match estimated values.

To evaluate the effects of brine inflow on low-biased groundwater TDS concentrations, the time-varying TDS mass flux of brine from the breccia into the alluvial aquifer was first simulated as a constant flux with the same long-term average value as the 33-year simulation (table 8). The inflow representing deep breccia underflow was simulated with a constant concentration of 354 kg/m<sup>3</sup>, which is the saturated concentration of sodium-chloride salt in water, multiplied by the

average inflow rate from the 33-year simulation ( $971.14 \text{ m}^3/\text{d}$ ) distributed equally across 31 cells in model layer 7. Mass-flux results from the constant-breccia flux simulation provided results similar to the 33-year calibrated simulation (table 8) and provided an improved match between simulated and estimated transient patterns of PVU withdrawals (fig. 19). As expected, because the mass-flux values were similar between the constant-breccia flux simulation and the 33-year calibration, the constant-breccia flux representation of brine inflow did not substantially increase the overall groundwater TDS concentrations or mass-flux rates from PVU pumping wells (fig. 19; table 8). The constant-breccia flux simulation reduced the TDS mass flux to the Dolores River by about  $14,000 \text{ kg}/\text{d}$  (fig. 20). These results indicated that the constant-breccia flux simulation best replicated the transient pattern in observed TDS mass flux from PVU pumping wells and that the 8-month time lag of precipitation rates in the La Sal Mountains used to simulate brine inflow in the calibrated model may be an overly complex representation, which does not substantially change or improve the model.

To explore the use of the brine source to replicate estimated PVU pumping concentrations and mass-flux rates, the flow rate in the constant-breccia flux simulation was incrementally increased until a reasonable match was achieved between simulated and estimated TDS mass-flux withdrawal from PVU pumping wells (fig. 19). The inflow was simulated with a constant concentration of  $354 \text{ kg}/\text{m}^3$ , the saturation concentration of sodium chloride in water, multiplied by the average inflow rate of  $2,145 \text{ m}^3/\text{d}$  distributed equally across 31 cells in model layer 7. Results from this increased constant-breccia flux simulation (table 8) successfully replicated the PVU TDS mass-flux withdrawal rate, indicating that a stronger brine-source term can raise groundwater TDS concentrations, overcome numerical dispersion, and match estimated PVU TDS mass-flux withdrawal rates. Although the increased constant-breccia flux simulation provided a close match between simulated and estimated PVU TDS mass-flux withdrawal rates, the simulation also substantially increased the TDS mass flux to the Dolores River and overestimated this value compared to estimated TDS mass flux to the river (table 8; fig. 20). The increased mass flux from the breccia also increased outflows to ET and storage (table 8). Neither the 33-year simulation nor the two constant-breccia flux simulations correctly replicated the transient pattern of low estimated TDS mass flux to the river during drought periods (fig. 20). These results indicate several alternative model parameters and conceptual models that could be considered in additional model configurations, as described in the “Other Sources of Model Uncertainty” section of this report.

## Other Sources of Model Uncertainty

Numerical dispersion and the breccia-source term were explored as sources of uncertainty related to PVU pumping wells, yet questions remain. For the post-PVU period,

simulated TDS mass flux from PVU pumping wells was about 26 percent less than estimated, simulated TDS mass flux to the Dolores River was about 41 percent greater than estimated, and these results are accentuated during drought. Increasing brine inflow resulted in an improved match between simulated and estimated TDS mass flux from PVU pumping wells, but the resulting simulated mass flux to the Dolores River was much greater than observed conditions, and the difference increased during drought, indicating processes other than the brine source are affecting TDS mass flux to the river. Seasonal estimates of TDS mass flux to the Dolores River indicate that brine discharge is minimal during spring runoff when river stage and groundwater levels are highest, suppressing discharge of brine to the river (Mast, 2017; Mast and Terry, 2019). In addition, previous studies (Mast, 2017; Mast and Terry, 2019) observed that TDS mass flux to the river is greatest during low-flow winter periods when the surficial freshwater lens is minimal and upward gradients allow brine to discharge to the river. Presumably, drought conditions would be similar to observed low-flow conditions, which are reasonably simulated by the model; however, conditions observed during the drought periods from June 2000 to March 2003, May 2012 to June 2013, and October 2013 to October 2014 indicate that TDS concentrations and mass flux to the river are minimal during prolonged drought periods in direct opposition to the observed seasonal patterns. These results indicate that TDS discharge to the river during drought conditions may be affected by processes different than those during seasonal low-flow conditions and these differences are not well represented by the model.

During model calibration, several model parameters were identified as highly sensitive in the evaluation of model results. The most sensitive parameters were the vertical hydraulic conductivity of the alluvial aquifer, conductance of the Dolores River streambed sediments (streambed conductance), recharge rate, and ET extinction depth and rate. (table 3). Simulated transport of TDS to the river could perhaps be reduced by decreasing vertical hydraulic conductivity for cells representing the alluvial aquifer near the river, decreasing the streambed conductance, or adjusting the simulated representation of recharge and ET. Alluvial-aquifer hydraulic conductivity presently is simulated as a constant value across the model domain, and although the available data are not sufficient to provide a spatial distribution of hydraulic conductivity, there may be spatial variation or zonation of this parameter near the river that could be explored with additional field efforts and model configurations. Similarly, the streambed conductance serves as a “valve” in the model that allows water and TDS to discharge to the river. The model presently uses a single value for streambed conductance. Like hydraulic conductivity, the value and spatial zonation of the streambed conductance parameter could be evaluated by additional model configurations. Reducing this parameter value could also reduce TDS mass flux to the river.

**Table 8.** Simulated total dissolved solids mass-flux budget components for average 33-year, constant-breccia flux, and increased constant-breccia flux simulations for the Paradox Valley, Colo. (Heywood and others, 2024).

[Pre-PVU period is October 1987–June 1996. Post-PVU period is June 1996–November 2020; Constant-breccia flux is set to match average flux rate in the 33-year simulation. Increased constant-breccia flux is set to match estimated flux rate from PVU pumping wells. Total storage is confined plus unconfined storage. Flux also provided in tons per year for consistency with Bureau of Reclamation reporting preferences. PVU, Paradox Valley Unit; kg/d, kilograms per day; tons/yr, tons per year]

| Budget component            | 33-year simulation |                |                 | Constant-breccia flux |                |                 | Increased constant-breccia flux |                |                 |
|-----------------------------|--------------------|----------------|-----------------|-----------------------|----------------|-----------------|---------------------------------|----------------|-----------------|
|                             | 33-year period     | Pre-PVU period | Post-PVU period | 33-year period        | Pre-PVU period | Post-PVU period | 33-year period                  | Pre-PVU period | Post-PVU period |
| Mass-flux inflows, in kg/d  |                    |                |                 |                       |                |                 |                                 |                |                 |
| Infiltrated precipitation   | 0                  | 0              | 0               | 0                     | 0              | 0               | 0                               | 0              | 0               |
| Irrigation-return flow      | 0                  | 0              | 0               | 0                     | 0              | 0               | 0                               | 0              | 0               |
| Northwest underflow         | 0                  | 0              | 0               | 0                     | 0              | 0               | 0                               | 0              | 0               |
| Deep breccia underflow      | 343,784            | 379,861        | 332,772         | 343,782               | 343,782        | 343,782         | 598,455                         | 598,455        | 598,455         |
| Stream leakage inflow       | 161                | 225            | 142             | 164                   | 229            | 144             | 153                             | 215            | 135             |
| PVU pumping wells           | 767                | 941            | 714             | 1,481                 | 2,602          | 1,114           | 474                             | 586            | 438             |
| Total storage               | 317,061            | 401,741        | 291,214         | 298,640               | 422,577        | 266,979         | 291,696                         | 374,621        | 272,109         |
| Total in                    | 661,773            | 782,768        | 624,842         | 644,067               | 769,190        | 612,019         | 890,778                         | 973,877        | 871,137         |
| Mass-flux outflows, in kg/d |                    |                |                 |                       |                |                 |                                 |                |                 |
| Evapotranspiration          | -64,293            | -113,043       | -49,413         | -59,851               | -103,241       | -47,109         | -91,927                         | -135,293       | -79,161         |
| Stream leakage outflow      | -198,795           | -309,958       | -164,865        | -177,201              | -266,853       | -150,870        | -311,662                        | -399,195       | -285,396        |
| PVU pumping wells           | -144,731           | -33,365        | -178,724        | -147,025              | -34,445        | -181,363        | -176,103                        | -36,319        | -218,768        |
| Total storage               | -253,953           | -326,401       | -231,839        | -259,990              | -364,651       | -232,676        | -311,086                        | -403,070       | -287,813        |
| Total out                   | -661,772           | -782,767       | -624,841        | -644,067              | -769,190       | -612,018        | -890,778                        | -973,877       | -871,138        |
| Net mass flux, in kg/d      |                    |                |                 |                       |                |                 |                                 |                |                 |
| Net flux to Dolores River   | -198,634           | -309,733       | -164,723        | -177,037              | -266,624       | -150,726        | -311,509                        | -398,980       | -285,261        |
| Net PVU pumping wells       | -143,964           | -32,424        | -178,010        | -145,544              | -31,843        | -180,249        | -175,629                        | -35,733        | -218,330        |
| Net total storage           | 63,108             | 75,340         | 59,375          | 38,650                | 57,926         | 34,303          | -19,390                         | -28,449        | -15,704         |
| Net mass flux, in tons/yr   |                    |                |                 |                       |                |                 |                                 |                |                 |
| Net flux to Dolores River   | -79,974            | -124,705       | -66,321         | -71,279               | -107,348       | -60,685         | -125,420                        | -160,637       | -114,852        |
| Net PVU pumping wells       | -57,963            | -13,055        | -71,670         | -58,599               | -12,821        | -72,572         | -70,712                         | -14,387        | -87,904         |
| Net total storage           | 25,409             | 30,333         | 23,906          | 15,561                | 23,322         | 13,811          | -7,807                          | -11,454        | -6,323          |

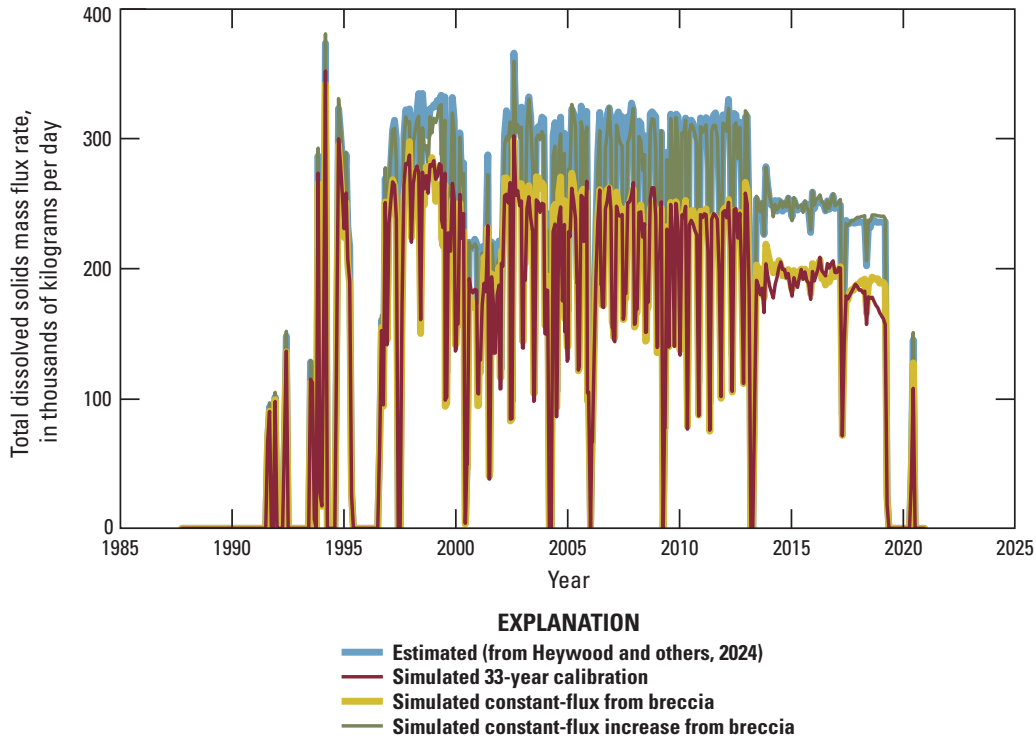


**Figure 19.** Estimated and simulated total dissolved solids mass flux removed by Paradox Valley Unit (PVU) pumping wells for the 33-year simulation and alternative representations of the breccia as a constant-flux source in the Paradox Valley, Colo., 1987–2020 (Heywood and others, 2024).

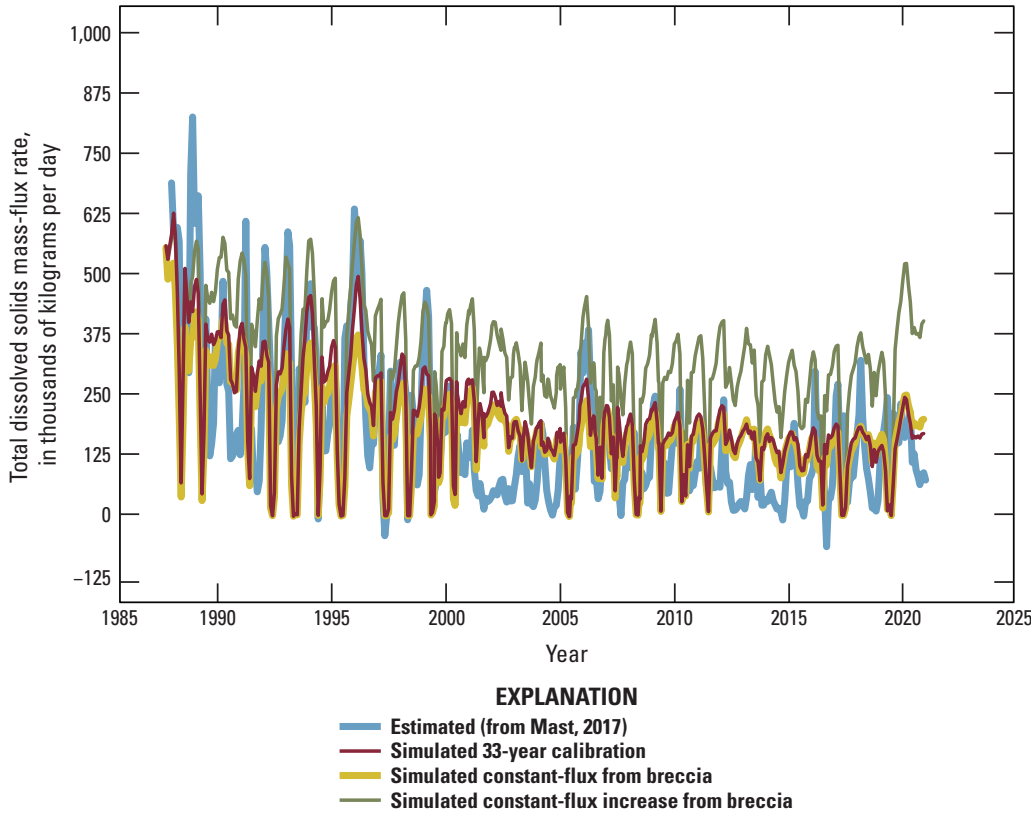


**Figure 20.** Estimated and simulated total dissolved solids mass flux to the Dolores River for the 33-year simulation and alternative representations of the breccia as a constant-flux source in the Paradox Valley, Colo., 1987–2020 (Heywood and others, 2024).

The differences between estimated and simulated TDS concentration and mass flux to the Dolores River are greater during the post-PVU period than during the pre-PVU period, and this difference is exaggerated during drought. In general, there has been a substantial reduction in streamflow of the Dolores River since the impoundment of McPhee Reservoir in 1985 (Voggeser, 2001) and the onset of drier conditions in the late 1990s (fig. 6), and this reduction in streamflow could result in changing conditions in the Paradox Valley that are not well represented in the model. Correcting the difference between estimated and simulated TDS mass flux to the Dolores River during drought could perhaps be achieved by examining sensitive recharge and ET parameters and representation. Precipitation recharge is simulated as 6 percent of the actual precipitation, and lesser percentages of precipitation recharge could be considered. For example, Paschke (2011) estimated groundwater recharge as 1–2 percent of precipitation for the Denver Basin aquifer system in eastern Colorado. Recharge from the La Sal Mountains presently is configured as a constant inflow and is another potential source of model uncertainty. Representing this source of recharge as a transient function related to precipitation rates rather than a constant inflow could perhaps improve model fit.

Evapotranspiration extinction depth and rates also were identified as sensitive model parameters. During periods of low streamflow, simulated TDS mass flux to ET is somewhat less than during periods of higher streamflow. Because ET is computed as a function of depth to water, simulated ET mass-flux rates during periods of low streamflow would indicate that simulated depths to water are greater than the assigned simulation ET extinction depth of 1 m. Increasing the ET extinction depth or ET rates would increase the TDS mass flux to ET and decrease simulated TDS mass flux to the river, especially during drought when the water table would be lowest. In the physical system, TDS removed from the groundwater system by ET would be precipitated as an evaporative mineral and accumulate in the unsaturated zone above the water table, which is supported by observations of evaporative salt deposits at the land surface in the Paradox Valley. These evaporative deposits could then be an additional source of TDS to the Dolores River and the groundwater system. Evaporative processes that precipitate salts near the land surface, coupled with the seasonal rise and fall of river stage and the water table could dissolve evaporative salt deposits and result in near-surface circulation of TDS that is not represented by the model.

## Brine Management Scenarios

Since 2019, injection-pressure limits have constrained the volume of brine that could be pumped into the existing PVU injection well, which consequently limited the quantity of brine that was withdrawn from the PVU pumping wells (Reclamation, 2022). To inform decisions regarding alternative

strategies for brine-discharge management, five 5-year scenarios for the period from 2020 to 2025 were simulated. Scenario 1 is a simulation of future conditions with zero PVU pumping after March 2019, which would be a continuation of the cessation of operations since the March 14, 2019, earthquake. This simulation serves as a base case for comparison to the other scenarios. Scenarios 2 and 3 simulate alternative schedules for withdrawing about 161,443 kg/d (65,000 tons/yr) of TDS at the PVU pumping wells, which is about two-thirds of the rate achieved during 2010 through 2018 and is referred to as the target rate in figure 21. Scenario 4 simulates the possible effect of better irrigation efficiency and decreased irrigation-return flow on brine discharge. Scenario 5 simulates the effect of a prolonged 5-year drought with cessation of PVU withdrawals and zero irrigation-return flows.

For management scenarios 1 through 4, simulated conditions on December 31, 2020, were used as starting conditions. Average monthly streamflow during 1987 through 2020 at the upstream streamgage was specified as inflow to the Dolores River (fig. 7). For seasonal ET, diversions from West Paradox Creek, and agricultural recharge (irrigation-return flow), the values used were those specified during the 33-year simulation. For groundwater underflow, precipitation recharge, and West Paradox Creek inflow, the values used were those specified for the 1,000-year simulation. Because 7 of the final 9 years of the 33-year simulation produced below average values of groundwater recharge and streamflow, the specification of average values as input for recharge, inflows, and groundwater underflows during the scenarios simulates a recovery from drought conditions and results in increased groundwater flux toward the Dolores River.

For management scenario 5 (drought scenario), simulated conditions on December 31, 2020, were used as starting conditions. For the first 6 months of the drought scenario, monthly streamflow measured at the upstream streamgage from December 2020 through May 2021 was specified as inflow to the river. For the subsequent 54 months, average monthly streamflow measured during 3 drought years (2002, 2018, and 2020) was specified as inflow to the river. For the drought scenario, infiltration of precipitation and irrigation-return flow were assumed to be zero, and no values were specified. Because there were no releases from Buckeye Reservoir during the spring of 2021, and such releases would be unlikely during a prolonged drought, the inflow to West Paradox Creek was set to a base-flow value of 1,223 m<sup>3</sup>/d, coming from groundwater seepage originating from outside the model domain. The average groundwater underflow specified for the drought was the same as that used in the other management scenarios.



### Scenario 1: Simulated Brine Discharge with No Brine Extraction

The first scenario simulates brine discharge to the Dolores River for the period 2021–25, using average hydro-logic conditions from the 33-year simulation but with no pumping at PVU extraction wells beginning in 2019. The simulated concentration in the Dolores River in this scenario varies by month because of the specified seasonal variabilities in Dolores River streamflow and evapotranspiration. These simulated conditions approximate historical conditions since PVU operations ceased after the magnitude 4.5 earthquake on March 4, 2019. The simulated TDS mass flux to the Dolores River during this 5-year scenario is 143,719 kg/d or about 57,864 tons/yr (table 9).

### Scenario 2: Simulated Brine Discharge with Reduced Brine Extraction

High pressures in the PVU injection reservoir have likely induced seismicity (King and others, 2014), which may limit future injection volumes to about two-thirds (630 m<sup>3</sup>/d [60.8 million gallons per year]) of the average annual volume since 1996. Scenario 2 simulates reduced withdrawals pumped continuously and equally from the six PVU pumping wells that were used for 98 percent of the brine withdrawals during 2010–20. As discussed in the “Model Uncertainty and Limitations” section of this report, simulated TDS

concentrations for PVU pumping wells of about 193,000 mg/L are less than the observed concentrations of around 257,000 mg/L. With the continuous-pumping schedule, scenario 2 results in a simulated TDS mass flux from PVU pumping wells of 121,363 kg/d (48,863 tons/yr; table 9), which is about 25 percent less than the target rate of 65,000 tons/yr (fig. 21). In this scenario, the average reduction in TDS flux to the Dolores River is 22 percent less than scenario 1 (no pumping).

### Scenario 3: Simulated Brine Discharge with Brine Extraction for 9 Months Each Year

Modeling of scenario 3 was motivated by the observation that brine discharge is reduced when the Dolores River stage is high, which decreases the upward gradient of the groundwater hydraulic head from the aquifer to the river (Mast and Terry, 2019). It was hypothesized that efficiency of TDS mass-flux reduction might be improved if PVU pumping was suspended during times of high river stage, when less brine discharges to the river and pumping may withdraw diluted brine. It was further reasoned that withdrawals could then be proportionately increased when river stage was lower and brine discharge was higher. For scenario 3, the annual withdrawal volume was the same as that specified for scenario 2, and it was distributed in similar proportions amongst the six PVU pumping wells. However, because pumping only occurred for 9 months each year (July through March), the total rate of 840 m<sup>3</sup>/d was higher than the rate of 630 m<sup>3</sup>/d for scenario 2. Specification

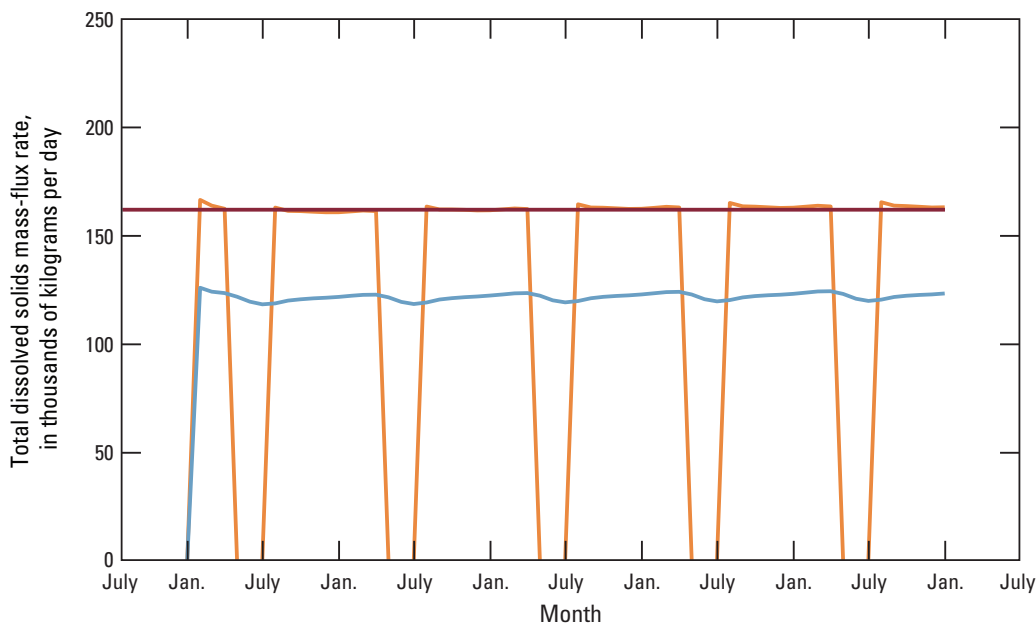


**Figure 21.** Simulated total dissolved solids mass flux withdrawn from Paradox Valley Unit pumping wells in scenarios 2 and 3 for the Paradox Valley, Colo., 2021–2025 (Heywood and others, 2024).

**EXPLANATION**

- Target: 160 thousands of kilograms per day (65,000 tons per year)
- Scenario 2: Pump continuously
- Scenario 3: Pump 9 months each year

**Table 9.** Simulated 5-year average values of total dissolved solids mass flux withdrawn from the Paradox Valley Unit pumping wells and total dissolved solids mass flux to the Dolores River and evapotranspiration for five management scenarios for the Paradox Valley, Colo., 2021–2025 (Heywood and others, 2024).

[Flux also presented in tons per year for consistency with Bureau of Reclamation reporting. TDS, total dissolved solids; PVU, Paradox Valley Unit; —, not determined]

| Scenario                              | TDS mass flux withdrawn from PVU pumping wells | TDS mass flux to the Dolores River | TDS mass flux difference from scenario 1 | Percent change of TDS mass flux from scenario 1 | TDS mass flux to evapotranspiration |
|---------------------------------------|--|------------------------------------|--|---|-------------------------------------|
| TDS mass flux in kilograms per day    |  |                                    |  |   |                                     |
| 1: No pumping                         | 0  | 143,719                            | —  | —   | 55,983                              |
| 2: Pumping every month                | 121,363  | 112,424                            | –31,295                                  | –22   | 47,116                              |
| 3: Pumping for 9 months               | 121,760  | 111,425                            | –32,293                                  | –23   | 47,914                              |
| 4: No irrigation recharge, no pumping | 0  | 139,998                            | –3,721                                   | –2.6  | 55,487                              |
| 5: Drought conditions, no pumping     | 0  | 165,349                            | 21,631                                   | +15   | 27,952                              |
| TDS mass flux in tons per year        |  |                                    |  |   |                                     |
| 1: No pumping                         | 0  | 57,864                             | —  | —   | 22,540                              |
| 2: Pumping every month                | 48,863   | 45,264                             | –12,600                                  | –22   | 18,970                              |
| 3: Pumping for 9 months               | 49,023   | 44,862                             | –13,002                                  | –23   | 19,291                              |
| 4: No irrigation recharge, no pumping | 0  | 56,366                             | –1,498                                   | –2.6  | 22,340                              |
| 5: Drought conditions, no pumping     | 0  | 66,573                             | 8,709                                    | +15   | 11,254                              |

of this withdrawal schedule produced a 23-percent annual reduction in TDS mass flux to the Dolores River compared to scenario 1 (no pumping) but resulted in little change to the TDS mass flux to the river compared to the continuous pumping schedule in scenario 2.

### Scenario 4: Simulated Brine Discharge with Reduced Irrigation-Return Flow

Recharge to groundwater from irrigation-return flow is caused by the amount of water used for irrigation exceeding the amount consumed by crops. It was reasoned that improvements to irrigation efficiency might reduce this component of recharge and, hence, reduce the shallow groundwater flow that mixes with brine before discharging into the river. In scenario 4, the effect of irrigation-return flow on brine discharge was evaluated by setting this component of recharge to zero. This simulation of “perfect” irrigation efficiency (zero groundwater recharge) yielded an annual reduction in TDS mass flux to the Dolores River of about 2.6 percent compared to that of scenario 1, which uses the value of irrigation-return flow estimated for the 33-year simulation.

### Scenario 5: Simulated Brine Discharge During a 5-Year Drought with No Brine Extraction

Interest in scenario 5 was motivated by the drought conditions that existed as of June 2021 and the need to improve model fit during drought. As in scenario 1, this simulation had no PVU pumping or irrigation-return flows, but scenario 5 also had no precipitation recharge to simulate a persistent 5-year drought. Although the decreased groundwater recharge simulated in this scenario tends to decrease the groundwater discharge to the Dolores River, the lower simulated stage of the Dolores River causes an increased net value of TDS mass flux to the river (table 9). The simulated value of annual TDS mass flux to the Dolores River for the drought conditions in scenario 5 is 15 percent greater than the average hydrologic conditions simulated in scenario 1. Although drought conditions would presumably be like observed low-flow conditions, TDS mass flux to the river observed during the drought periods from June 2000 to March 2003, May 2012 to June 2013, and October 2013 to October 2014 was notably less than the simulated mass flux during these three periods (fig. 18). Results from scenario 5 indicate that the model input parameters are not accurately simulating TDS mass flux to the river during drought conditions. These results further indicate that adjusting only recharge parameters does not result in a satisfactory model fit during drought and that perhaps adjusting

aquifer properties, such as vertical hydraulic conductivity of the alluvial aquifer, streambed conductance, and ET parameters, would lead to improved model fit.

### Scenario Comparison

The water levels and concentrations measured and simulated for November 2020 occurred after an unusually dry period in which streamflow and precipitation were below historical norms during 7 of the preceding 9 years. Because these November 2020 water levels and concentrations were used as the initial conditions for all the scenario simulations and because the average hydrologic conditions specified for scenarios 1 through 4 are wetter than the drier-than-normal conditions observed during most of the last decade (2011–20), the increased groundwater flux caused by these wetter conditions increased the simulated TDS mass flux to the river, which is illustrated by the generally upward 5-year trends for scenarios 1 through 4 (fig. 22). Scenario 5, however, simulates drought conditions for an additional 5 years, which is a continuation of antecedent drought conditions observed during most of the last decade. The downward 5-year trend of simulated TDS mass flux to the river in this scenario (fig. 22) is a consequence of the lower-than-normal values for groundwater recharge that were used for scenario 5.

Scenario 1 simulates no future PVU pumping, and scenario 2 simulates resumption of PVU pumping at two-thirds of the historical extraction rate, as necessitated by earthquake-avoidance injection-pressure constraints. The modified 9-month pumping schedule simulated in scenario 3 predicts a minor decrease in TDS mass flux to the river as compared to the results of scenario 2. Such a minor improvement in efficiency may not warrant the additional complexity of timing episodic pumping with river stage, although seasonal pumping may offer opportunities for system maintenance during periods when PVU pumping does not substantially affect TDS concentrations in the river (Paschke and others, 2024). Similarly, the 2.6-percent decrease in TDS mass discharged to the river predicted by scenario 4 may not justify the considerable effort required to improve irrigation efficiencies.

Results from all simulations indicate that ET is a substantial process to consider in simulating TDS mass flux to the river. For this study, simulated TDS mass flux to ET was greatest for scenarios 1 and 4, which had no PVU pumping. Similarly, simulated TDS mass flux to ET for scenarios 2 and 3 was less than for scenario 1, indicating that PVU wells may capture some TDS that would have otherwise been removed from the system via ET. For scenario 5, TDS mass flux to ET was about half of that from scenario 1 likely because ET is simulated as a function of depth to the water table (extinction

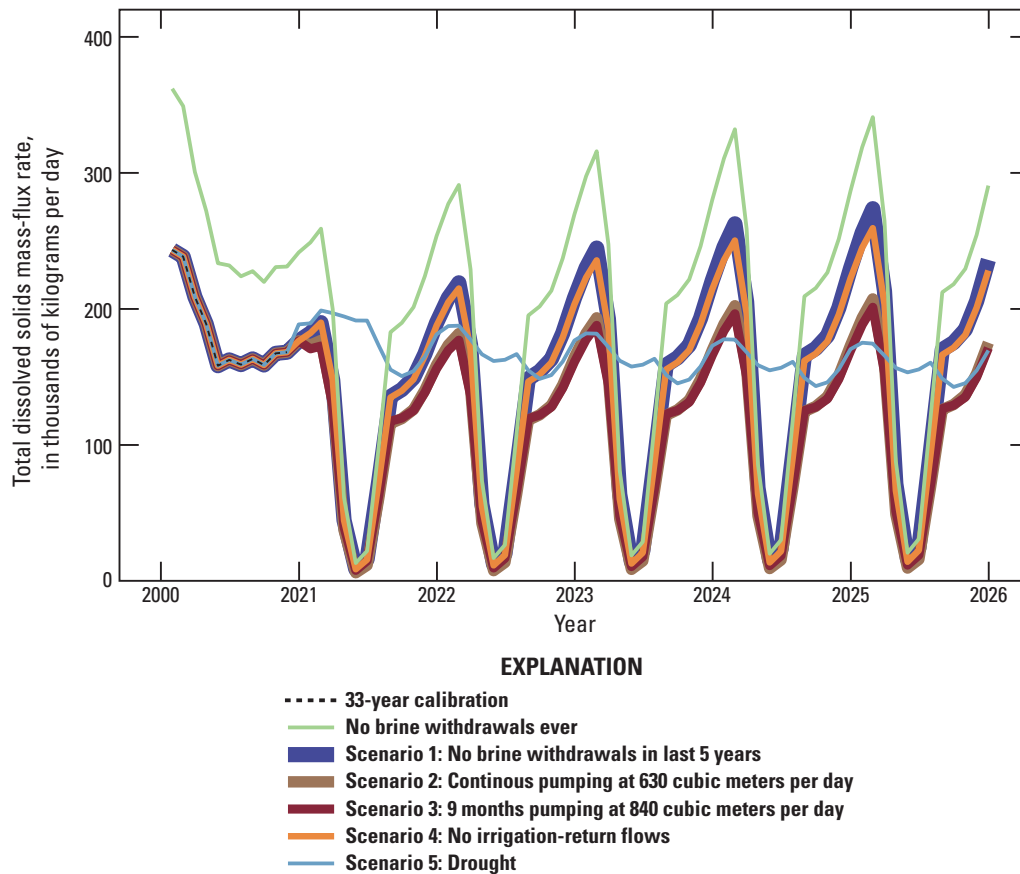


**Figure 22.** Simulated total dissolved solids mass flux to the Dolores River for five management scenarios at the Paradox Valley Unit, Paradox Valley, Colo. Continuous pumping rate simulated at 630 cubic meters per day and 9-month pumping rate simulated at 840 cubic meters per day, 2021–2025 (Heywood and others, 2024).

depth), and the water table is lowered during drought. Adjustments to recharge in scenario 5 did not adequately represent observed drought conditions and further indicate that additional model configurations could consider the effects ET processes and parameters on model results.

As discussed previously, numerical dispersion of simulated concentrations limits the accuracy of the simulated freshwater-brine interface, and other model uncertainties may also affect the magnitude of simulated TDS mass flux to the Dolores River in the scenarios. Although magnitudes varied, relative differences between the scenarios remained consistent during sensitivity tests of model-parameter values, and therefore may be used to inform PVU operational decisions.

## Additional Research

The distribution of simulated TDS mass flux to the Dolores River depends on properties of the groundwater and surface-water systems, and simulation accuracy could be improved by better estimates of some properties of the surface-water system that affect interaction with the groundwater system. For example, the specified streambed altitude controls the simulated river stage, which affects simulated groundwater levels. Changes in streambed slope affect the river stage and areas of inflow compared to outflow between the shallow alluvial aquifer and the Dolores River. More detailed specification of the Dolores River streambed widths and altitudes could improve the accuracy of simulation of zones of TDS mass flux to the river. To address this data gap, a survey of streambed altitude and width at several locations along the Dolores River could be considered using drone or ground-based lidar methods.

West Paradox Creek may contribute substantial groundwater recharge, which in turn affects groundwater flux and brine discharge to the river; however, streamflow in West Paradox Creek has not been measured since 1973. The accuracy of the simulation could be improved with more recent streamflow data from West Paradox Creek and measurements of altitudes and widths of the creek bed.

Although the approximate depths of groundwater observation wells near the Dolores River have been measured, their screened-interval depth is unknown, and this knowledge gap limits the utility of available water-level observations in these wells. The use of video logging or another technique to determine the actual screened intervals in these wells may be possible. Additional water-level observations farther from the river in the Paradox Valley could also enable improved estimation of the hydraulic conductivities and flux of groundwater through the valley to the river. Depth-specific pressure head differentials in observation wells could also be used to provide measures of the TDS concentration and hydraulic-head gradients and the location of the freshwater-brine interface, which could be used to improve model fit and guide PVU operations.

The stage of the Dolores River affects hydraulic gradients and flow of groundwater in the alluvial aquifer; therefore, loci of brine discharge may vary with river stage. To help delineate zones of enhanced brine discharge to the river, additional geophysical techniques, such as electromagnetic and subsurface resistivity surveys around and along the river, could be completed during times of low river stage, such as those that existed during the drought conditions in spring 2021. Additional surveys of river-SC during low-flow conditions may be beneficial for comparison to the 2013 survey and for identifying reaches where brine discharge is occurring (fig. 8). Furthermore, real-time measurements of pressure head and groundwater SC at varying depths in observation wells could provide a measure of the position of the freshwater-brine interface as well as seasonal changes at a given location.

Although the surficial distribution of alluvium and surrounding consolidated rocks in the Paradox Valley has been mapped, the alluvial thickness and distribution of hydrogeologic units beneath the alluvium is not well constrained. The depth to the collapse breccia in the Paradox Formation is known where it has been identified in the drilling logs of the PVU wells, but the extent of the breccia has only been hypothesized based on interpretations of bedrock altitudes (Paschke and Mast, 2024), and the extent remains highly uncertain. Near the PVU pumping wells and areas downstream where the Dolores River exits the Paradox Valley, low-permeability bedrock crops out at the edges of the alluvial aquifer and collapse breccia and may be controlling groundwater flow and brine discharge. To remedy these knowledge gaps, additional geophysical surveys including surface resistivity, electromagnetic, and passive seismic methods could help to better constrain the subsurface distribution of the collapse breccia and other hydrogeologic units. Drilling of additional boreholes for pumping or observation wells and additional water-level and water-quality monitoring of such wells also could further the understanding of subsurface geology and hydraulic gradients. Finally, a refined three-dimensional hydrogeologic framework model could improve the hydraulic-parameter definition in additional groundwater models, which could likely also enhance the accuracy of the simulated distributions of subsurface brine and discharge.

With respect to model conceptualization and calibration, further research could investigate the model limitations and sources of uncertainty to improve the match between simulated and estimated TDS mass flux from PVU pumping wells and to the Dolores River. Potential sources of uncertainty that limit the model include numerical dispersion, representation of the brine source, estimated aquifer parameters, and representation of recharge and ET processes. During model calibration, the most sensitive parameters were the vertical hydraulic conductivity of the alluvial aquifer, conductance of the Dolores River streambed, recharge rate, and ET extinction depth and rate (table 3). Exploratory simulations of the brine source indicated that an increased constant-breccia flux simulation best replicated the transient pattern observed for TDS mass flux from PVU pumping wells (fig. 19). Model

parameters for vertical hydraulic conductivity of the alluvial aquifer, streambed conductance, and ET extinction depth could be explored by additional modeling efforts to improve the model fit between simulated and observed TDS mass flux to the Dolores River.

Modeling results and system understanding could also benefit from the use of advanced modeling tools for model development and calibration. For example, FloPy (Hughes and others, 2023) is a Python package for creating, running, and post-processing MODFLOW-6 models. FloPy can be used to generate graphics of model input and output to facilitate interpretation of model results and incorporates related MODFLOW-6 programs for model calibration and particle tracking (Hughes and others, 2023). The model also could benefit from a formal parameter-estimation and sensitivity analysis completed with MODFLOW-6 compatible programs, such as PEST++ (White and others, 2020), which is available within FloPy. Using PEST++ and FloPy, multiple model realizations and predictions can be efficiently created, executed, and evaluated to potentially improve model performance and further inform system understanding for the Paradox Valley.

## Summary

Salinity, or total dissolved solids (TDS), of the Colorado River affects agricultural, municipal, and industrial water users and is an important concern in the Western United States. The Dolores River is a major tributary of the Colorado River historically accounting for about 6 percent of the salinity load to the Colorado River, and the primary source of salinity to the Dolores River is the Paradox Valley in southwest Colorado. Formation of the Paradox Valley began during the Miocene, and subsequent erosion exposed the core of a salt-valley anticline where cap rock, collapse features, breccia, and salt-saturated brine developed at the top of the exposed salt diapir. The brine is estimated as at least 10,000 years old and is much older than fresh groundwater in the overlying alluvial aquifer. The brine is dense because of its salt content, and the density difference between the brine and the overlying freshwater aquifer drives upward density-dependent gradients and flow of brine into the base of the alluvial aquifer and the Dolores River. It is this discharge of brine to the Dolores River that causes the observed increases in TDS salinity as the river crosses the Paradox Valley.

Beginning in 1996, the Bureau of Reclamation (Reclamation) began operating a series of pumping wells as part of the Paradox Valley Unit (PVU), which withdraw brine from the alluvial aquifer adjacent to the river to reduce the discharge of brine into the river. The withdrawn brine is disposed of into a 4,570-meter-deep injection well located about 3 miles southwest of the Paradox Valley. The PVU system was developed in the 1970s and 1980s with a test phase of intermittent pumping and injection occurring from 1991 to 1993. Regular operation of the PVU began July 1, 1996, and

by 2015, the PVU had reduced TDS concentrations in the Dolores River by as much as 70 percent compared to pre-PVU conditions. After more than 20 years of injection, seismicity induced by PVU injection has increased, and, on March 4, 2019, injection and thus PVU pumping, were immediately suspended after the occurrence of a 4.5 magnitude earthquake in the region. Except for a short pumping period in the spring 2020, PVU operations remained ceased from March 2019 to June 2022, and on June 1, 2022, the PVU temporarily resumed operations for a six-month trial period with a reduced injection rate of about 625 m<sup>3</sup>/d, or about two thirds of past operations, to gather additional information and guide future operational decisions.

This report describes a MODFLOW-6 three-dimensional numerical model of variable-density groundwater flow and TDS transport for the Paradox Valley, Colorado, developed by the U.S. Geological Survey (USGS) in cooperation with Reclamation for the purposes of evaluating the effect of PVU pumping operations on TDS discharge to the river and guiding additional research. The finite-difference model grid consists of 76 rows and 48 columns oriented from northwest to southeast in alignment with valley topography and groundwater-flow in the near-surface freshwater aquifer. A 7-layer hydro-geologic framework was developed from existing datasets to represent groundwater flow and TDS transport from the underlying Paradox Formation salt to the Dolores River. The model represents a 33-year calibration period from 1987 through 2020 that includes pre-PVU conditions from October 1987 through June 1996 and post-PVU conditions from July 1996 through 2020.

The model simulates the density-dependent transport of dissolved solutes from within the groundwater system into the Dolores River and the resulting river TDS concentrations. Because the MODFLOW-6 groundwater flow and transport equations are coupled by an equation of state that calculates the groundwater density from the simulated solute concentration, the specified initial conditions for groundwater TDS concentrations can substantially affect the simulated transient flow and TDS concentrations of groundwater. Effective model calibration required simulating 1,000-years of steady-state groundwater flow and coupled TDS transport to produce quasi-equilibrium in the distributions of groundwater hydraulic-head altitudes and TDS concentrations. These equilibrated values were subsequently specified as initial conditions for a 33-year transient simulation (1987–2020).

Observations of precipitation, evaporation, agricultural land use, and PVU brine pumping rates were used to specify appropriate boundary conditions to the model representing time-varying recharge, tributary streamflow, groundwater underflow, evapotranspiration (ET), and PVU pumping. Values for average monthly streamflow and TDS concentration at the upstream streamgage the Dolores River at Bedrock (USGS streamgage 09169500) were specified as model input where the Dolores River enters the Paradox Valley. Observed pumping from the PVU, water levels and TDS concentrations in groundwater, and streamflow and estimated TDS

concentrations at the downstream streamgage the Dolores River near Bedrock (USGS streamgage 09171100) were calibration targets that constrained the manual calibration of model parameters representing aquifer hydraulic conductivity, storage, streambed conductance, recharge, and ET. During model calibration, the most sensitive parameters were identified as vertical hydraulic conductivity of the alluvial aquifer, conductance of the Dolores River streambed, recharge rate, and ET extinction depth and rate.

Two primary model-calibration targets were the match between observed and simulated TDS mass flux from PVU pumping wells and the match between estimated and simulated TDS mass flux to the Dolores River. The simulated TDS mass withdrawn by PVU pumping wells is calculated by the model as the product of the assigned pumping rate and simulated TDS concentrations in the aquifer. Because actual pumping rates were assigned as simulated values, the total simulated PVU pumping for the 33-year calibration is within 0.5 percent of the observed values. However, simulated concentrations of TDS withdrawn by the PVU pumping wells are calculated based on the simulated groundwater TDS concentrations. For all the simulated time periods (33-year simulation, pre-PVU, and post-PVU), simulated TDS concentrations and thus TDS mass flux from PVU wells were consistently about 26 percent less than observed values. The representation of brine inflow to the model was explored as a source of this model uncertainty, and results indicated that an increased constant-breccia flux simulation best replicated the magnitude and transient pattern observed for TDS mass flux from PVU pumping wells.

The simulated TDS mass flux to the Dolores River is compared to estimates based on observed streamflow and specific conductance (SC) data for the downstream streamgage. The calibrated model provided a close fit of simulated to measured streamflow at the downstream streamgage, and the calibrated model fit of simulated to measured TDS concentrations at the downstream streamgage was reasonable with the greatest differences occurring during drought periods. Before the start of PVU operations in 1996, simulated peak TDS concentrations in the river at the downstream streamgage are generally less than estimated concentrations. After 1996, simulated peak concentrations often match, but sometimes exceed, peak estimated concentrations. Estimated concentration minima occur during spring runoff when the river stage is greatest and are generally accurately simulated. In general, simulated mass flux to the river for the pre-PVU period is in good agreement with estimated values (2-percent difference). However, the average simulated TDS mass flux to the river for the post-PVU period is greater than estimated values. Simulated TDS concentrations in the river also are greater than estimated concentrations during the drought periods from June 2000 to March 2003, May 2012 to June 2013, and October 2013 to October 2014, and the model overestimated TDS mass flux to the river by about 41 percent during the post-PVU period (simulated value of 164,724 kg/d or 66,321 tons/yr compared to the estimated value of 108,713 kg/d or 43,770 tons/yr).

Model uncertainty with respect to TDS mass flux to the river indicates other processes or parameters not well represented in the model are affecting the system, especially during drought. Model parameters for vertical hydraulic conductivity of the alluvial aquifer, streambed conductance, and ET extinction depth could be explored by additional modeling efforts to improve the model fit between simulated and observed TDS mass flux to the Dolores River.

Five scenarios of 5-year durations for 2021–25 were simulated to assist evaluation of alternative strategies to manage the discharge of brine into the Dolores River. The first scenario simulates no future withdrawals at PVU pumping wells and serves as a base case for comparison to the other scenarios. Two scenarios simulate the effect of varying the timing of withdrawals from PVU pumping wells on TDS mass flux to the Dolores River. Comparison of these scenarios indicates that scheduling brine pumping during times of low river stage is nearly as effective as pumping brine year-round. This low-flow scenario may be advantageous as an alternative schedule for brine injection and seismic-risk reduction. The fourth scenario simulates the effect of reduced irrigation-return flow on TDS mass flux to the river and predicts a slight reduction of TDS flux to the Dolores River but not as great a reduction as that of using the PVU to remove brine. The fifth scenario simulates 5 years of prolonged drought conditions without PVU pumping and indicates that brine discharge during drought would be about 15 percent greater than during average hydrologic conditions, presumably because of low river stage. Results from scenario 5 are consistent with the 33-year calibrated model and indicate that aquifer properties and ET processes and parameters may be affecting simulation results during drought.

The Paradox Valley groundwater flow and TDS transport model provides a reasonable overall match to observed conditions in the Dolores River; however, discrepancies between and relations among model results and observations indicate there are sources of model uncertainty. The model is useful for evaluating relative differences between brine management scenarios to inform PVU operational decisions and to identify gaps in data and process understanding. Representation of the brine source, hydraulic-conductivity parameters, and recharge and ET processes were identified as areas for potential additional field and modeling research. Additional research in the Paradox Valley might include field-data collection that provides additional information on the hydrogeologic framework, groundwater levels, groundwater TDS concentrations, stream characteristics, and aquifer properties. Additional modeling efforts could benefit from applying advanced tools for model development, calibration, and visualization including parameter-estimation and sensitivity analysis. Statistical evaluation of model limitations and sources of uncertainty could improve the match between simulated and estimated TDS mass flux from PVU pumping wells and to the Dolores River to further inform model predictions and system understanding for the Paradox Valley.

## Acknowledgments

The authors thank U.S. Geological Survey colleagues Patrick Lambert and John Masterson for providing thoughtful reviews on a previous version of this report.

## References Cited

- Bakker, M., Schaars, F., Hughes, J.D., Langevin, C.D., and Dausman, A.M., 2013, Documentation of the seawater intrusion (SWI2) package for MODFLOW: U.S. Geological Survey Techniques and Methods, book 6, chap. A46, 47 p., accessed October 4, 2022, at <https://pubs.usgs.gov/tm/6a46>.
- Ball, L.B., Bedrosian, P.A., and Minsley, B.J., 2020, High-resolution mapping of the freshwater–brine interface using deterministic and Bayesian inversion of airborne electromagnetic data at Paradox Valley, USA: *Hydrogeology Journal*, v. 28, p. 941–954, accessed October 4, 2022, at <https://doi.org/10.1007/s10040-019-02102-z>.
- Ball, L.B., Bloss, B.R., Bedrosian, P.A., Grauch, V.J.S., and Smith, B.D., 2015, Airborne electromagnetic and magnetic survey data of the Paradox and San Luis Valleys, Colorado: U.S. Geological Survey Open-File Report 2015–1024, 19 p., accessed December 17, 2020, at <https://doi.org/10.3133/ofr20151024>.
- Banta, E.R., 2000, MODFLOW-2000, the U.S. Geological Survey Modular Ground-Water Model; documentation of packages for simulating evapotranspiration with a segmented function (ETS1) and drains with return flow (DRT1): U.S. Geological Survey Open-File Report 2000–466, 127 p., accessed April 23, 2024, at <https://doi.org/10.3133/ofr00466>.
- Barnes, H.H., 1967, Roughness characteristics of natural channels: U.S. Geological Survey Water-Supply Paper 1849, 213 p., accessed April 23, 2024, at <https://doi.org/10.3133/wsp1849>.
- Block, L.V., Wood, C.K., Yeck, W.L., and King, V.M., 2015, Induced seismicity constraints on subsurface geological structure, Paradox Valley, Colorado: *Geophysical Journal International*, v. 200, no. 2, p. 1172–1195, accessed December 17, 2020, at <https://doi.org/10.1093/gji/ggu459>.
- Bureau of Reclamation [Reclamation], 1978a, Paradox Valley Unit definite plan report: Bureau of Reclamation, Colorado River Basin Salinity Control Project, 91 p., accessed March 12, 2021, at <https://www.usbr.gov/uc/progact/paradox/docs/DPR-1978.pdf>.
- Bureau of Reclamation [Reclamation], 1978b, Paradox Valley Unit definite plan report, Appendix B—Hydrosalinity: Bureau of Reclamation, Colorado River Basin Salinity Control Project, accessed March 12, 2021, at <https://www.usbr.gov/uc/progact/paradox/docs/DPR1978-Appdx-B.pdf>.
- Bureau of Reclamation [Reclamation], 2021, Colorado River Basin salinity control program: Bureau of Reclamation website, accessed February 3, 2021, at <http://www.usbr.gov/uc/progact/salinity/index.html>.
- Bureau of Reclamation [Reclamation], 2022, Paradox Valley Unit: Bureau of Reclamation website, accessed February 16, 2022, at <https://www.usbr.gov/uc/progact/paradox/index.html>.
- Cater, F.W., and Craig, L.C., 1970, Geology of the salt anticline region in southwestern Colorado: U.S. Geological Survey Professional Paper 637, 80 p., 2 pls. [Available at <https://doi.org/10.3133/pp637>.]
- Colorado Water Conservation Board and Colorado Division of Water Resources, 2005, Division 7 San Juan/Dolores—Irrigated lands 2005, [dataset]: State of Colorado, Colorado’s Decision Support Systems, accessed March 11, 2021, at <https://cdss.colorado.gov/gis-data/division-7-san-juan/dolores>.
- Colorado Water Conservation Board and Colorado Division of Water Resources, 2021, GIS data by the category: State of Colorado, Colorado’s Decision Support System, accessed July 22, 2021, at <https://cdss.colorado.gov/gis-data/gis-data-by-category>.
- Denlinger, R.P., and O’Connell, D.R.H., 2020, Evolution of faulting induced by deep fluid injection, Paradox Valley, Colorado: *Bulletin of the Seismological Society of America*, v. 110, no. 5, p. 2308–2327, accessed December 17, 2020, at <https://doi.org/10.1785/0120190328>.
- Elston, D.P., and Shoemaker, E.M., 1961, Preliminary structure contour map on top of salt in the Paradox Formation of the Hermosa Group in the salt anticline region, Colorado and Utah: U.S. Geological Survey Oil and Gas Investigations Map OM–209, scale 1:250,000, accessed April 23, 2024, at <https://doi.org/10.3133/om209>.
- Essaid, H.I., 1990, The computer model SHARP, a quasi-three-dimensional finite-difference model to simulate freshwater and saltwater flow in layered coastal aquifer systems: U.S. Geological Survey Water-Resources Investigations Report 90–4130, 181 p., accessed April 23, 2024, at <https://doi.org/10.3133/wri904130>.
- Fenneman, N.M., 1931, *Physiography of Western United States*: New York, McGraw-Hill Book Co., 534 p.
- Fetter, C.W., 1994, *Applied hydrogeology—Third Edition*: New York, N.Y., Macmillan College Publishing Company, 691 p.
- Gardner, P.M., and Newman, C.P., 2023, Recharge temperatures and groundwater-age models for the Paradox Valley alluvial aquifer, 2011, Colorado: U.S. Geological Survey data release, <https://doi.org/10.5066/P9FMWX2J>.
- Geldon, A.L., 2003, Geology of Paleozoic rocks in the upper Colorado River Basin in Arizona, Colorado, New Mexico, Utah, and Wyoming, excluding the San Juan Basin: U.S. Geological Survey Professional Paper 1411–A, 85 p., 18 pls. [Available at <https://doi.org/10.3133/pp1411A>.]

- Gutiérrez, F., 2004, Origin of the salt valleys in the Canyonlands section of the Colorado Plateau—Evaporite-dissolution collapse versus tectonic subsidence: *Geomorphology*, v. 57, no. 3–4, p. 423–435, accessed October 4, 2022, at [https://doi.org/10.1016/S0169-555X\(03\)00186-7](https://doi.org/10.1016/S0169-555X(03)00186-7).
- Hem, J.D., 1985, Study and interpretation of the chemical characteristics of natural water: U.S. Geological Survey Water Supply Paper 2254, 263 p., accessed February 16, 2022, at <https://doi.org/10.3133/wsp2254>.
- Heywood, C.E., Mast, M.A., and Paschke, S.S., 2024, MODFLOW-6 model of variable-density groundwater flow and brine discharge to the Dolores River in Paradox Valley, Colorado: U.S. Geological Survey data release, at <https://doi.org/10.5066/P9ZW0FH5>.
- Hite, R.J., and Lohman, S.W., 1973, Geologic appraisal of Paradox basin salt deposits for waste emplacement: U.S. Geological Survey Open-File Report 73–114, 75 p., accessed April 23, 2024, at <https://doi.org/10.3133/ofr73114>.
- Hood, J.W., and Waddell, K.M., 1968, Hydrologic reconnaissance of Skull Valley, Tooele County, Utah: State of Utah, Department of Natural Resources Technical Publication no. 18, 57 p., accessed April 23, 2024, at <https://waterrights.utah.gov/docSys/v920/w920/w920008g.pdf>.
- Hubbert, M.K., 1953, Entrapment of petroleum under hydrodynamic conditions: *American Association of Petroleum Geologists Bulletin*, v. 37, no. 8, p. 1954–2026.
- Hughes, J.D., Langevin, C.D., Paulinski, S.R., Larsen, J.D., and Brakenhoff, D., 2023, FloPy workflows for creating structured and unstructured MODFLOW models: *Groundwater*, v. 62, no. 1, p. 124–139. [Available at <https://doi.org/10.1111/gwat.13327>.] <https://doi.org/10.1111/gwat.13327>
- Kenney, T.A., Gerner, S.J., Buto, S.G., and Spangler, L.E., 2009, Spatially referenced statistical assessment of dissolved-solids load sources and transport in streams of the Upper Colorado River Basin: U.S. Geological Survey Scientific Investigations Report 2009–5007, 50 p., accessed October 4, 2022, at <https://doi.org/10.3133/sir20095007>.
- King, V.M., Block, L.V., Yeck, W.L., Wood, C.K., and Derouin, S.A., 2014, Geological structure of the Paradox Valley Region, Colorado, and relationship to seismicity induced by deep well injection: *Journal of Geophysical Research Solid Earth*, v. 119, no. 6, p. 4955–4978, accessed May 21, 2021, at <https://doi.org/10.1002/2013JB010651>.
- Konikow, L.F., and Bedinger, M.S., 1978, Evaluation of hydrogeologic aspects of proposed salinity control in Paradox Valley, Colorado: U.S. Geological Survey Open-File Report 78–27, 56 p., accessed October 4, 2022, at <https://doi.org/10.3133/ofr7827>.]
- Langevin, C.D., Hughes, J.D., Banta, E.R., Niswonger, R.G., Panday, S., and Provost, A.M., 2017, Documentation for the MODFLOW 6 Groundwater Flow Model: U.S. Geological Survey Techniques and Methods, book 6, chap. A55, 197 p., accessed May 7, 2020, at <https://doi.org/10.3133/tm6A55>.
- Langevin, C.D., Hughes, J.D., Banta, E.R., Provost, A.M., Niswonger, R.G., and Panday, S., 2021, MODFLOW 6 Modular Hydrologic Model version 6.2.2: U.S. Geological Survey Software Release, released July 30, 2021, accessed August 1, 2021, at <https://www.usgs.gov/software/modflow-6-usgs-modular-hydrologic-model>.
- Langevin, C.D., Panday, S., and Provost, A.M., 2020, Hydraulic-head formulation for density-dependent flow and transport: *Groundwater*, v. 58, no. 3, p. 349–362, accessed May 7, 2020, at <https://doi.org/10.1111/gwat.12967>.
- Mast, M.A., 2017, Estimation of salt loads for the Dolores River in the Paradox Valley, Colorado, 1980–2015: U.S. Geological Survey Scientific Investigations Report 2017–5059, 20 p., accessed February 17, 2022, at <https://doi.org/10.3133/sir20175059>.
- Mast, M.A., and Terry, N., 2019, Controls on spatial and temporal variations of brine discharge to the Dolores River in the Paradox Valley, Colorado, 2016–18: U.S. Geological Survey Scientific Investigations Report 2019–5058, 25 p., accessed February 17, 2022, at <https://doi.org/10.3133/sir20195058>.
- Natural Resources Conservation Service, 2020, Natural water and climate center—Report generator 2.0: U.S. Department of Agriculture, accessed December 10, 2020, at <https://wcc.sc.egov.usda.gov/reportGenerator>.
- Newman, C.P., 2021, Water-level and pumping data, water-level models, and estimated hydraulic properties for the Paradox Valley alluvial aquifer in Montrose County, Colorado, 2013: U.S. Geological Survey data release, accessed February 17, 2022, at <https://doi.org/10.5066/P9NV5U6F>.
- Paschke, S.S., ed., 2011, Groundwater availability of the Denver Basin aquifer system, Colorado: U.S. Geological Survey Professional Paper 1770, 274 p., accessed October 4, 2022, at <https://doi.org/10.3133/pp1770>.
- Paschke, S.S., and Mast, M.A., 2024, Geospatial datasets developed for a groundwater model of brine discharge to the Dolores River, Paradox Valley, Colorado: U.S. Geological Survey data release, <https://doi.org/10.5066/P9CJQDDU>.
- Paschke, S.S., Mast, M.A., Gardner, P.M., Newman, C.P., and Watts, K.R., 2024, Hydrogeologic conceptual model of groundwater occurrence and brine discharge to the Dolores River in the Paradox Valley, Montrose County, Colorado: U.S. Geological Survey Scientific Investigations Report 2023–5094, 58 p., <https://doi.org/10.3133/sir20235094>.



- PRISM Climate Group, 2021, PRISM climate data website: Northwest Alliance for Computational Science & Engineering, Oregon State University, accessed July 31, 2021, at <https://prism.oregonstate.edu/>.
- Provost, A.M., and Voss, C.I., 2019, SUTRA, a model for saturated-unsaturated, variable-density groundwater flow with solute or energy transport—Documentation of generalized boundary conditions, a modified implementation of specified pressures and concentrations or temperatures, and the lake capability: U.S. Geological Survey Techniques and Methods, book 6, chap. A52, 62 p., accessed February 17, 2022, at <https://doi.org/10.3133/tm6A52>.
- Shah, N., Nachabe, M., and Ross, M., 2007, Extinction depth and evapotranspiration from ground water under selected land covers: *Groundwater*, v. 45, no. 3, p. 329–338, accessed October 4, 2022, at <https://doi.org/10.1111/j.1745-6584.2007.00302.x>.
- Tuttle, M.L., and Grauch, R.I., 2009, Salinization of the upper Colorado River—Fingerprinting geologic salt sources: U.S. Geological Survey Scientific Investigations Report 2009–5072, 62 p., accessed October 4, 2022, at <https://doi.org/10.3133/sir20095072>.
- U.S. Geological Survey, 2022, USGS water data for the Nation: U.S. Geological Survey National Water Information System database, accessed February 16, 2022, at <https://doi.org/10.5066/F7P55KJN>.
- U.S. Geological Survey, 2023, 1-meter Digital Elevation Models (DEMs), accessed October 6, 2023, at <https://data.usgs.gov/datacatalog/data/USGS:77ae0551-c61e-4979-aedd-d797abcdce0e>.
- U.S. Geological Survey, 2024a, USGS 09169500 Dolores River at Bedrock, CO, *in* USGS water data for the Nation: U.S. Geological Survey National Water Information System database, accessed March 29, 2024, at <https://doi.org/10.5066/F7P55KJN>. [Site information directly accessible at <https://waterdata.usgs.gov/monitoring-location/09169500/all-graphs/#period=P7D>.]
- U.S. Geological Survey, 2024b, USGS 09171100 Dolores River near Bedrock, CO, *in* USGS water data for the Nation: U.S. Geological Survey National Water Information System database, accessed March 29, 2024, at <https://doi.org/10.5066/F7P55KJN>. [Site information directly accessible at <https://waterdata.usgs.gov/monitoring-location/09171100/all-graphs/#period=P7D>.]
- Voggeser, Garrit, 2001, The Dolores Project, Bureau of Reclamation history; accessed July 3, 2023, at <https://www.usbr.gov/projects/pdf.php?id=113>.
- Watts, K.R., 2000, Effects of the Paradox Valley Unit on dissolved solids, sodium, and chloride in the Dolores River near Bedrock, Colorado, water years 1988–98: U.S. Geological Survey Water-Resources Investigations Report 00–4011, 8 p., accessed December 17, 2020, at <https://pubs.usgs.gov/wri/wri00-4011/>.
- Weir, J.E., Jr., Maxfield, E.B., and Zimmerman, E.A., 1983, Regional hydrology of the Dolores River Basin, eastern Paradox Basin, Colorado and Utah: U.S. Geological Survey Water-Resources Investigations Report 83–4127, 53 p., accessed April 23, 2024 at <https://doi.org/10.3133/wri834217>.
- Western Regional Climate Center, 2020, Desert research institute website: Western Regional Climate Center accessed December 11, 2020, at <https://wrcc.dri.edu/>.
- White, J.T., Hunt, R.J., Fienen, M.N., and Doherty, J.E., 2020, Approaches to highly parameterized inversion—PEST++ version 5, a software suite for parameter estimation, uncertainty analysis, management optimization and sensitivity analysis: U.S. Geological Survey Techniques and Methods, book 7, chap. C26, 52 p., accessed October 4, 2022, at <https://doi.org/10.3133/tm7C26>.
- Wollitz, L.E., Thordarson, W., Whitfield M.S., Jr., and Weir, J.E., Jr., 1982, Results of hydraulic tests in U.S. Department of Energy’s wells DOE-4, 5, 6, 7, 8, and 9, Salt Valley, Grand County, Utah: U.S. Geological Survey Open-File Report 82–346, 71 p., accessed December 17, 2020, at <https://doi.org/10.3133/ofr82346>.

For additional information contact:

Director, Colorado Water Science Center  
U.S. Geological Survey  
Box 25046, Mail Stop 415  
Denver, CO 80225  
<https://co.water.usgs.gov>

Publishing support provided by the U.S. Geological Survey  
Science Publishing Network, Denver, Reston, and Sacramento  
Publishing Service Centers

